Supplementary information for "Classification in biological networks with hypergraphlet kernels"

Jose Lugo-Martinez
Computational Biology Department, Carnegie Mellon University
Pittsburgh, Pennsylvania, U.S.A.
jlugomar@cs.cmu.edu

Daniel Zeiberg
Khoury College of Computer Sciences, Northeastern University
Boston, Massachusetts, U.S.A.
zeiberg.d@northeastern.edu

Thomas Gaudelet
Department of Computer Science, University College London
London WC1E 6BT, U.K.
thomas.gaudelet.16@cs.ucl.ac.uk

Noël Malod-Dognin
Department of Life Sciences, Barcelona Supercomputing Center
Barcelona, 08034 Spain
noel.malod@bsc.es

Nataša Pržulj
Department of Life Sciences, Barcelona Supercomputing Center
Barcelona, 08034 Spain
ICREA, Pg. Lluis Companys 23
08010 Barcelona, Spain
natasa@cs.ucl.ac.uk

Predrag Radivojac*
Khoury College of Computer Sciences, Northeastern University
Boston, Massachusetts, U.S.A.
predrag@northeastern.edu

*To whom correspondence should be addressed.

1 Enumeration of labeled hypergraphlets

Here we characterize the feature space of fully labeled hypergraphlets by describing the dimensionality of count vectors $\phi_{(n,\tau)}(v)$. We are interested in the order of growth of $\kappa(n, \Sigma, \Xi)$ as a function of n, Σ and Ξ, as introduced in the main text.

Suppose that G and H are base hypergraphlets with n vertices and m hyperedges. We say that G and H belong to the same equivalence class if and only if the total number of (non-isomorphic) fully labeled hypergraphlets corresponding to the base cases G and H are equal for any Σ and Ξ. The total counts of labeled hypergraphlets over all alphabet sizes induce a partition of base hypergraphlets into equivalence classes. We

Table S1: **Equivalence classes over vertex- and hyperedge-labeled hypergraphlets.** List of equivalence classes and their cardinality produced by partitioning the set of undirected base hypergraphlets for $n \in \{1, 2, 3, 4\}$ over vertex-labels alphabet Σ and hyperedge-labels alphabet Ξ. We also list the number of vertex-labeled n-hypergraphlets over an alphabet Σ denoted as $m_i(n, \Sigma, 1)$, as well as fully labeled n-hypergraphlets over an alphabet Σ and Ξ denoted as $m_i(n, \Sigma, \Xi)$.

Vertex-labeled hypergraphlets		
$S_i(n)$	$\lvert S_i(n)\rvert$	$m_i(n, \Sigma, 1)$
$S_1(1)$	1	$\lvert\Sigma\rvert$
$S_1(2)$	1	$\lvert\Sigma\rvert^2$
$S_1(3)$	3	$\lvert\Sigma\rvert^3$
$S_2(3)$	6	$1/2(\lvert\Sigma\rvert^3 + \lvert\Sigma\rvert^2)$
$S_1(4)$	221	$\lvert\Sigma\rvert^4$
$S_2(4)$	212	$1/2(\lvert\Sigma\rvert^4 + \lvert\Sigma\rvert^3)$
$S_3(4)$	28	$1/6(\lvert\Sigma\rvert^4 + 3 \cdot \lvert\Sigma\rvert^3 + 2 \cdot \lvert\Sigma\rvert^2)$
Fully-labeled hypergraphlets		
$S_i(n)$	$\lvert S_i(n)\rvert$	$m_i(n, \Sigma, \Xi)$
$S_1(1)$	1	$\lvert\Sigma\rvert$
$S_1(2)$	1	$\lvert\Sigma\rvert^2 \cdot \lvert\Xi\rvert$
$S_1(3)$	1	$\lvert\Sigma\rvert^3 \cdot \lvert\Xi\rvert^3$
$S_2(3)$	2	$\lvert\Sigma\rvert^3 \cdot \lvert\Xi\rvert^2$
$S_3(3)$	1	$1/2(\lvert\Sigma\rvert^3 \cdot \lvert\Xi\rvert^4 + \lvert\Sigma\rvert^2 \cdot \lvert\Xi\rvert^3)$
$S_4(3)$	2	$1/2(\lvert\Sigma\rvert^3 \cdot \lvert\Xi\rvert^3 + \lvert\Sigma\rvert^2 \cdot \lvert\Xi\rvert^2)$
$S_5(3)$	1	$1/2(\lvert\Sigma\rvert^3 \cdot \lvert\Xi\rvert^2 + \lvert\Sigma\rvert^2 \cdot \lvert\Xi\rvert^2)$
$S_6(3)$	1	$1/2(\lvert\Sigma\rvert^3 \cdot \lvert\Xi\rvert^2 + \lvert\Sigma\rvert^2 \cdot \lvert\Xi\rvert)$
$S_7(3)$	1	$1/2(\lvert\Sigma\rvert^3 \cdot \lvert\Xi\rvert + \lvert\Sigma\rvert^2 \cdot \lvert\Xi\rvert)$

denote the set of all equivalence classes over the hypergraphlets of order n as $S(n) = \{S_1(n), S_2(n), \ldots\}$. For example, the set of vertex- and hyperedge-labeled 3-hypergraphlets can be partitioned into either: two symmetry classes when $|\Xi| = 1$: $S_1(3) = \{3_2, 3_4, 3_7\}$ and $S_2(3) = \{3_1, 3_3, 3_5, 3_6, 3_8, 3_9\}$, or seven symmetry classes when $|\Xi| > 1$: $S_1(3) = \{3_2\}$, $S_2(3) = \{3_4, 3_7\}$, $S_3(3) = \{3_9\}$, $S_4(3) = \{3_6, 3_8\}$, $S_5(3) = \{3_3\}$, $S_6(3) = \{3_5\}$ and $S_7(3) = \{3_1\}$. Table S1 summarizes equivalence classes induced by partitioning base hypergraphlets up to the order of 4 along with the cardinality of each set. Overall, observe that the cardinality of $S(n)$ can be significantly larger than those reported for graphlets [3] because the possible number of hyperedges in a hypergraphlet is generally much larger than the possible number of edges in a graphlet. Additionally, hyperedge-labels require base hypergraphlets G and H to have an equal number of hyperedges.

This approach can be generalized to hypergraphlets labeled by any alphabet Σ and Ξ, such that

$$\kappa(n, \Sigma, \Xi) = \sum_{i=1}^{|S(n)|} m_i(n, \Sigma, \Xi) \cdot |S_i(n)|,$$

where $m_i(n, \Sigma, \Xi)$ is the number of (non-isomorphic) fully labeled hypergraphlets corresponding to any base hypergraphlet from the equivalence class $S_i(n)$. We use this decomposition to compute the total dimensionality of the count vectors by first finding the equivalence classes corresponding to the base hypergraphlets and then counting the number of labeled hypergraphlets for any one member of the group.

In the case of undirected fully labeled hypergraphlets, $m_i(n, \Sigma, \Xi)$ can also be computed by applying the theory of enumeration developed by Pólya [5]. In order to get the derivation of the complete generating function for each equivalence class $S_i(n)$, we first define the automorphism group $\mathcal{A}$ of a given vertex- and hyperedge-labeled hypergraph $G = (V, E)$. That is, in the case of fully-labeled hypergraphs, set $\mathcal{A}$ is a collection of permutations (automorphisms) of V and E. Therefore, the counting problem can be re-formulated as follows: Let G be a base hypergraphlet of n vertices and m hyperedges, and $\mathcal{A}$ be the automorphism group of G over V and E. Then, each permutation $\alpha \in \mathcal{A}$ can be written uniquely as the

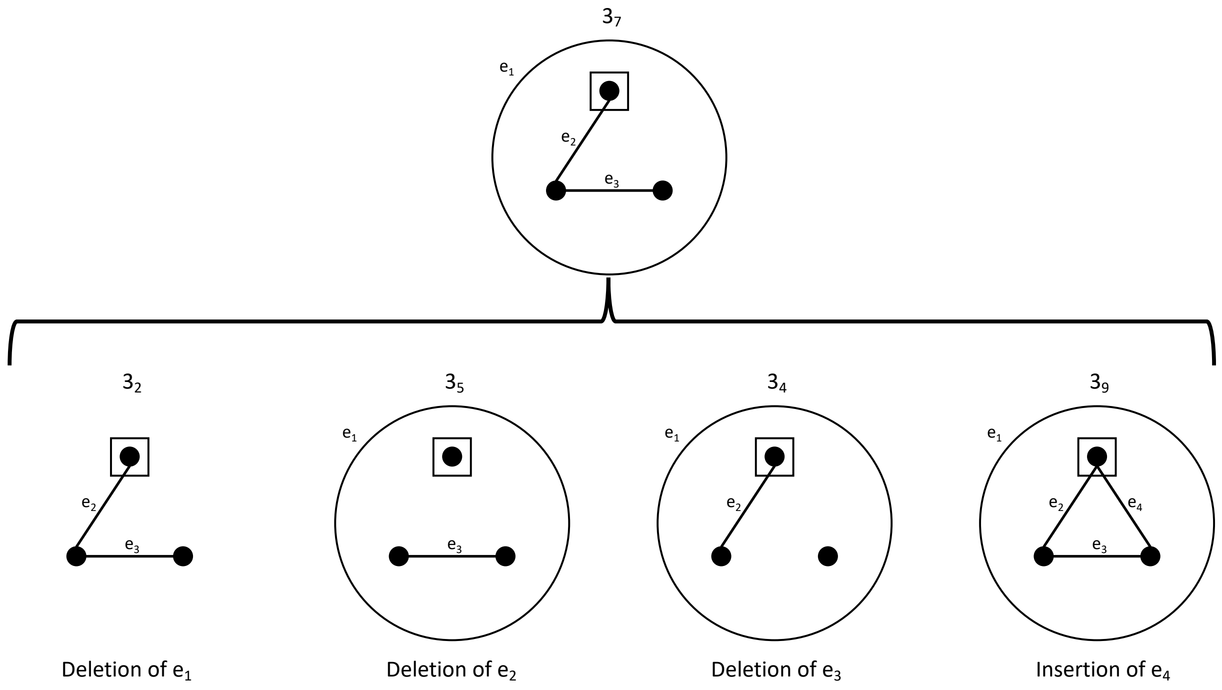

Figure S1: Example of precomputed level-1 insertions/deletions (indels) of hyperedges for base hypergraphlet 3_7. The precomputed level-1 indels include three hyperedge deletions and one hyperedge insertion.

product of disjoint cycles such that for each integer $k \in \{1, \ldots, n\}$ ($k' \in \{1, \ldots, m\}$), we define $j_k(\alpha)$ ($j_{k'}(\alpha)$) as the number of cycles of length k (k') in the disjoint cycle expansion of α. Interestingly, the generalized formula for the cycle index of $\mathcal{A}$, denoted as $Z(\mathcal{A})$, is a polynomial in $s_1, \ldots, s_n; s'_1, \ldots, s'_m$ given by

$$Z(\mathcal{A}; s_1, \ldots, s_n; s'_1, \ldots, s'_m) = \frac{1}{|\mathcal{A}|} \sum_{\alpha \in \mathcal{A}} \prod_{k=1}^{n} \prod_{k'=1}^{m} s_k^{j_k(\alpha)} \cdot s_{k'}^{j_{k'}(\alpha)}.$$

By applying Pólya's theorem in the context of enumerating vertex- and hyperedge-labeled hypergraphlets corresponding to any base hypergraphlet in $S_i(n)$, we get that $m_i(n, \Sigma, \Xi)$ is determined by substituting $|\Sigma|$ for each variable s_k and $|\Xi|$ for each variable $s'_{k'}$ in $Z(\mathcal{A})$. Hence,

$$m_i(n, \Sigma, \Xi) = Z(\mathcal{A}; |\Sigma|, |\Sigma|, \ldots, |\Sigma|; |\Xi|, |\Xi|, \ldots, |\Xi|),$$

where $\mathcal{A}$ is the automorphism group of a base hypergraphlet from $S_i(n)$. As an example, consider the equivalence class $S_3(3) = \{3_9\}$ with $\Sigma = \{A, B, C\}$ and $\Xi = \{X, Y\}$ (Figure 2 in the main paper illustrates an unlabeled version of hypergraphlet 3_9). The automorphism group is given by

$$\mathcal{A} = \{(v_1)(v_2)(v_3)(e_1)(e_2)(e_3)(e_4), (v_1)(v_2 v_3)(e_1 e_2)(e_3)(e_4)\},$$

thus, $Z(\mathcal{A}; s_1, s_2, s_3; s'_1, s'_2) = \frac{1}{2}(s_1^3 \cdot s'^4_1 + s_1 \cdot s_2 \cdot s'^2_1 \cdot s'_2)$. Therefore, it follows that, $m_3(3, \Sigma, \Xi) = Z(\mathcal{A}; 3, 3, 3; 2, 2) = \frac{1}{2}(3^3 \cdot 2^4 + 3 \cdot 3 \cdot 2^2 \cdot 2) = 252$.

2 Computational complexity

The implementation and the analysis of hypergraphlet kernels is an extension of the available solutions for string kernels [6]. Let $G_l(r) = (V_r, E_r)$ be a *neighborhood hypergraph* of a rooted hypergraph $G = (V, r, E)$ such that there exits a walk w of length at most l between any node $u \in V$ and root vertex r, denoted as $|w(u, r)| \leq l$. Formally, $E_r = \{e \,|\, e \in E \wedge e \subseteq V_r \wedge |w(u, r)| \leq l, \forall u \in V_r, l \geq 0, r \in V_r\}$. In this work, we consider the set of undirected base hypergraphlets for $n \in \{1, 2, 3, 4\}$, thus, neighborhood hypergraph $G_{n-1}(r)$ contains all possible n-hypergraphlets rooted at vertex r. Suppose $G_{n-1}(r)$ is significantly smaller than G. An upper bound on the complexity of the counting algorithm for all n-hypergraphlets rooted at vertex r is $\mathcal{O}(|V_r||E_r| + (\delta_{\max} d_{\max})^{n-1})$, where $d_{\max}$ is the maximum degree of a vertex in V_r and $\delta_{\max}$ is the maximum degree of a hyperedge in E_r. The first term is related to computing the neighbors for each node $v \in V_r$, whereas the second term reflects the cost of counting over all base hypergraphlets. Similarly, an upper bound on the complexity of generating the minimum cost edit path is $\mathcal{O}((n|\Sigma| + 2^n|\Xi|) + (2^n|\Xi|))$ per single hypergraphlet edit operation. In this case, the first term reflects the cost of generating all vertex and hyperedge label substitutions, whereas the second term corresponds to the cost of performing hyperedge insertions and deletions (indels); see Figure S1 for an example of level-1 indels on a base hypergraphlet. Therefore, for each vertex v an order of

$$\mathcal{O}(\min\{|V_r|^n, \kappa(n, \Sigma, \Xi)\}\,((n|\Sigma| + 2^n|\Xi|) + (2^n|\Xi|))^\tau)$$

operations are necessary, where the $|V_r|^n$ term enumerates possible n-hypergraphlets in $G_{n-1}(r)$. Note that the possible number of hyperedges in a hypergraph $|E_r|$ can be significantly larger than the possible number of edges in a standard graph. Hence, in a practical setting, the edit-distance hypergraphlet kernels could greatly benefit from effective sampling techniques or exploitation of special types of hypergraphlets. The proposed implementation for computing hypergraphlet kernel functions is computed in time linear in the number of non-zero elements.

2.1 Converting hypergraphs to graphs

A commonly used approach for learning from hypergraph data is to construct a standard graph representation from the input hypergraph and use well-established graph approaches. Among these hypergraph-to-graph transformations, the two most popular are *clique expansion* and *star expansion* [7]. A clique expansion of a hypergraph $G = (V, E)$ is defined as graph $G^x = (V, E^x \subseteq V^2)$ such that each hyperedge $e = \{v_1, \cdots, v_{\delta(e)}\} \in E$ is replaced with an edge for each pair of vertices in hyperedge e, thus, forming a clique in G^x; mathematically, $E^x = \{(u, v)\,|\,u, v \in e, e \in E\}$. A star expansion of a hypergraph $G = (V, E)$ is defined as a graph $G^* = (V^*, E^*)$ such that for each hyperedge $e = \{v_1, \cdots, v_{\delta(e)}\} \in E$, a new vertex e is introduced in G^* connecting e to each $v \in e$, hence, $V^* = V \cup E$; mathematically, $E^* = \{(v, e)\,|\,v \in e, e \in E\}$.

We used the clique expansion to evaluate the benefits of using hypregraphs in the second stage of our approach. Note that the first stage consists of converting graphs into dual extended hypergraphs and formulating edge classification and link prediction as a vertex classification approach on hypergraphs. A combination of the dual hypergraph construction, subsequent clique expansion, with graphlet kernel-based prediction is referred to here as *dual graphlet kernel* to distinguish this method from standard graphlet kernels used on the vertices of the original network (note that edge classification on standard graphs corresponds here to the vertex classification on line graphs). The dual graphlet kernels that here integrate vertex and edge alphabets into edit-distance similarity functions were not available in prior work and were implemented within our proposed methodology.

References

[1] A.L. Barabási et al. Evolution of the social network of scientific collaborations. *Physica A*, 311(3):590–614, 2002.

[2] I.A. Kovács et al. Network-based prediction of protein interactions. *Nat Commun*, 10:1240–1247, 2019.

[3] J. Lugo-Martinez and P. Radivojac. Generalized graphlet kernels for probabilistic inference in sparse graphs. *Network Science*, 2(2):254–276, 2014.

[4] Y. Park and E. M. Marcotte. Flaws in evaluation schemes for pair-input computational predictions. *Nat Methods*, 9(12):1134–1136, 2012.

[5] G. Pólya. Kombinatorische anzahlbestimmungen für gruppen, graphen und chemische verbindungen. *Acta Math*, 68:145–254, 1937.

[6] K. Rieck and P. Laskov. Linear-time computation of similarity measures for sequential data. *J Mach Learn Res*, 9:23–48, 2008.

[7] J. Y. Zien, M. D. F. Schlag, and P. K. Chan. Multilevel spectral hypergraph partitioning with arbitrary vertex sizes. *IEEE Trans Comput Aid Design*, 18(9):1389–1399, 1999.

Table S2: **Area under the ROC curve estimates for each method on the PPI data sets using 10-fold cross-validation based on the three categories C_1, C_2, C_3 of difficulty identified by Park and Marcotte [4].** The highest performance for each class and data set pair is shown in boldface. Since L3 framework relies on paths of a specific length, it cannot predict on all possible protein pairs. Therefore, the last two rows compare the AUC between L3 and the best hypergraphlet kernel on the same set of predicted protein pairs.

Method/Dataset	**EC**			**SP**			**RN**			**MM**			**CE**			**AT**		
	C_1	C_2	C_3	C_1	C_2	C_3	C_1	C_2	C_3	C_1	C_2	C_3	C_1	C_2	C_3	C_1	C_2	C_3
Without domain information, $\lvert\Sigma\rvert = 1$																		
Dual graphlet kernel ($\tau = 0$)	0.715	0.705	0.674	0.719	0.718	**0.712**	0.693	0.691	0.651	0.637	0.635	0.625	**0.873**	**0.872**	**0.872**	0.681	0.683	0.681
Section hypergraphlet kernel ($\tau = 0$)	0.724	0.713	0.719	0.639	0.646	0.628	0.671	0.672	0.664	0.628	0.630	0.633	0.762	0.755	0.774	0.578	0.563	0.588
Sub-hypergraphlet kernel ($\tau = 0$)	0.692	0.687	0.657	0.691	0.691	0.686	0.651	0.647	0.633	0.612	0.610	0.605	**0.873**	**0.872**	**0.872**	0.681	0.683	0.681
Dual graphlet kernel ($\tau = 1$)	0.678	0.669	0.649	0.698	0.699	0.691	0.671	0.670	0.648	0.623	0.620	0.614	0.869	0.869	0.869	0.672	0.671	0.670
Section hypergraphlet kernel ($\tau = 1$)	0.708	0.695	0.700	0.641	0.643	0.623	0.678	0.666	0.668	0.628	0.628	0.633	0.772	0.781	0.767	0.581	0.563	0.567
Sub-hypergraphlet kernel ($\tau = 1$)	0.681	0.682	0.660	0.686	0.687	0.682	0.649	0.649	0.634	0.611	0.610	0.606	0.871	0.870	0.870	0.683	0.684	0.682
L3 framework [2]	0.717	0.597	0.556	0.577	0.529	0.497	0.634	0.611	0.510	0.573	0.550	0.506	0.511	0.504	0.504	0.501	0.501	0.502
Preferential attachment [1]	0.814	0.675	0.639	0.492	0.456	0.453	0.552	0.504	0.511	0.498	0.485	0.463	0.660	0.523	0.549	0.449	0.441	0.463
With domain information, $\lvert\Sigma\rvert = \{4, 8, 16\}$; $\Sigma = \Sigma_{GO}$																		
Random walk	0.762	0.755	0.739	0.636	0.617	0.574	0.537	0.521	0.422	0.585	0.563	0.497	0.805	0.803	0.802	0.613	0.605	0.585
Random hyperwalk	0.815	0.817	0.786	0.610	0.599	0.550	0.599	0.587	0.484	0.588	0.567	0.531	0.597	0.595	0.594	0.608	0.601	0.580
Cumulative random walk	0.799	0.791	0.789	0.706	0.701	0.680	0.587	0.585	0.466	0.641	0.641	0.613	0.716	0.701	0.708	0.647	0.643	0.629
Cumulative random hyperwalk	0.848	0.841	0.820	0.681	0.666	0.641	0.647	0.616	0.524	0.670	0.669	0.646	0.569	0.552	0.561	0.637	0.614	0.624
Pairwise spectrum kernel ($k = \{3, 4, 5\}$)	0.816	0.754	0.618	0.584	0.505	0.432	0.716	0.648	0.580	0.689	0.632	0.548	0.754	0.659	0.650	0.629	0.616	0.541
Dual graphlet kernel ($\tau = 0$)	0.802	0.763	0.733	0.734	0.704	0.609	0.673	0.665	0.528	0.630	0.663	0.595	0.846	0.848	0.843	0.678	0.671	0.619
Section hypergraphlet kernel ($\tau = 0$)	0.861	0.840	0.815	0.677	0.664	0.634	0.698	0.670	0.637	0.655	0.647	0.641	0.804	0.799	0.798	0.559	0.567	0.535
Sub-hypergraphlet kernel ($\tau = 0$)	0.796	0.771	0.747	0.740	0.720	0.665	0.676	0.637	0.500	0.708	0.692	0.641	0.846	0.848	0.843	0.678	0.671	0.619
Dual graphlet kernel ($\tau = 1$)	0.816	0.776	0.742	0.745	0.719	0.630	0.682	0.691	0.559	0.702	0.673	0.611	0.853	0.854	0.851	0.699	0.687	0.633
Section hypergraphlet kernel ($\tau = 1$)	**0.875**	**0.843**	**0.830**	0.697	0.684	0.649	0.706	0.695	**0.686**	0.667	0.648	0.639	0.786	0.784	0.783	0.574	0.576	0.574
Sub-hypergraphlet kernel ($\tau = 1$)	0.812	0.776	0.772	**0.750**	**0.738**	**0.712**	**0.719**	**0.698**	0.563	**0.736**	**0.726**	**0.695**	0.860	0.860	0.861	**0.728**	**0.726**	**0.711**
L3 framework [2]	0.588	0.449	0.691	0.638	0.635	0.565	0.751	0.755	0.613	0.622	0.616	0.531	0.130	0.100	-	0.677	0.549	0.659
Hypergraphlet kernel (highest)	0.896	0.687	0.833	0.759	0.728	0.712	0.683	0.696	0.632	0.738	0.726	0.696	0.966	0.714	-	0.652	0.843	0.846

Table S3: **Area under the ROC curve estimates for each method on the DTI data sets using 10-fold cross-validation based on the three categories C_1, C_2, C_3 of difficulty identified by Park and Marcotte [4].** The highest performance for each class and data set pair is shown in boldface. Since L3 framework relies on paths of a specific length, it cannot predict on all possible drug-target pairs. Therefore, the last two rows compare the AUC between L3 and the best hypergraphlet kernel on the same set of predicted drug-target pairs.

Method/Dataset	**EZ**			**IC**			**GR**			**NR**		
	C_1	C_2	C_3	C_1	C_2	C_3	C_1	C_2	C_3	C_1	C_2	C_3
Without domain information, $\|\Sigma\| = 1$												
Dual graphlet kernel ($\tau = 0$)	0.871	0.865	0.838	0.759	0.729	0.714	0.624	0.606	0.525	0.714	0.676	0.712
Section hypergraphlet kernel ($\tau = 0$)	0.537	0.541	0.514	0.542	0.506	0.509	0.552	0.542	0.493	0.783	**0.772**	0.679
Sub-hypergraphlet kernel ($\tau = 0$)	0.788	0.786	0.778	0.711	0.697	0.680	0.579	0.566	0.484	0.732	0.719	**0.735**
Dual graphlet kernel ($\tau = 1$)	0.851	0.836	0.792	0.713	0.689	0.651	0.599	0.580	0.519	0.734	0.725	0.728
Section hypergraphlet kernel ($\tau = 1$)	0.535	0.541	0.502	0.550	0.510	0.524	0.542	0.504	0.513	**0.791**	0.736	0.704
Sub-hypergraphlet kernel ($\tau = 1$)	0.784	0.780	0.770	0.702	0.684	0.671	0.580	0.566	0.482	0.736	0.733	0.731
L3 framework [2]	0.629	0.626	0.500	0.642	0.534	0.500	0.596	0.584	0.500	0.505	0.420	0.500
Preferential attachment [1]	0.534	0.502	0.500	0.561	0.457	0.500	0.545	0.530	0.500	0.497	0.431	0.500
With domain information, $\|\Sigma\| = \{4, 8, 16\}$; $\Sigma = \Sigma_{GO} \bigcup \Sigma_{SS}$												
Dual graphlet kernel ($\tau = 0$)	0.952	0.914	0.830	0.883	0.830	0.659	0.756	0.679	0.534	0.771	0.709	0.694
Section hypergraphlet kernel ($\tau = 0$)	0.633	0.630	0.596	0.583	0.546	0.527	0.625	0.581	0.518	0.775	0.605	0.638
Sub-hypergraphlet kernel ($\tau = 0$)	0.936	0.885	0.801	0.879	0.834	0.678	0.724	0.641	0.531	0.757	0.717	0.709
Dual graphlet kernel ($\tau = 1$)	**0.953**	**0.923**	0.832	**0.900**	0.845	0.686	**0.758**	0.684	0.533	0.778	0.719	0.719
Section hypergraphlet kernel ($\tau = 1$)	0.637	0.605	0.605	0.585	0.543	0.523	0.619	0.591	**0.550**	0.777	0.707	0.713
Sub-hypergraphlet kernel ($\tau = 1$)	0.944	0.913	**0.845**	0.884	**0.852**	**0.715**	0.747	**0.693**	0.526	0.764	0.713	0.730
L3 framework [2]	0.658	0.668	-	0.655	0.534	-	0.624	0.609	-	0.577	0.501	-
Hypergraphlet kernel (highest)	0.953	0.921	-	0.900	0.858	-	0.760	0.687	-	0.802	0.818	-

Base hypergraphlets up to 4 vertices

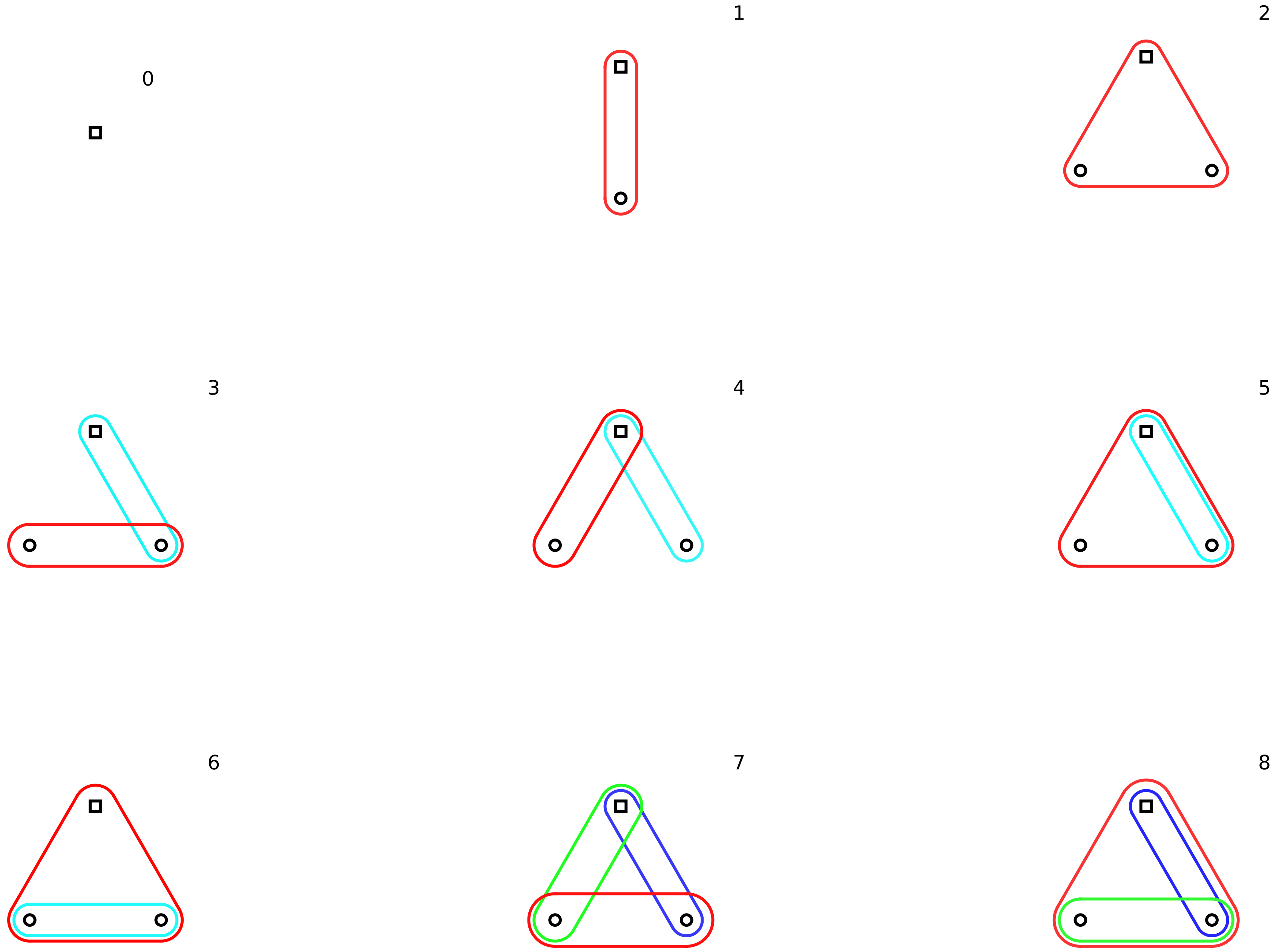

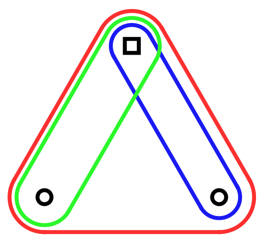
9

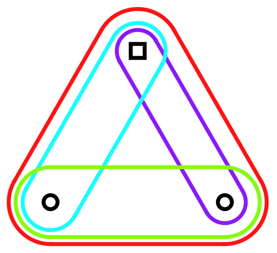
10

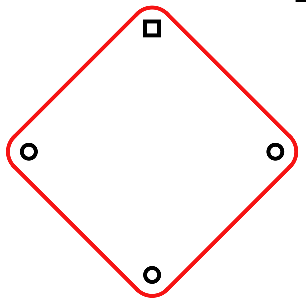
11

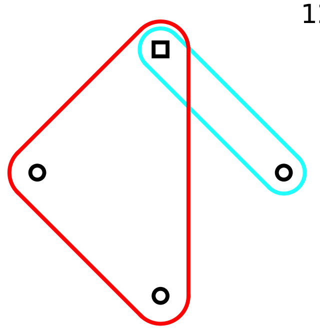
12

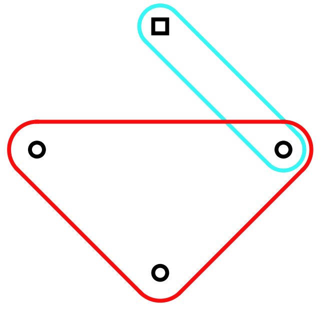
13

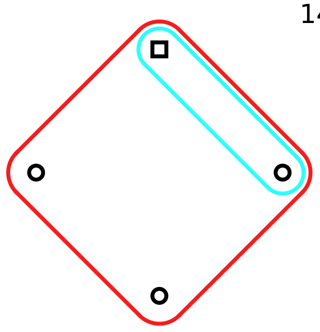
14

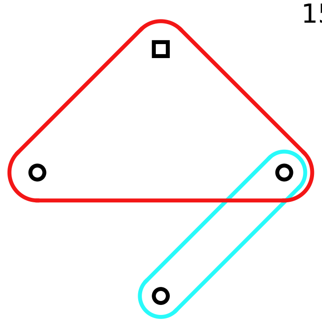
15

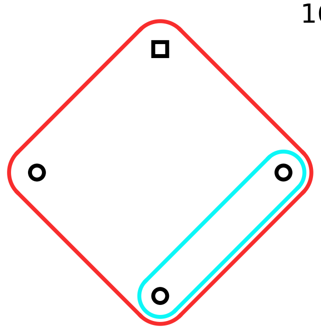
16

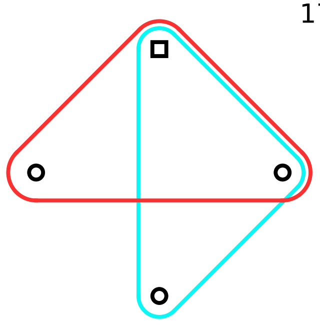
17

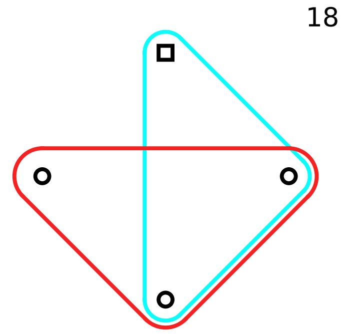
18

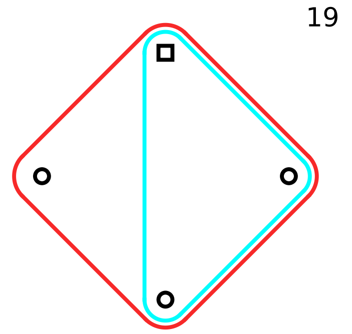
19

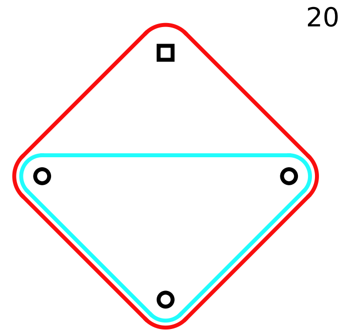
20

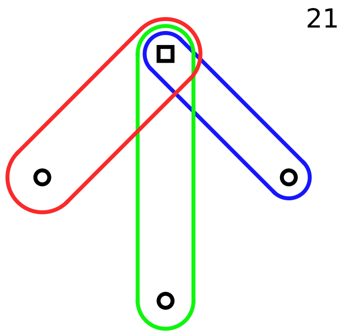
21

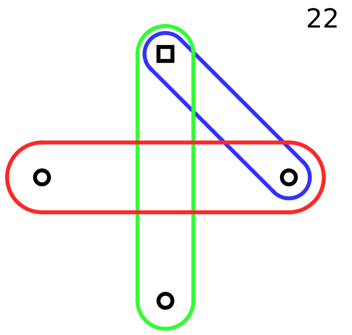
22

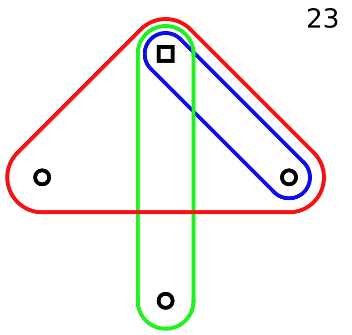
23

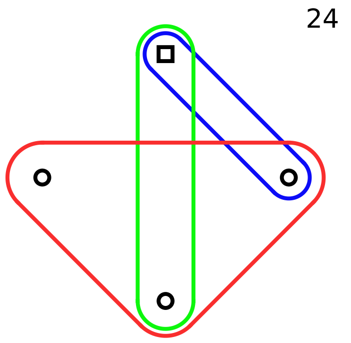
24

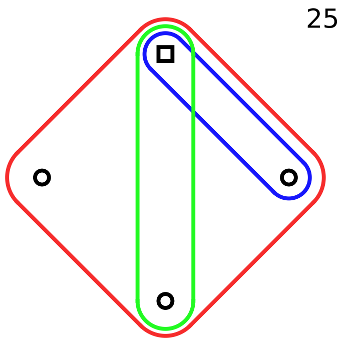
25

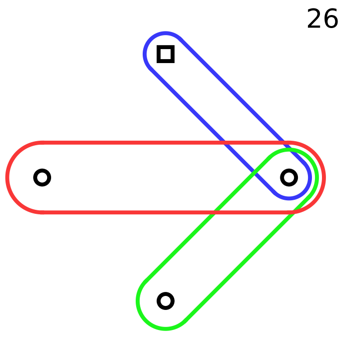
26

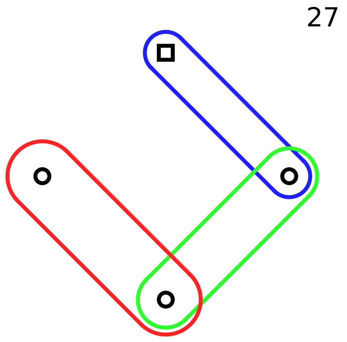
27

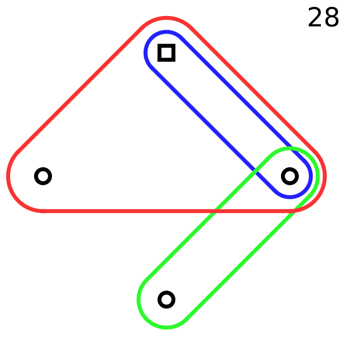
28

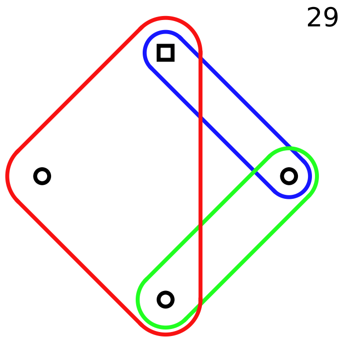
29

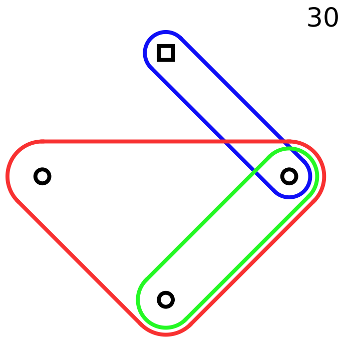
30

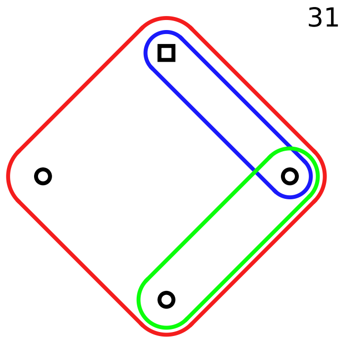
31

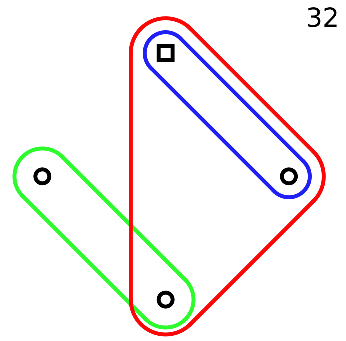
32

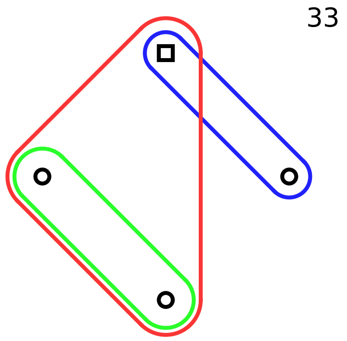
33

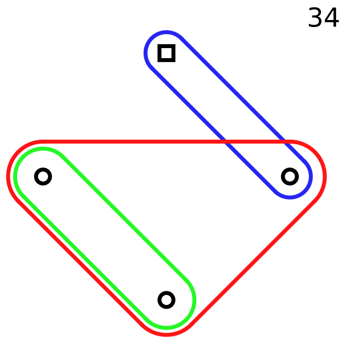
34

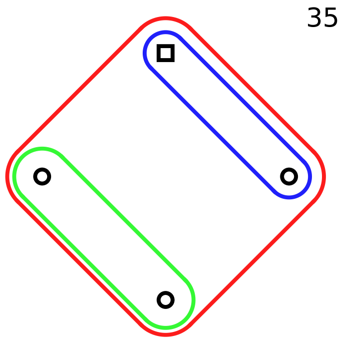
35

36

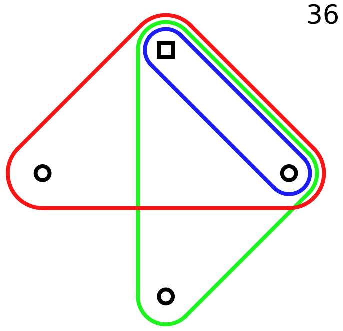

37

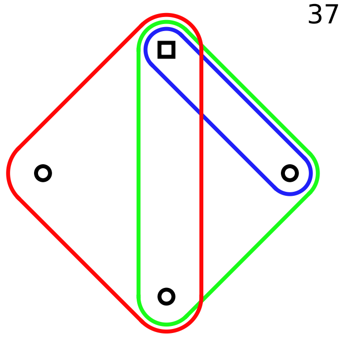

38

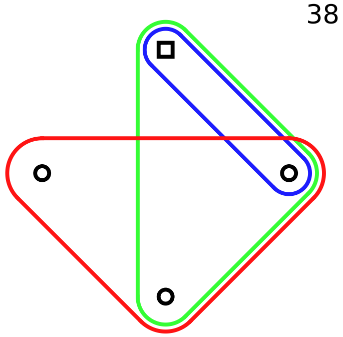

39

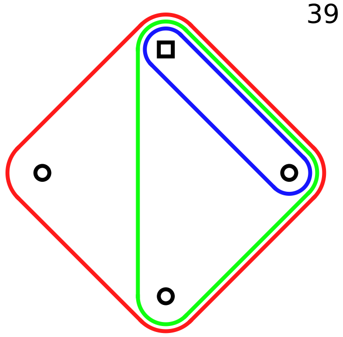

40

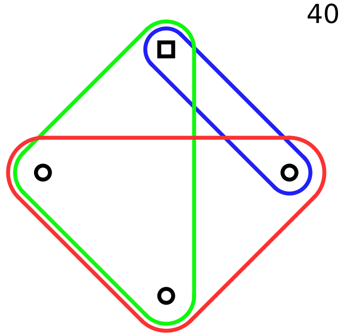

41

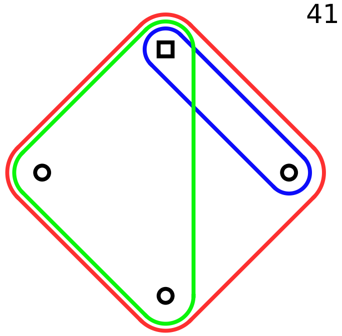

42

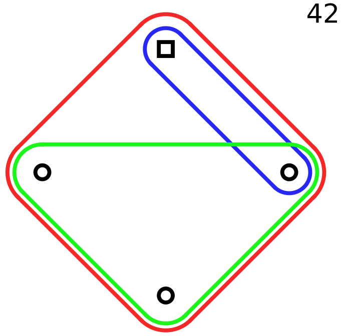

43

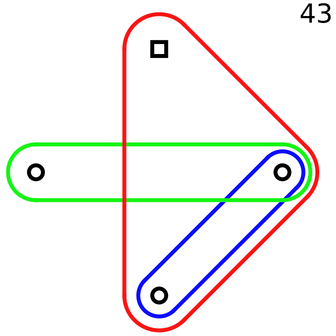

44

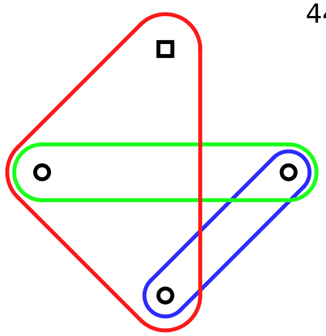

45

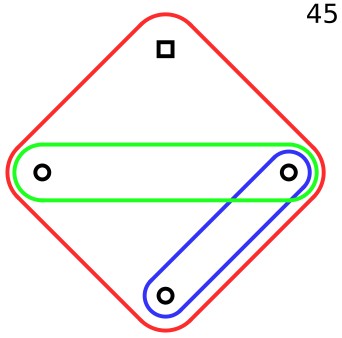

46

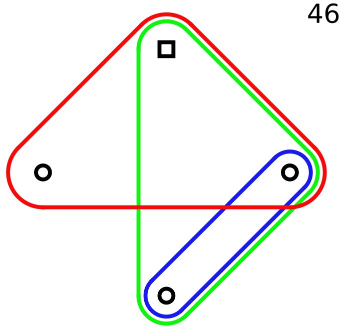

47

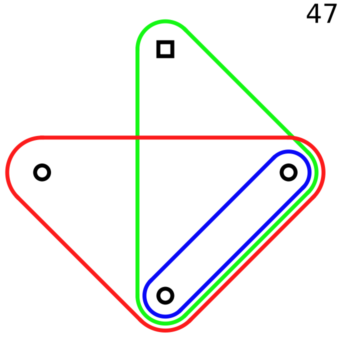

48

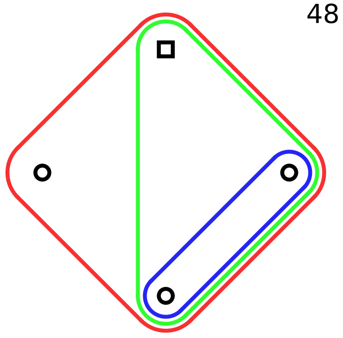

49

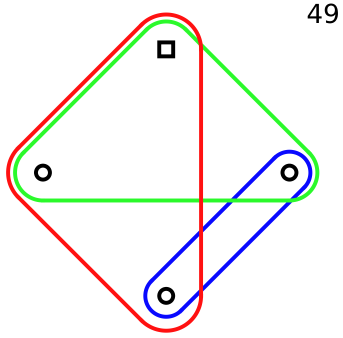

50

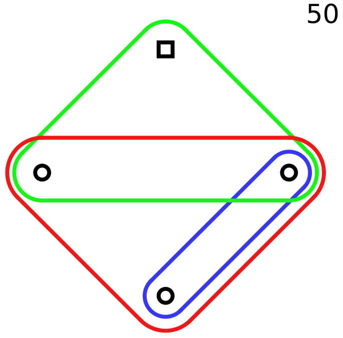

51

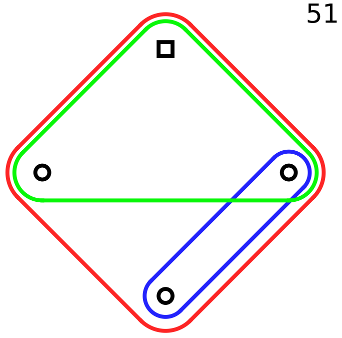

52

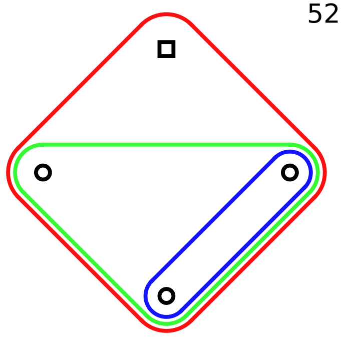

53

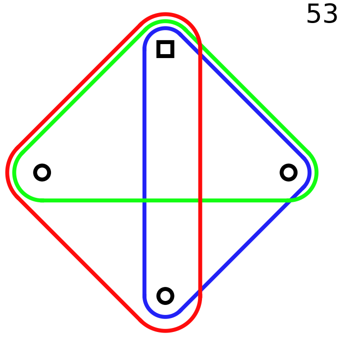

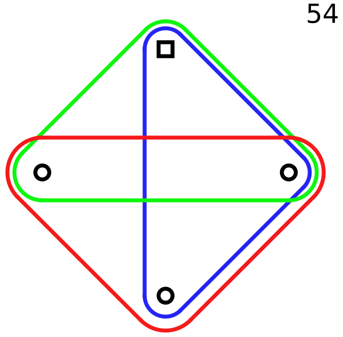
54

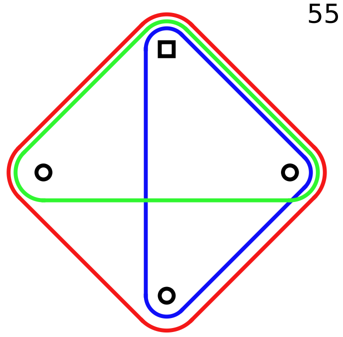
55

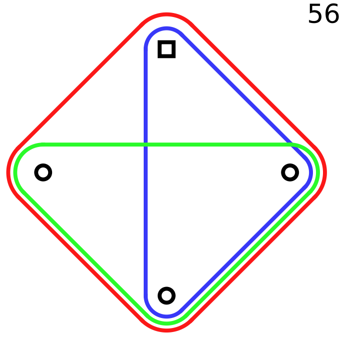
56

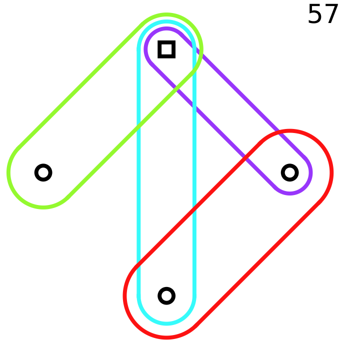
57

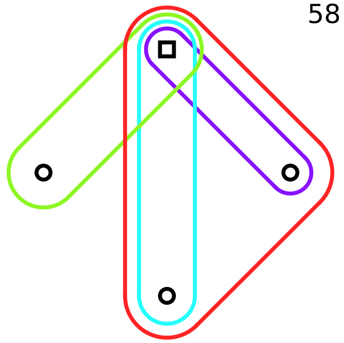
58

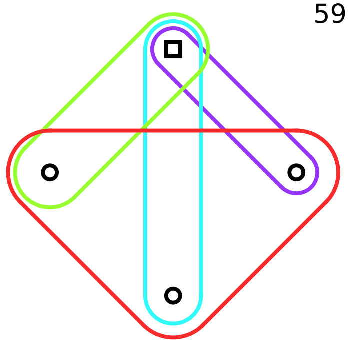
59

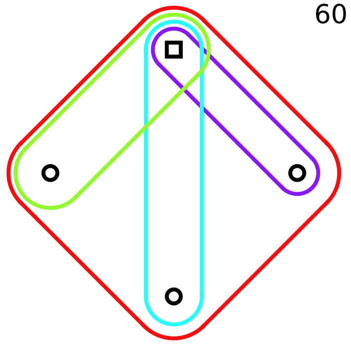
60

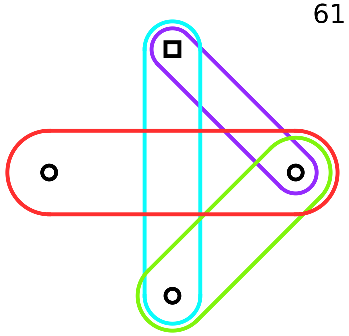
61

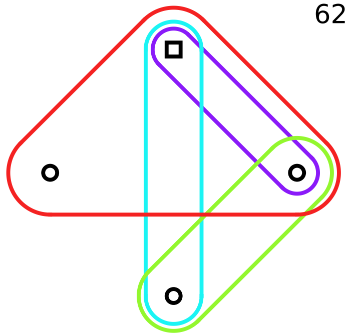
62

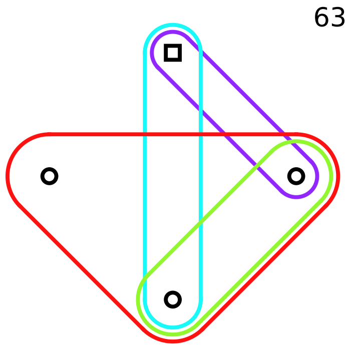
63

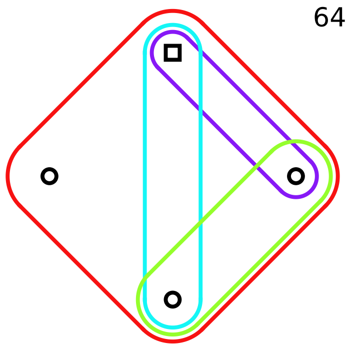
64

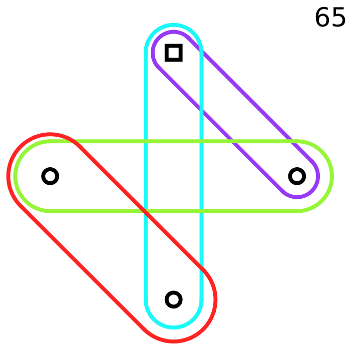
65

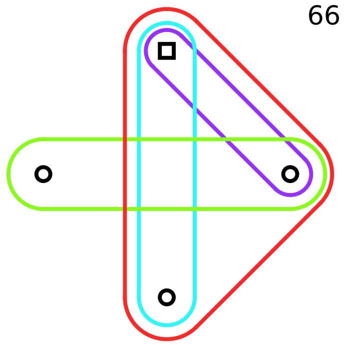
66

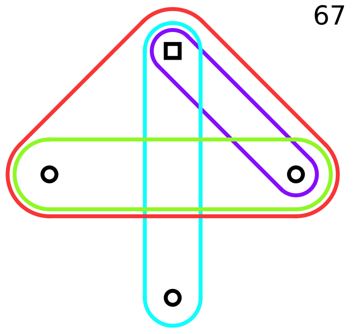
67

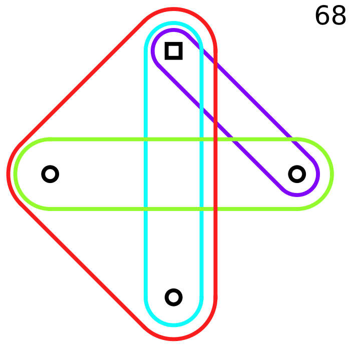
68

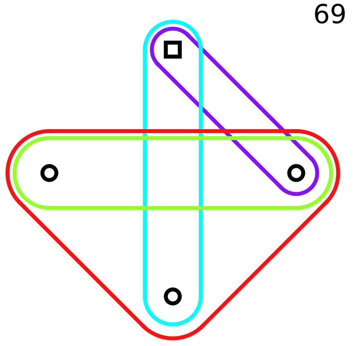
69

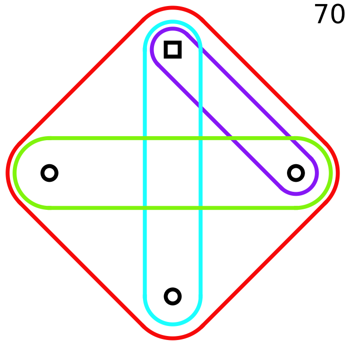
70

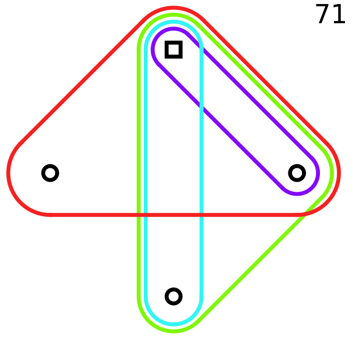
71

72

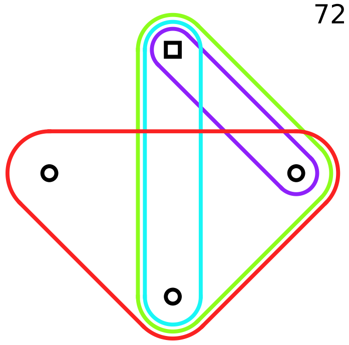

73

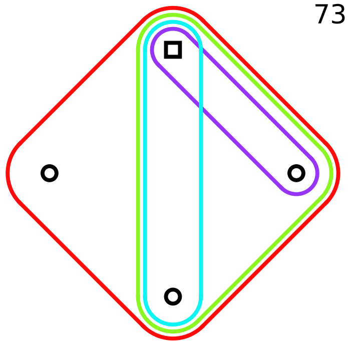

74

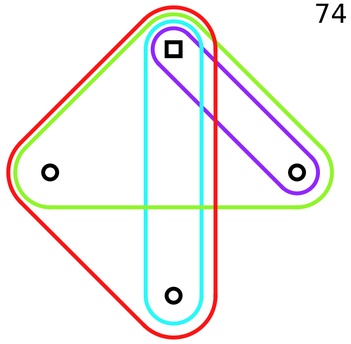

75

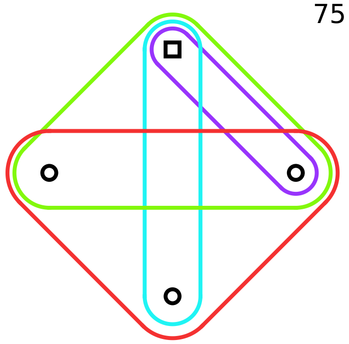

76

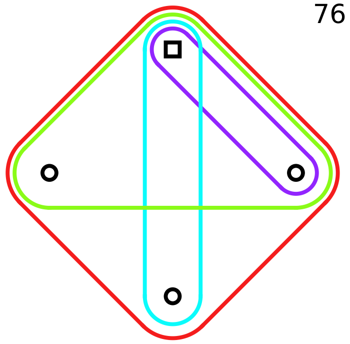

77

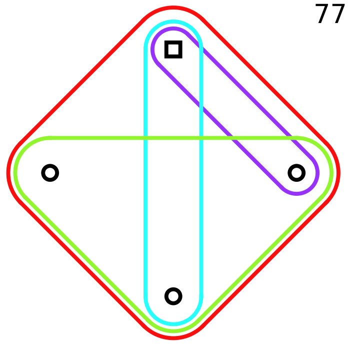

78

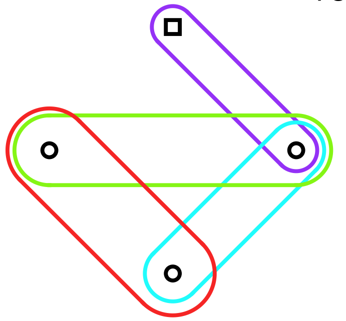

79

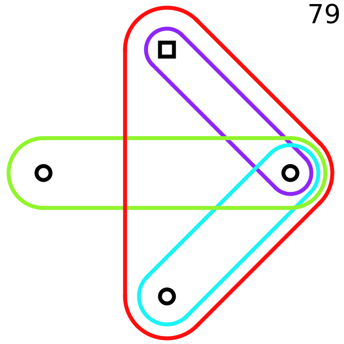

80

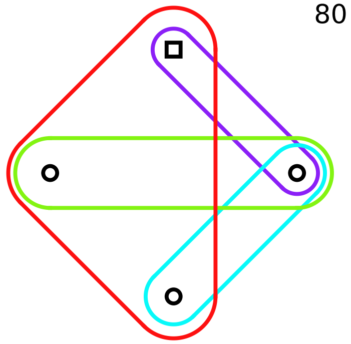

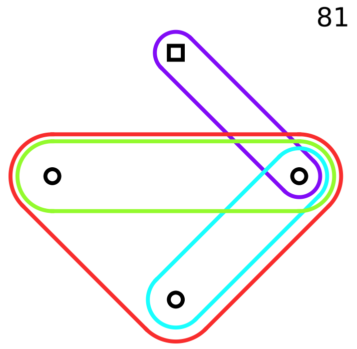
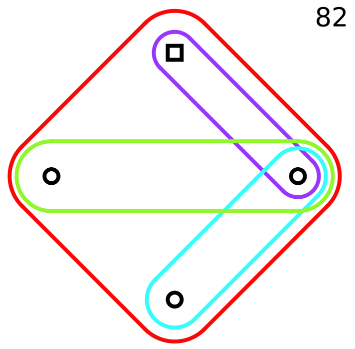
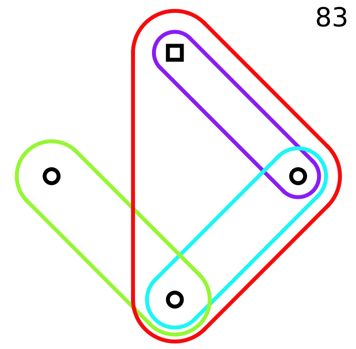
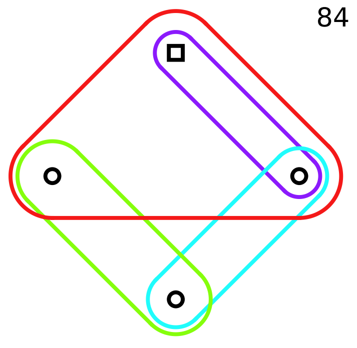
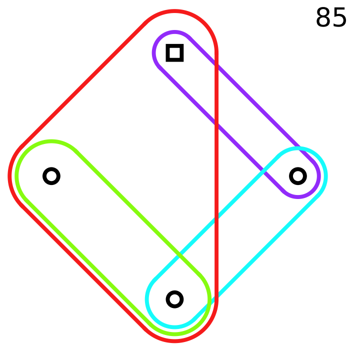
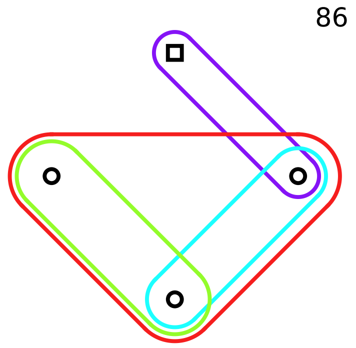
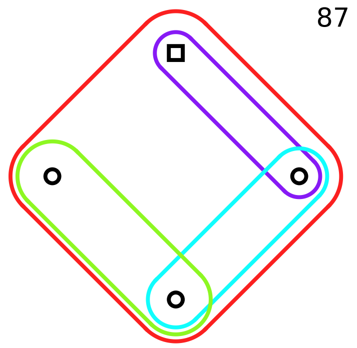
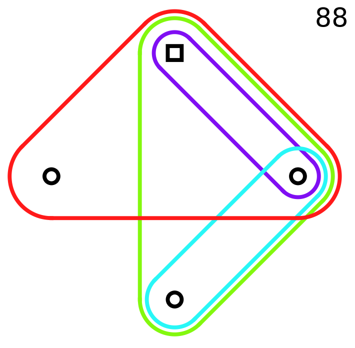
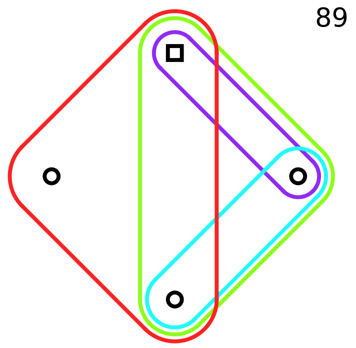
81
82
83
84
85
86
87
88
89

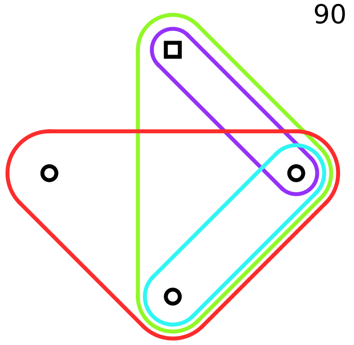
90
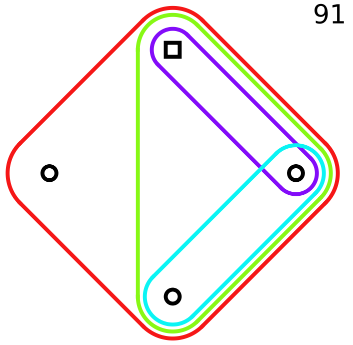
91
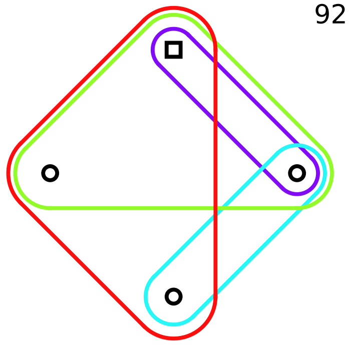
92
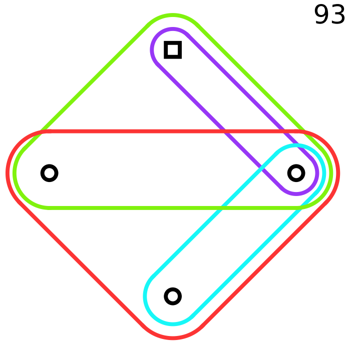
93
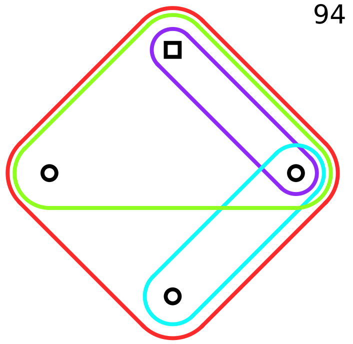
94
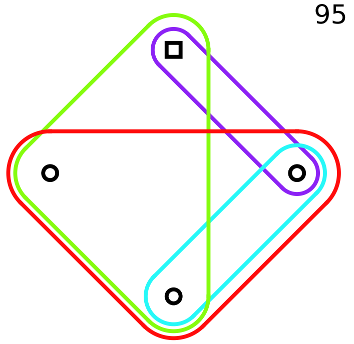
95
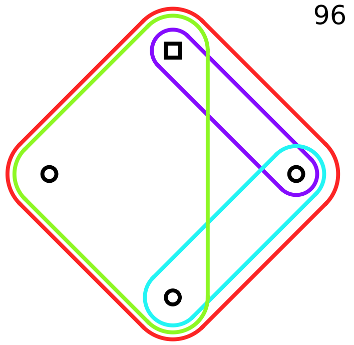
96
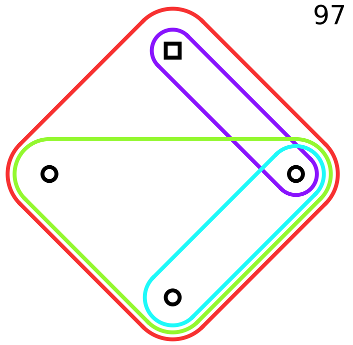
97
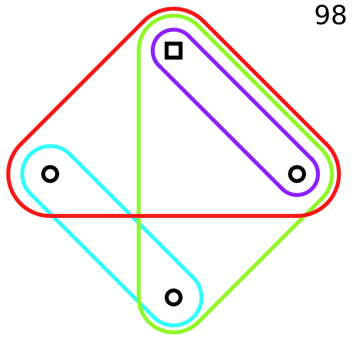
98

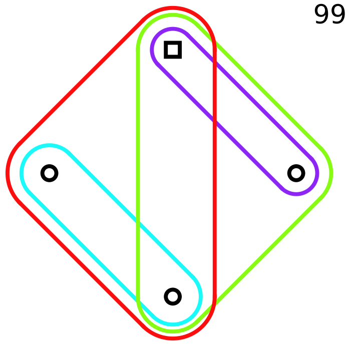
99

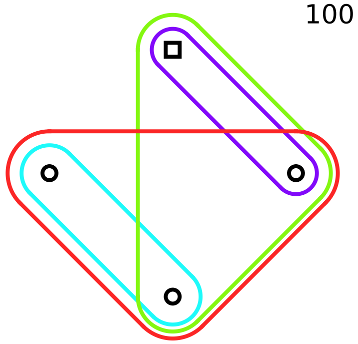
100

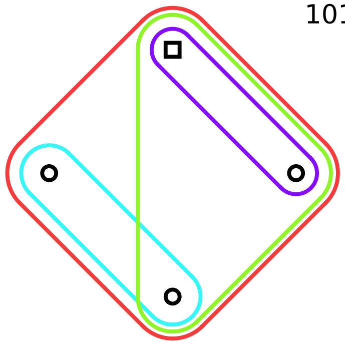
101

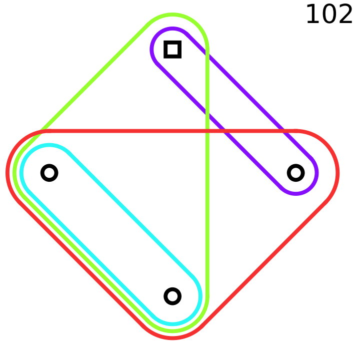
102

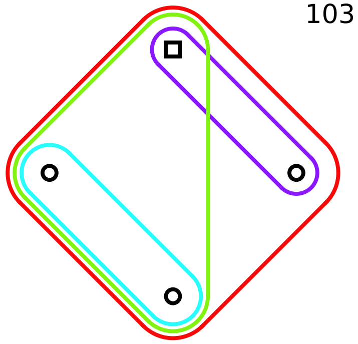
103

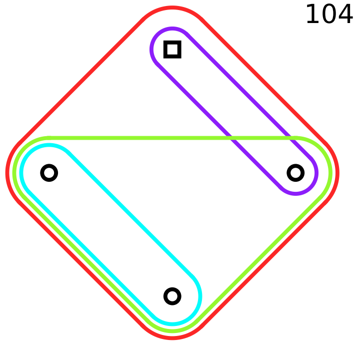
104

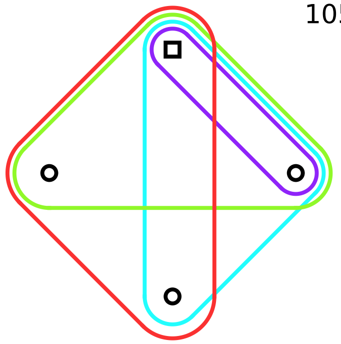
105

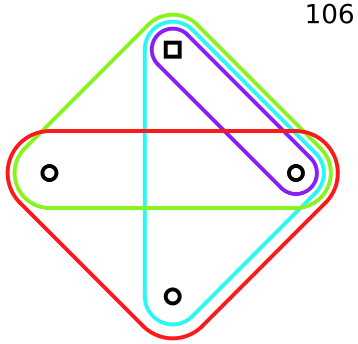
106

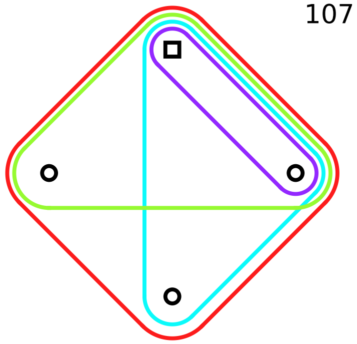
107

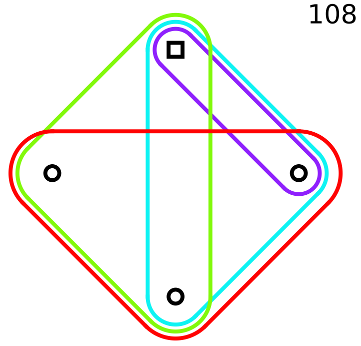
108

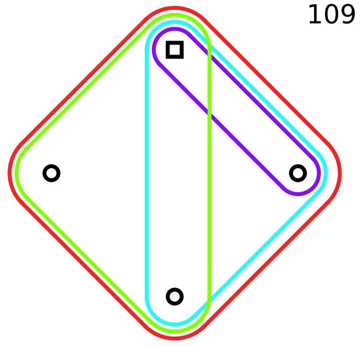
109

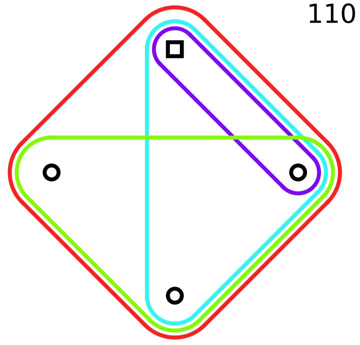
110

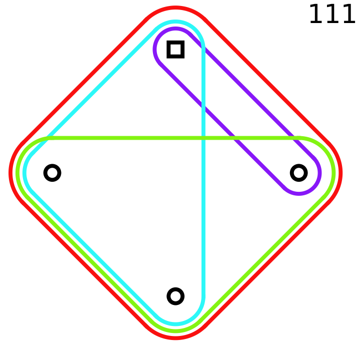
111

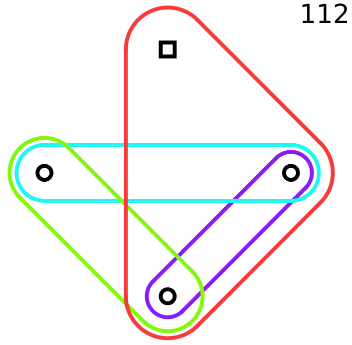
112

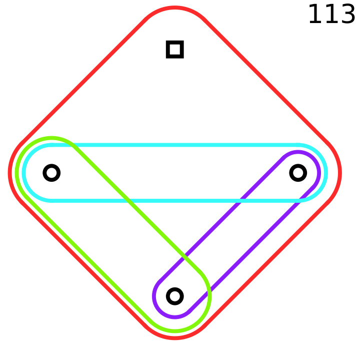
113

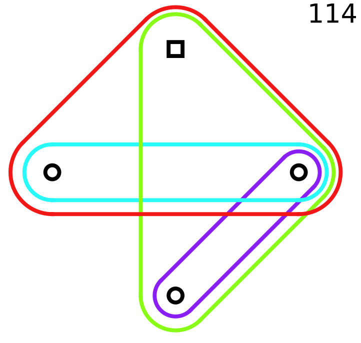
114

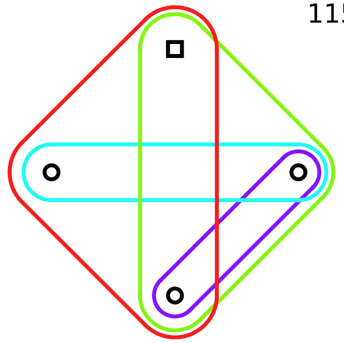
115

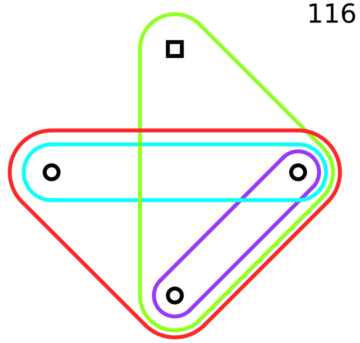
116

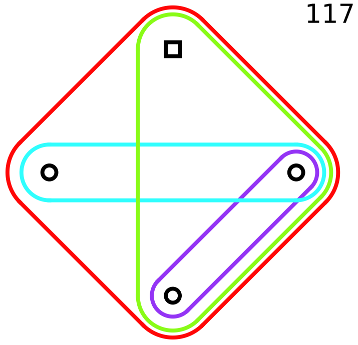
117

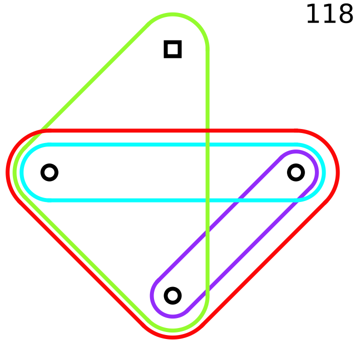
118

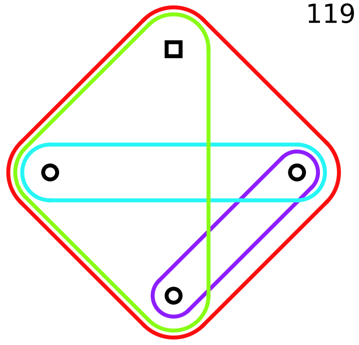
119

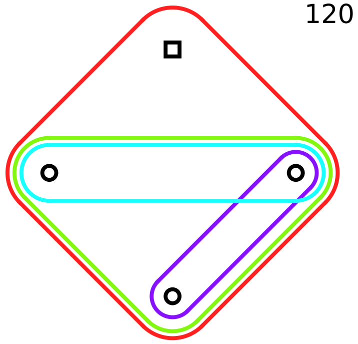
120

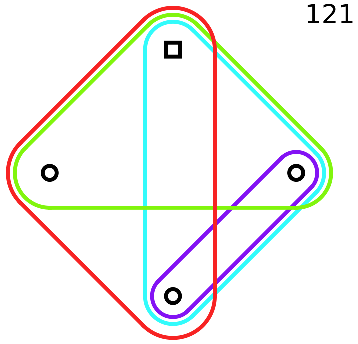
121

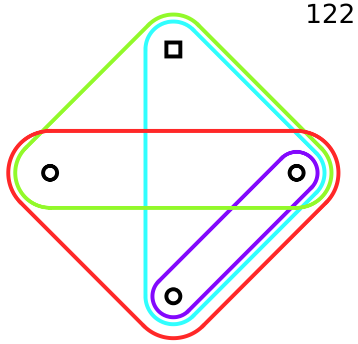
122

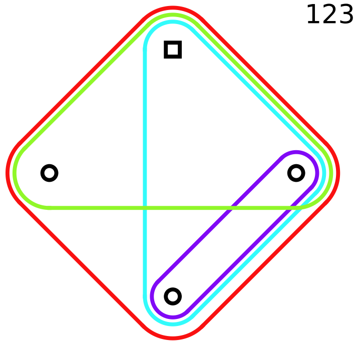
123

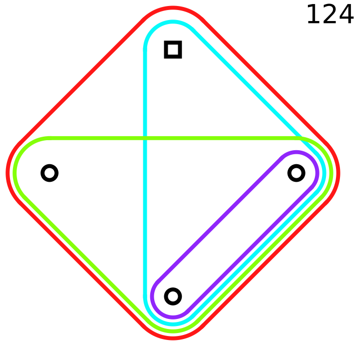
124

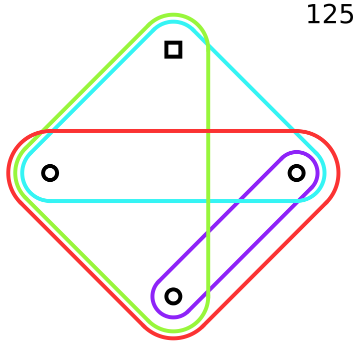
125

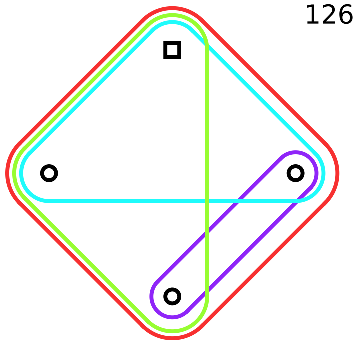
126

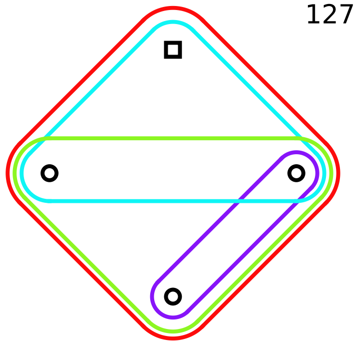
127

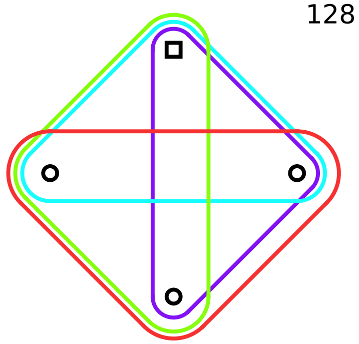
128

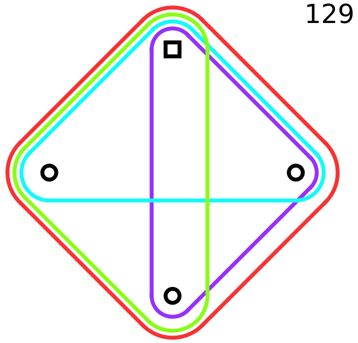
129

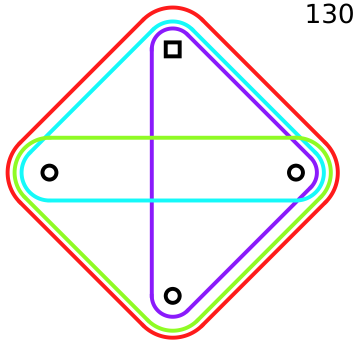
130

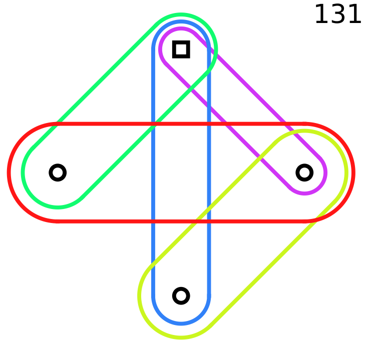
131

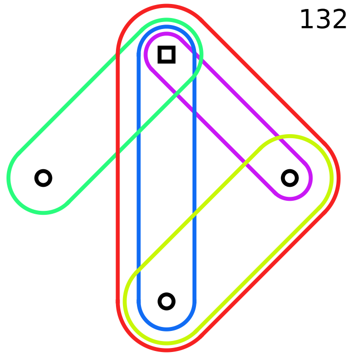
132

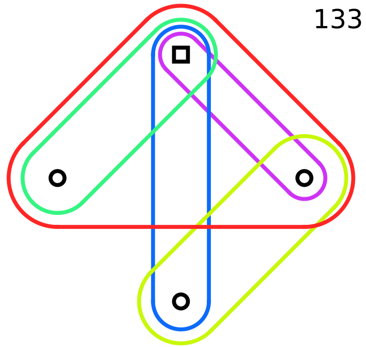
133

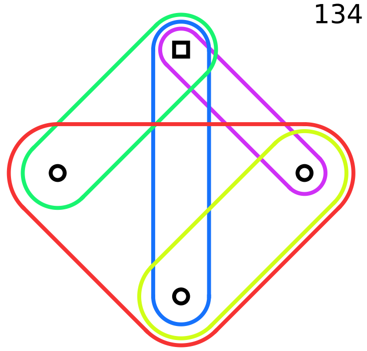
134

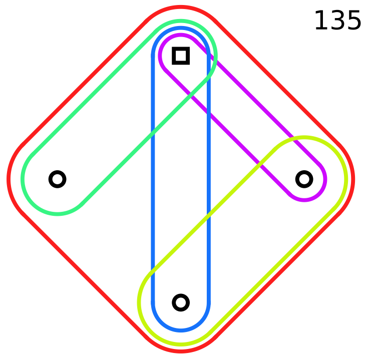
135

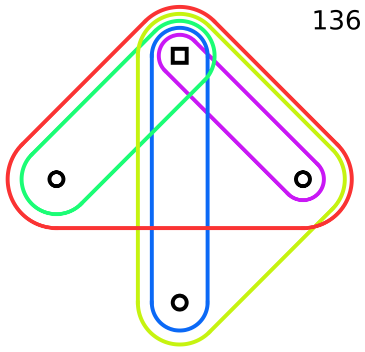
136

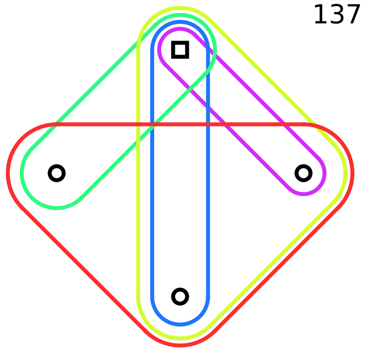
137

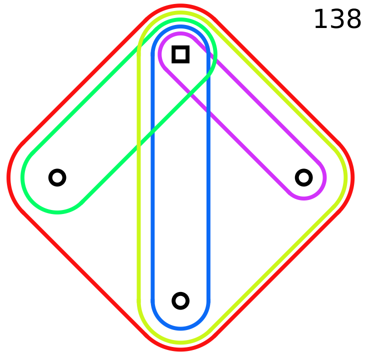
138

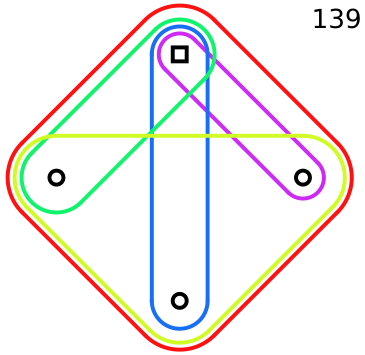
139

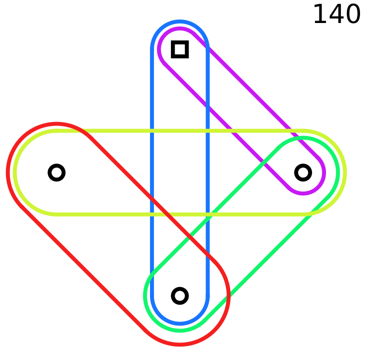
140

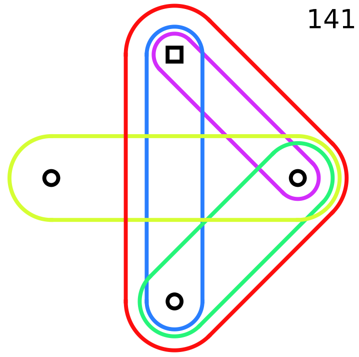
141

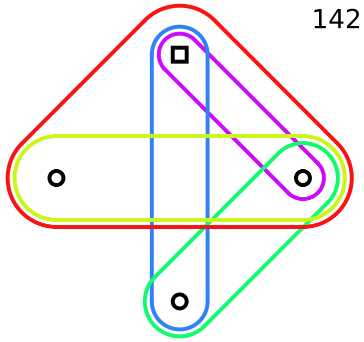
142

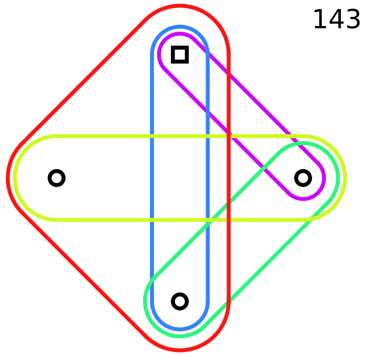
143

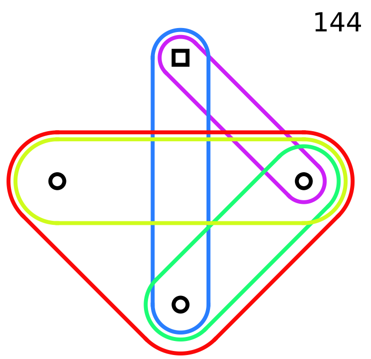
144

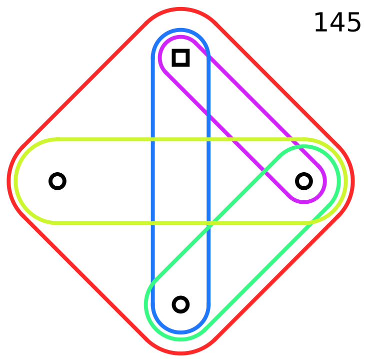
145

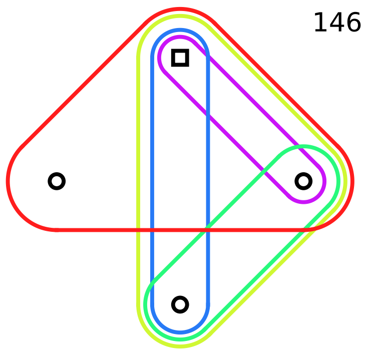
146

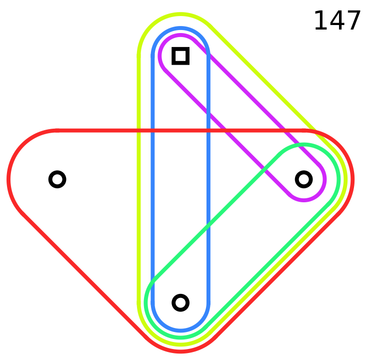
147

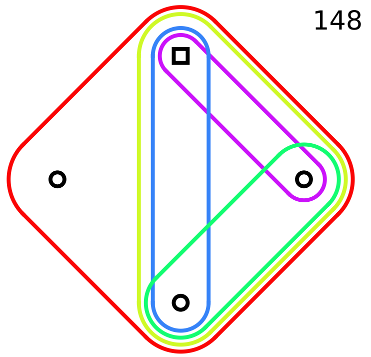
148

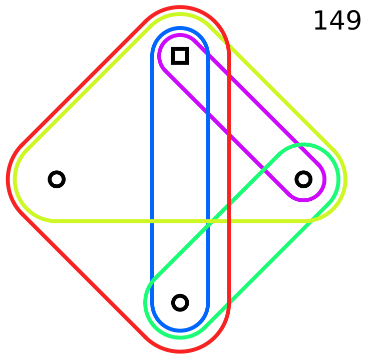
149

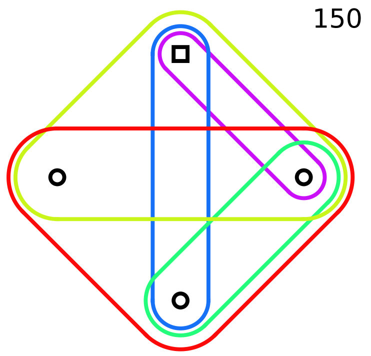
150

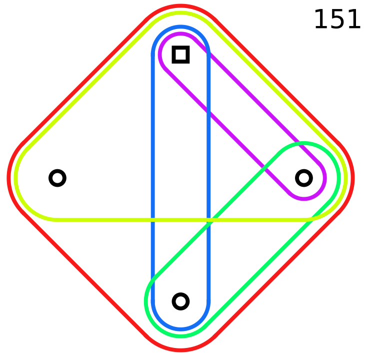
151

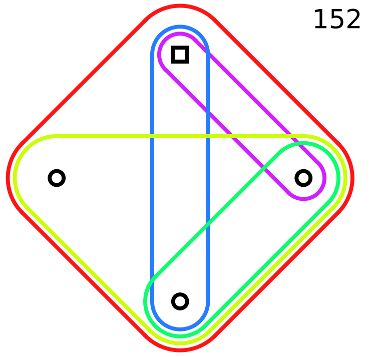
152

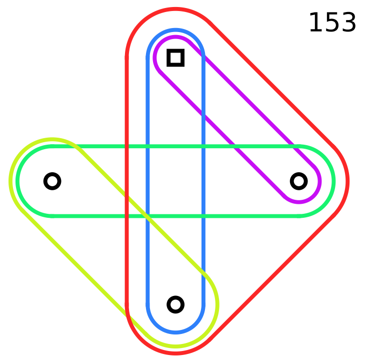
153

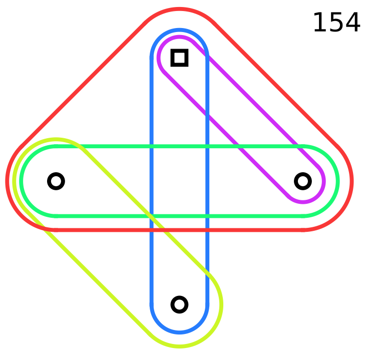
154

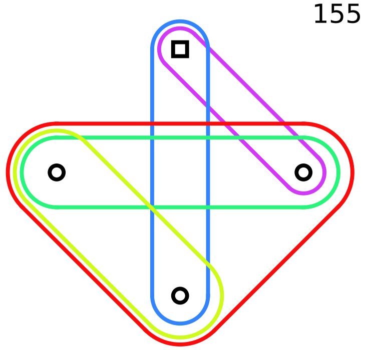
155

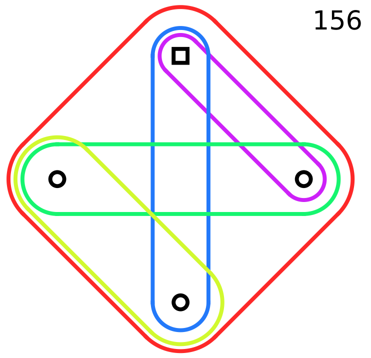
156

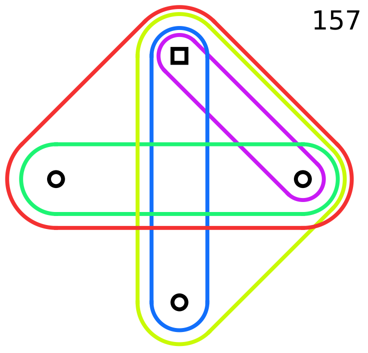
157

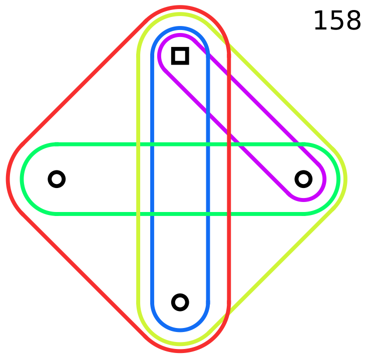
158

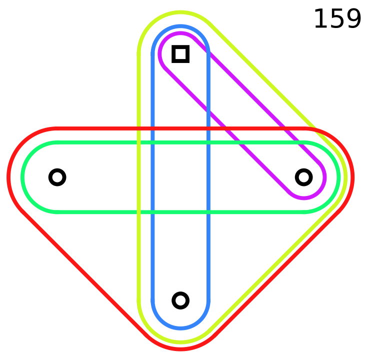
159

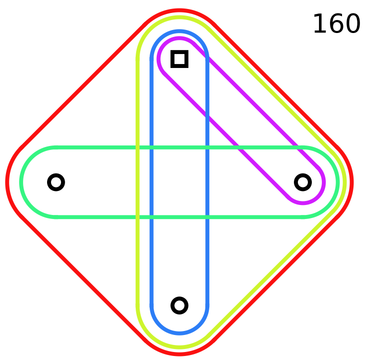
160

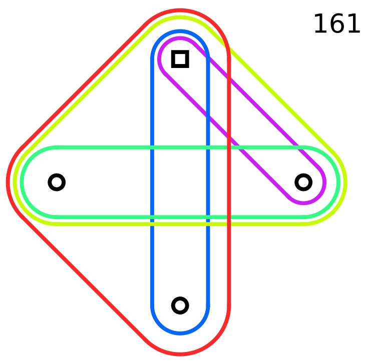
161

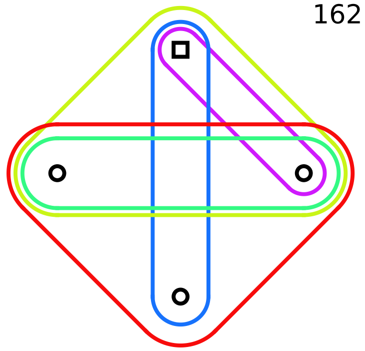
162

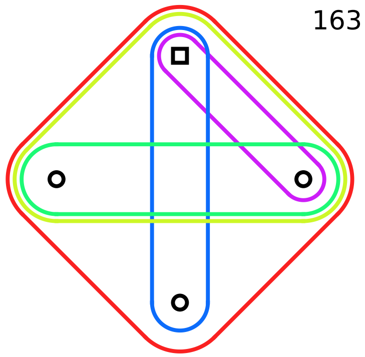
163

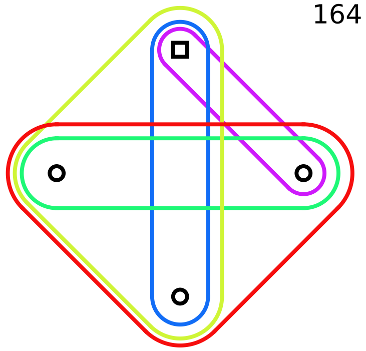
164

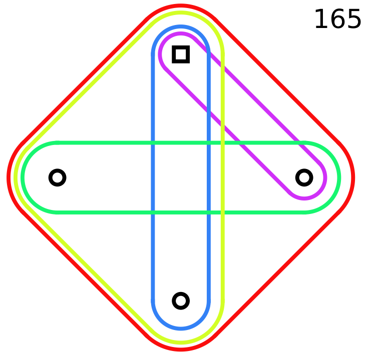
165

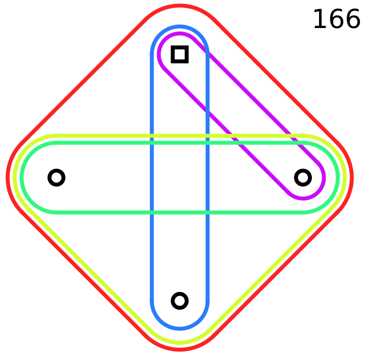
166

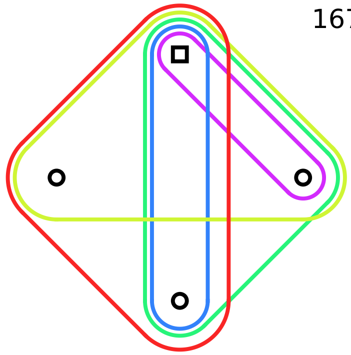
167

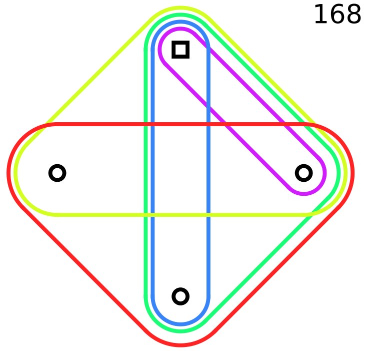
168

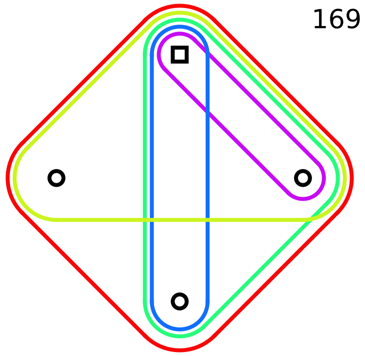
169

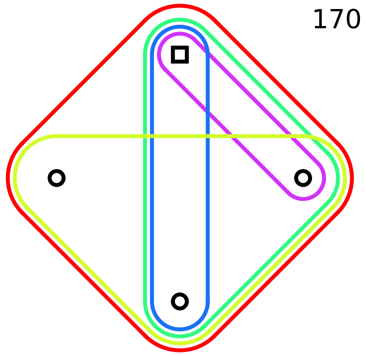
170

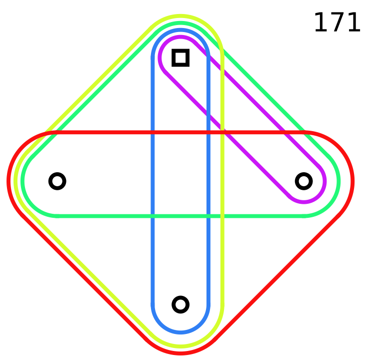
171

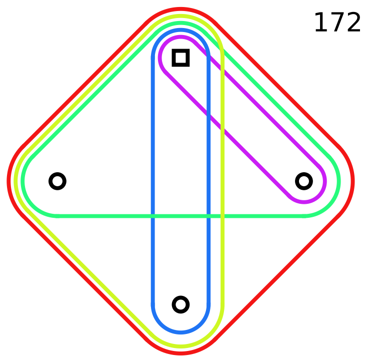
172

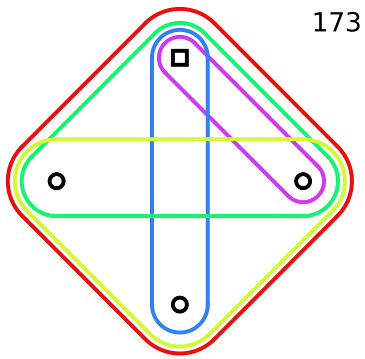
173

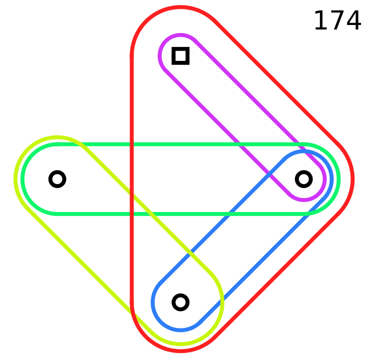
174

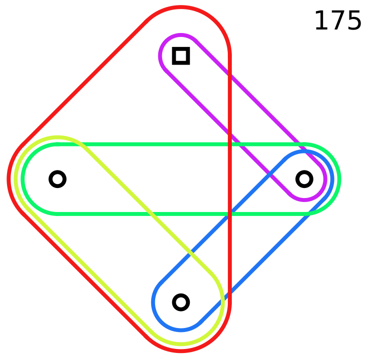
175

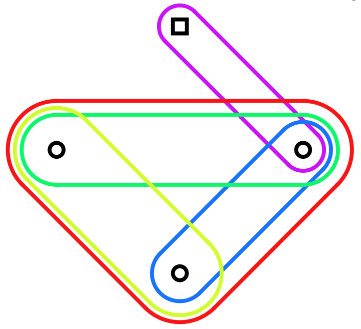
176

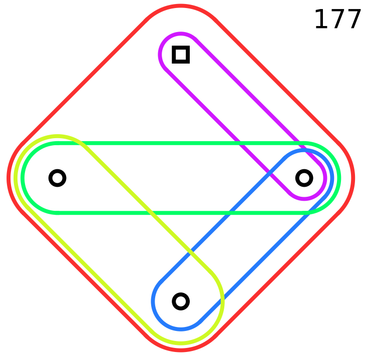
177

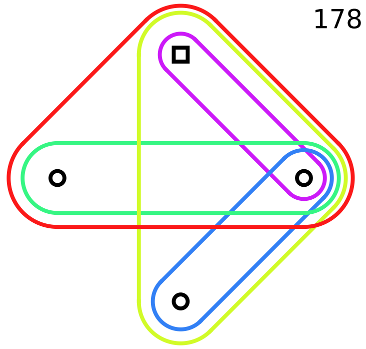
178

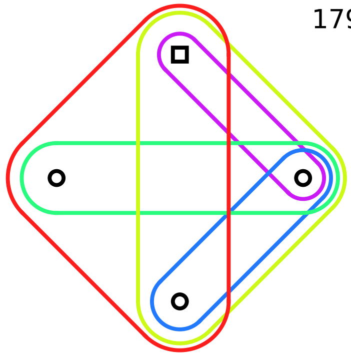
179

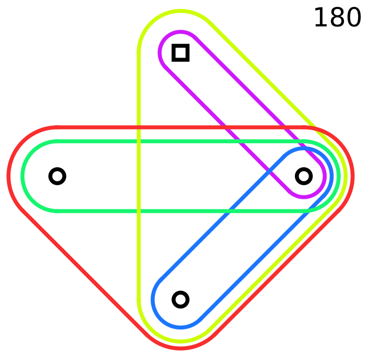
180

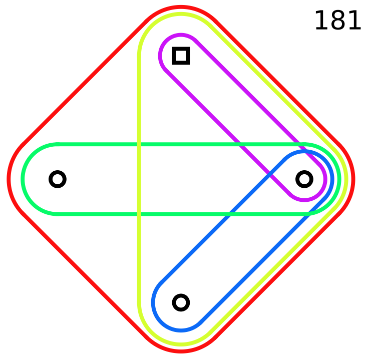
181

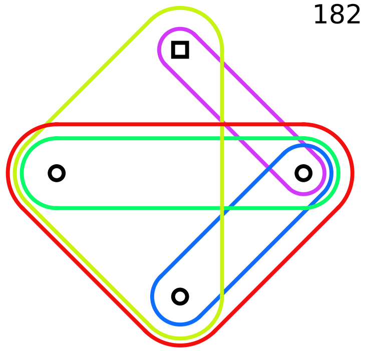
182

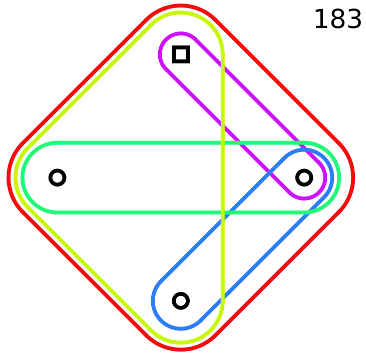
183

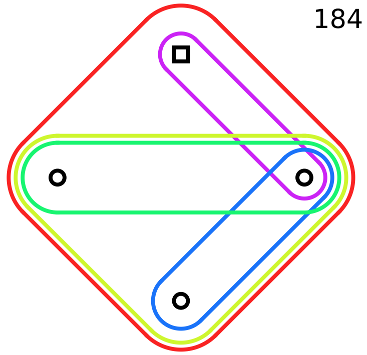
184

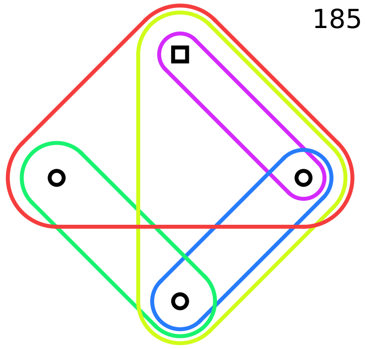
185

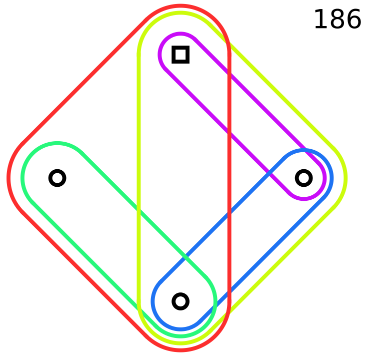
186

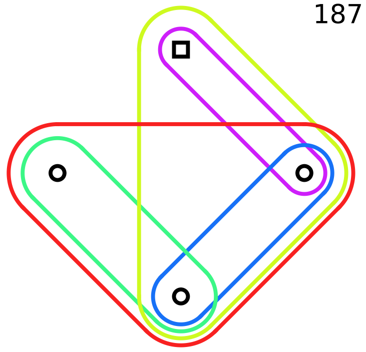
187

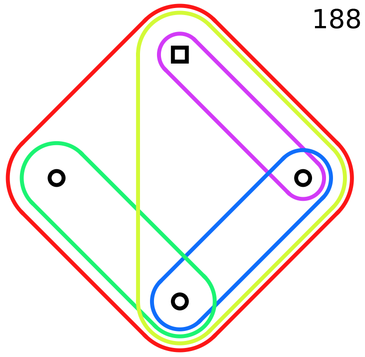
188

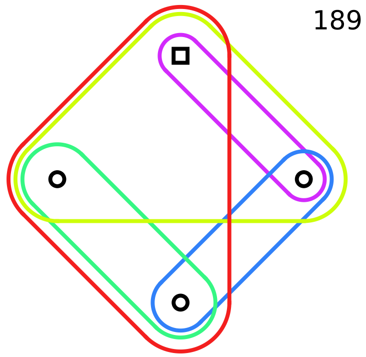
189

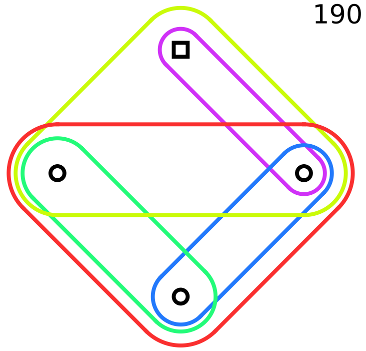
190

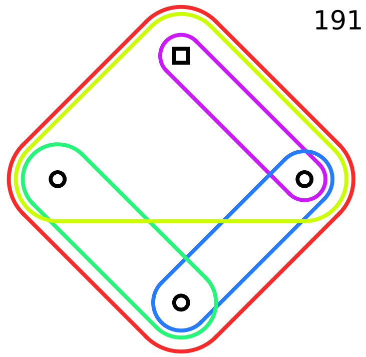
191

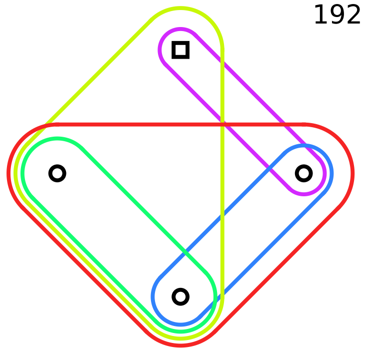
192

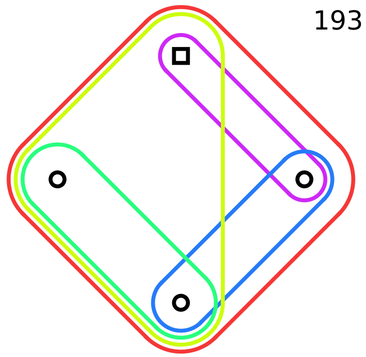
193

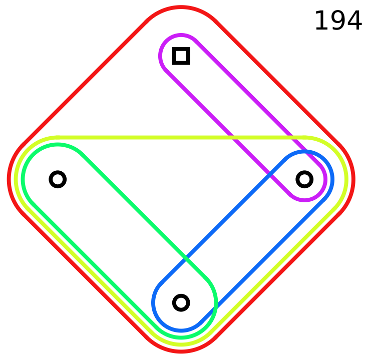
194

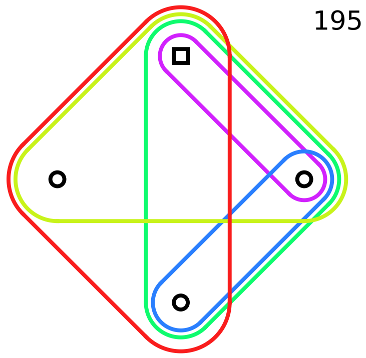
195

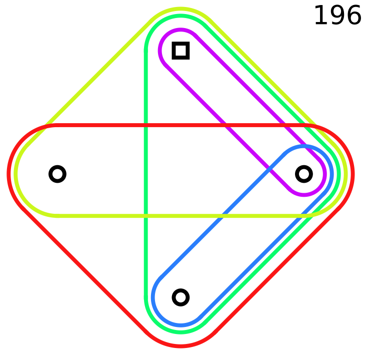
196

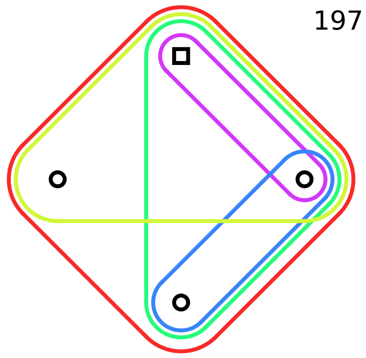
197

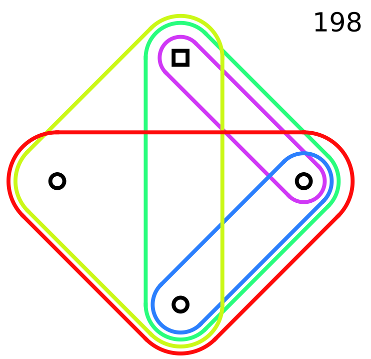
198

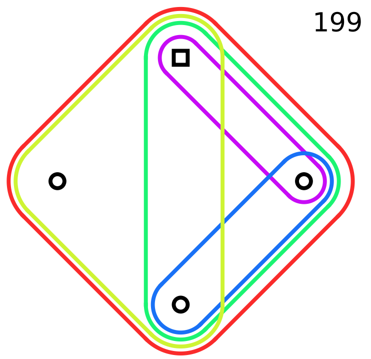
199

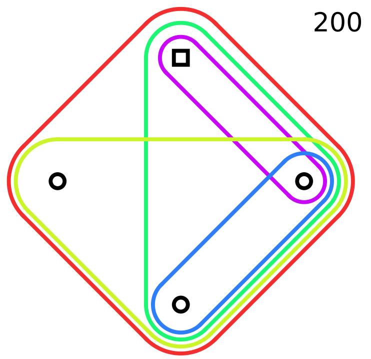
200

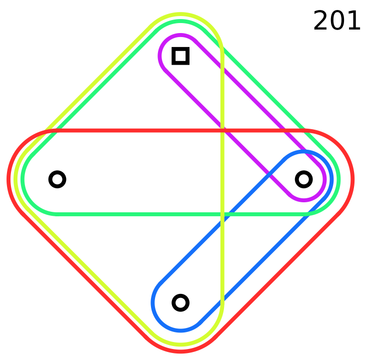
201

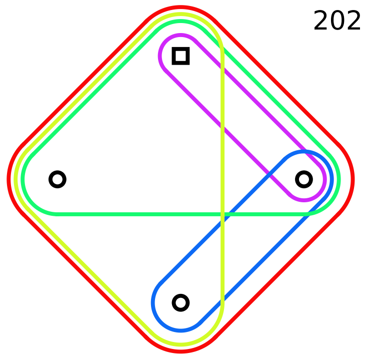
202

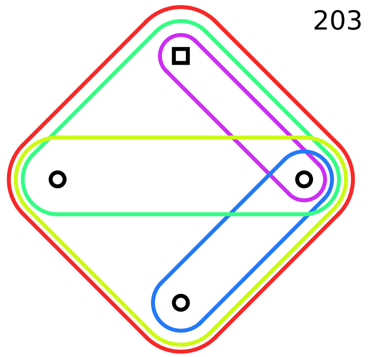
203

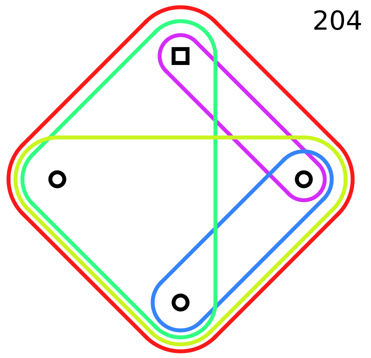
204

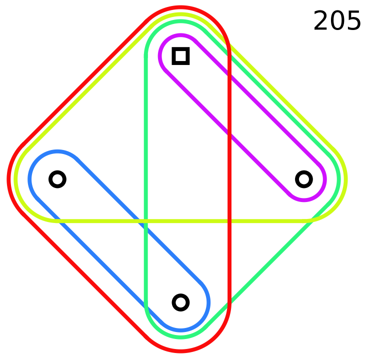
205

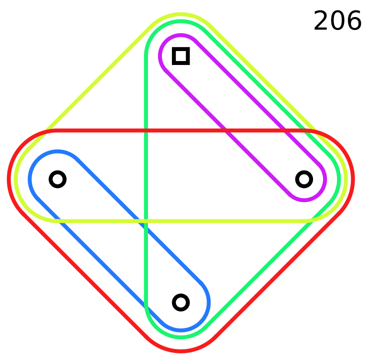
206

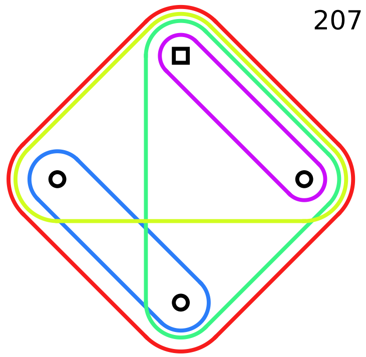
207

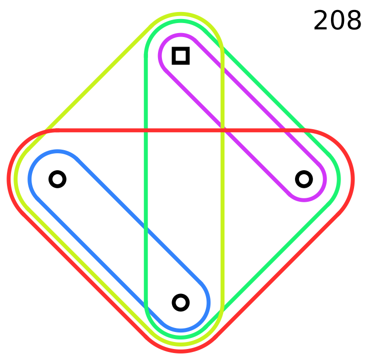
208

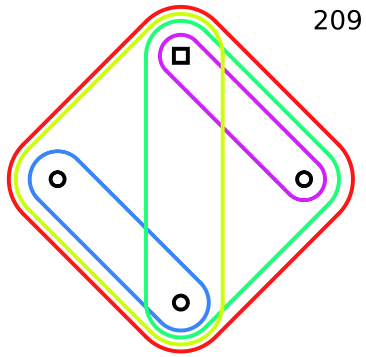
209

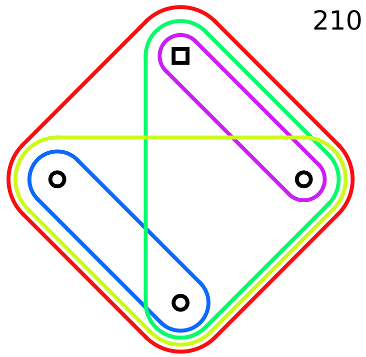
210

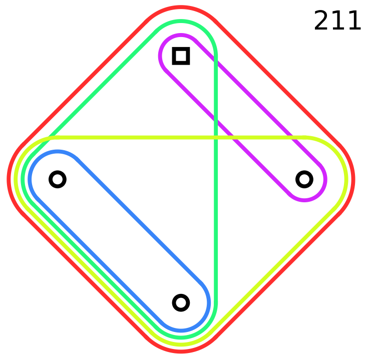
211

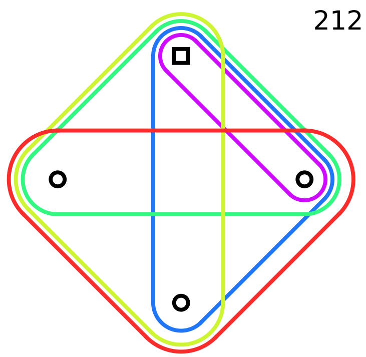
212

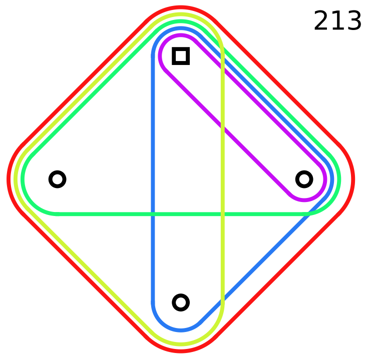
213

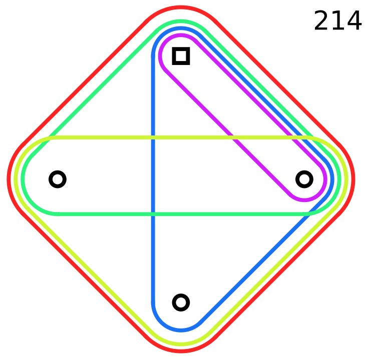
214

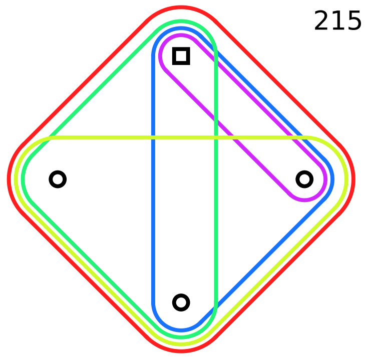
215

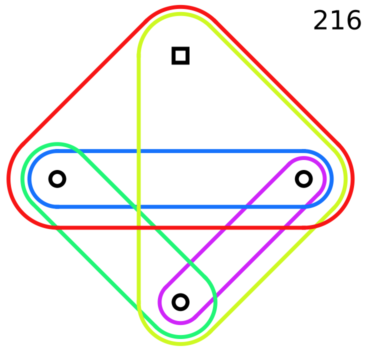
216

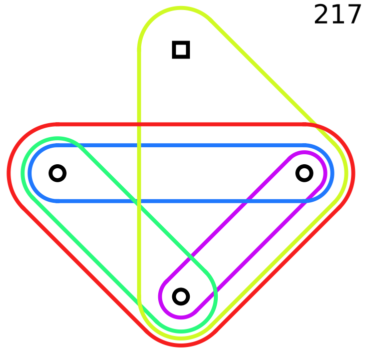
217

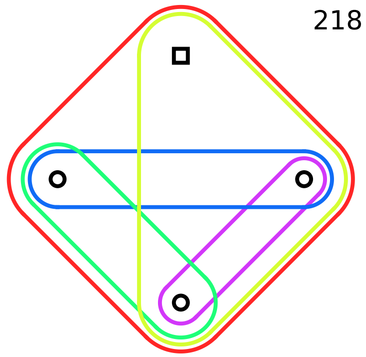
218

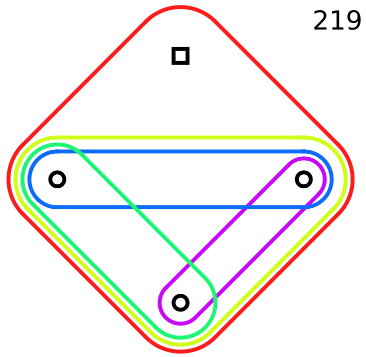
219

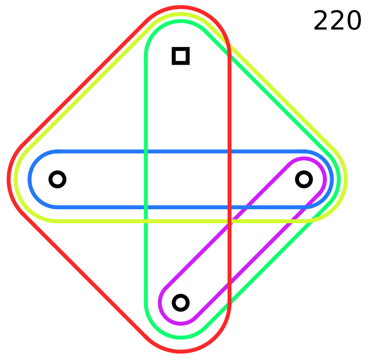
220

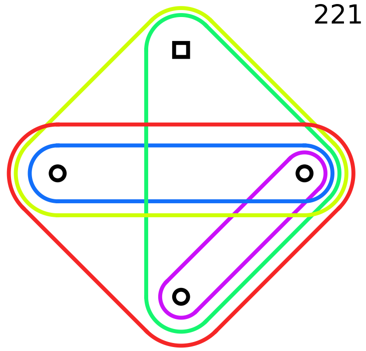
221

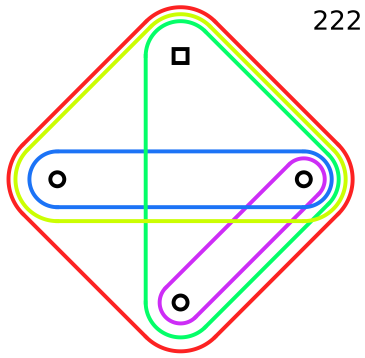
222

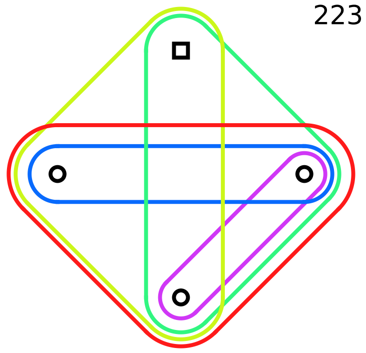
223

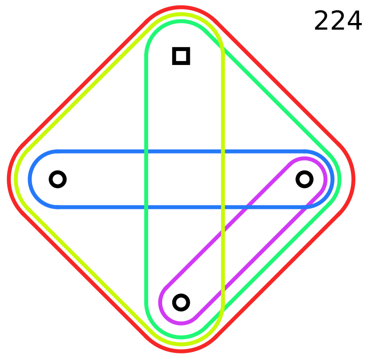
224

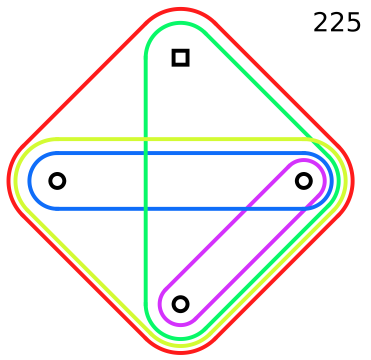
225
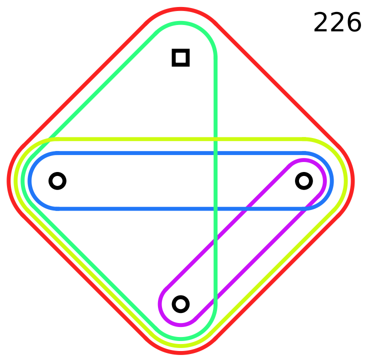
226
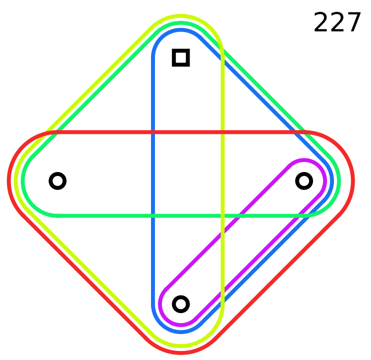
227
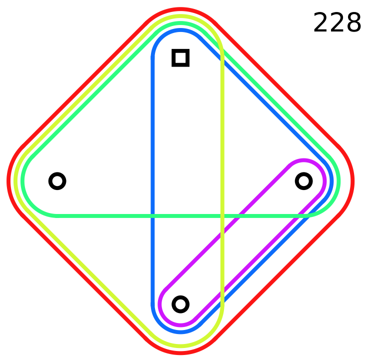
228
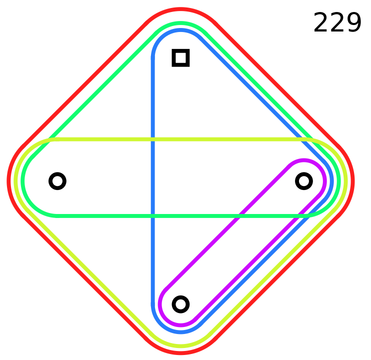
229
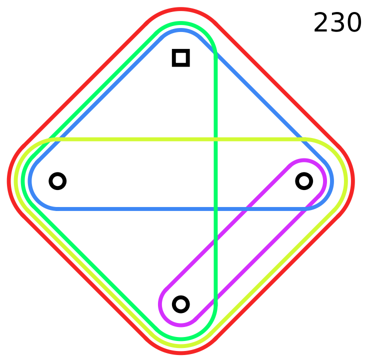
230
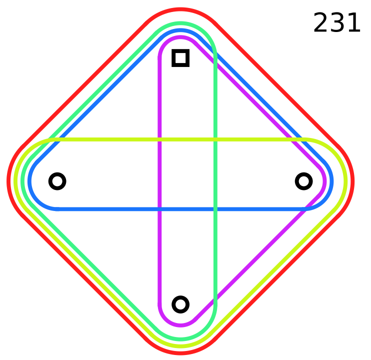
231
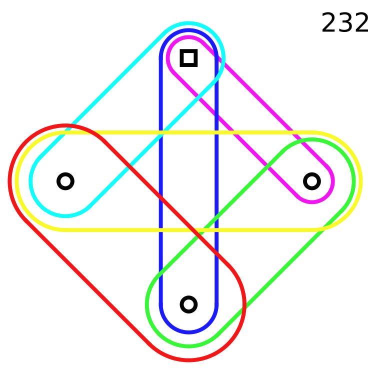
232
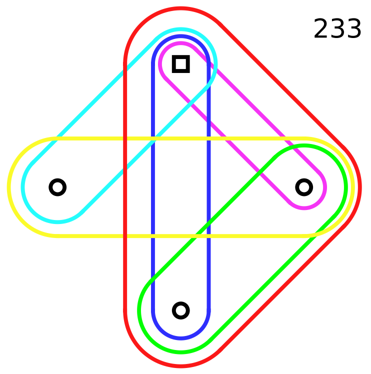
233

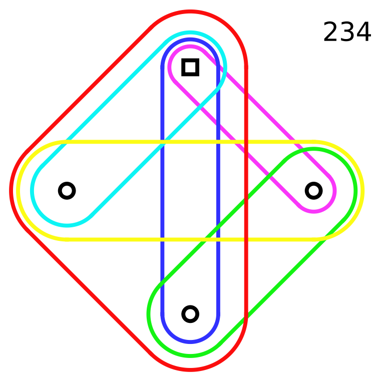
234

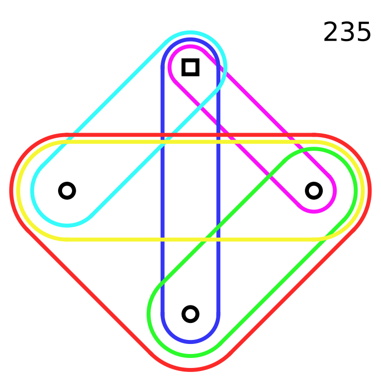
235

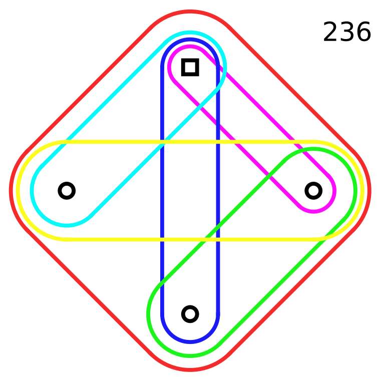
236

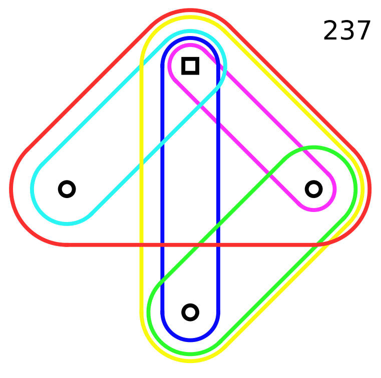
237

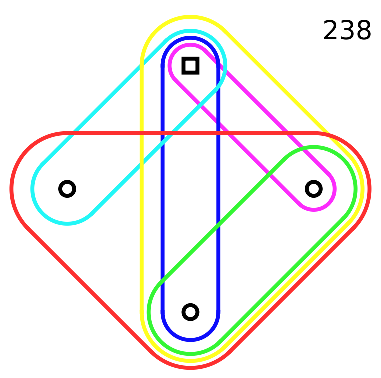
238

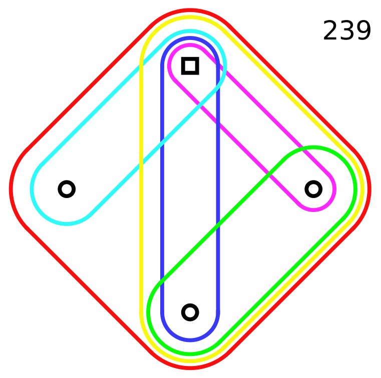
239

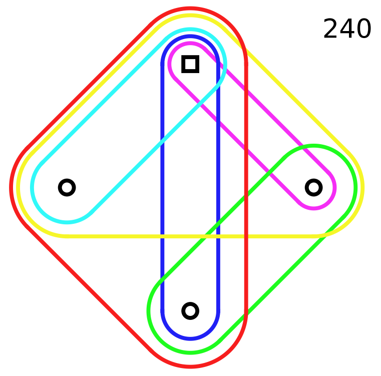
240

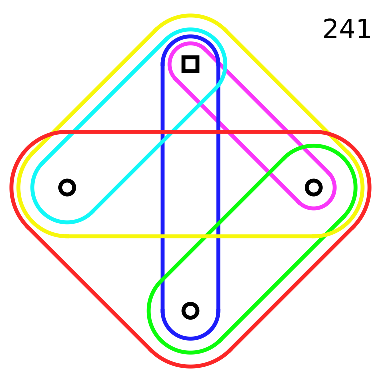
241

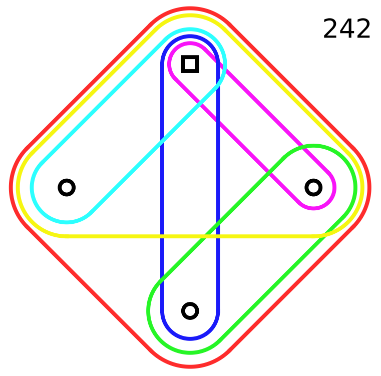
242

243
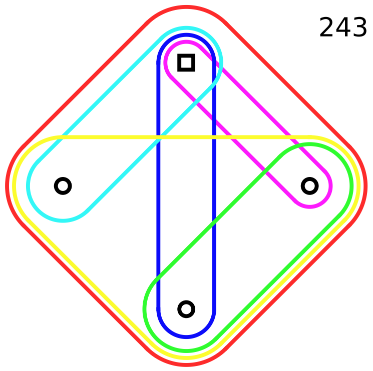

244
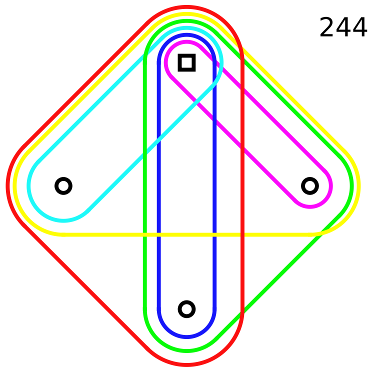

245
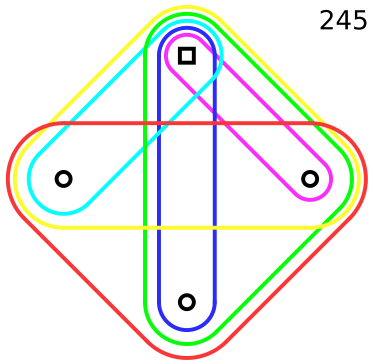

246
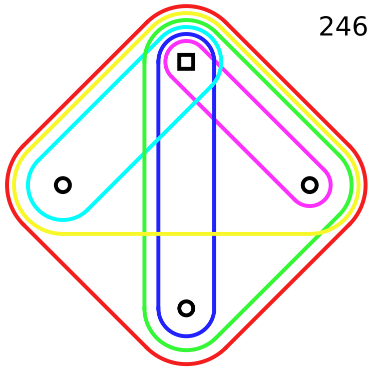

247
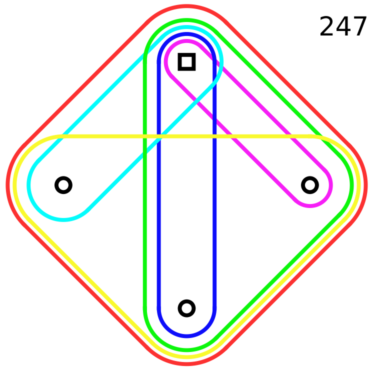

248
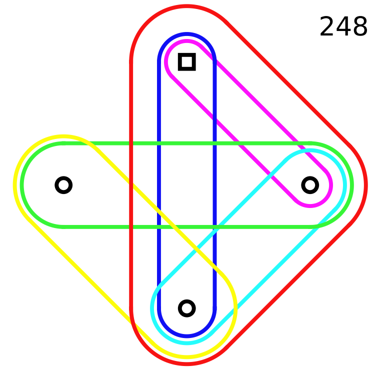

249
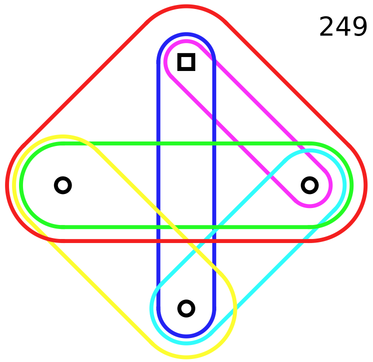

250
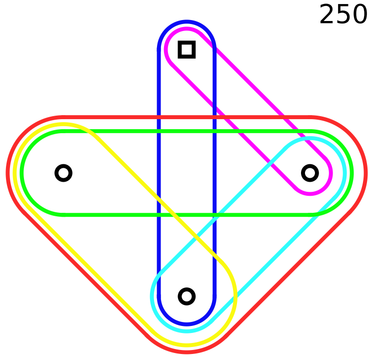

251
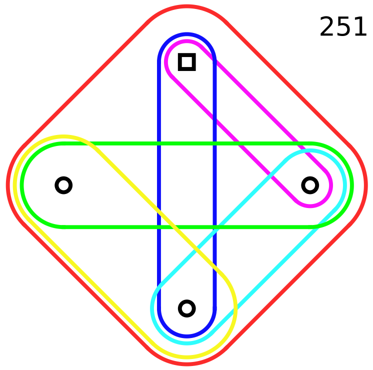

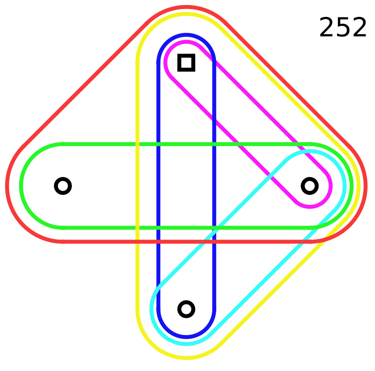
252

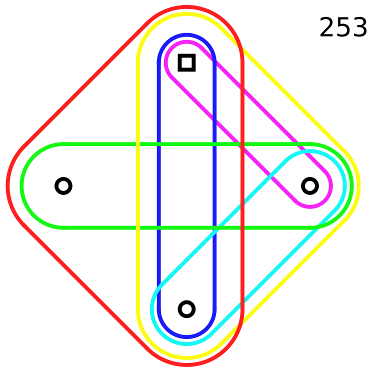
253

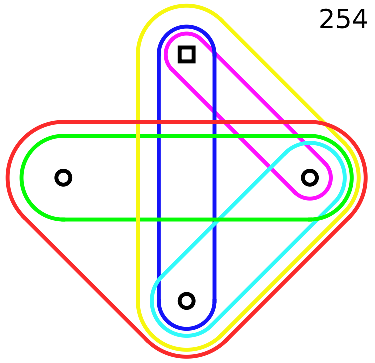
254

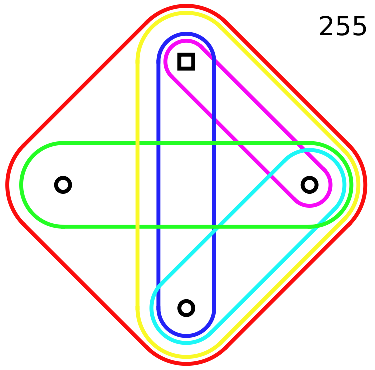
255

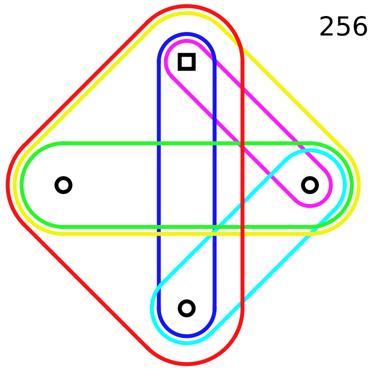
256

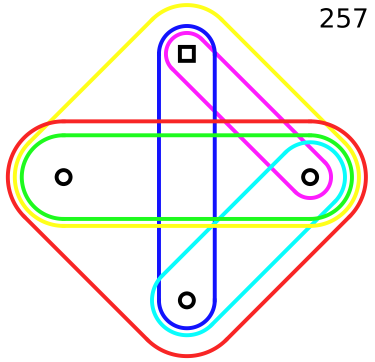
257

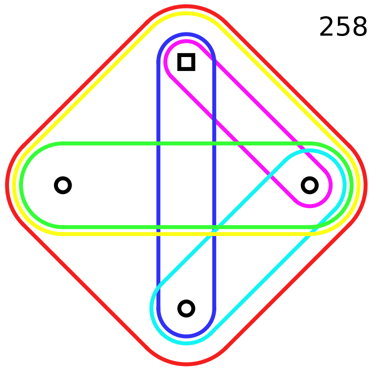
258

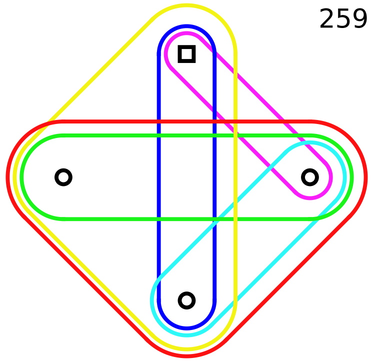
259

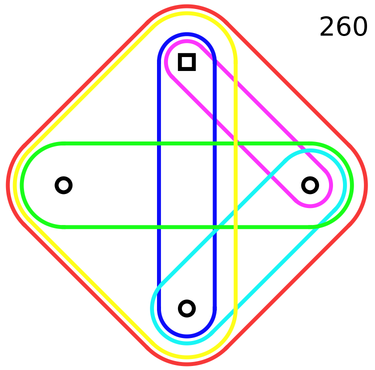
260

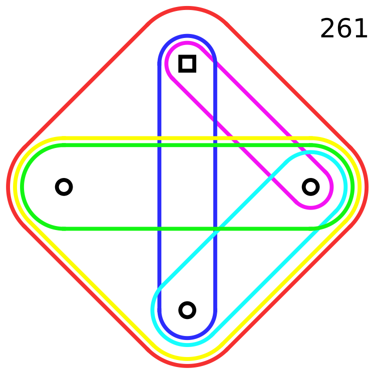
261

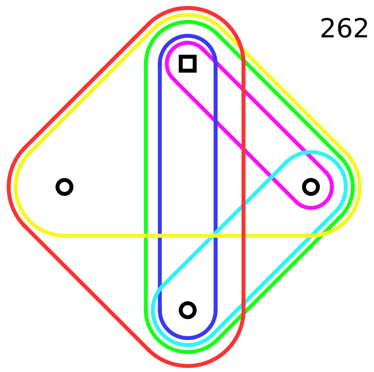
262

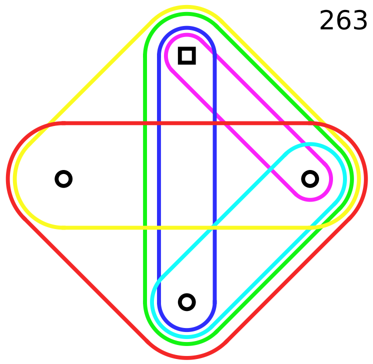
263

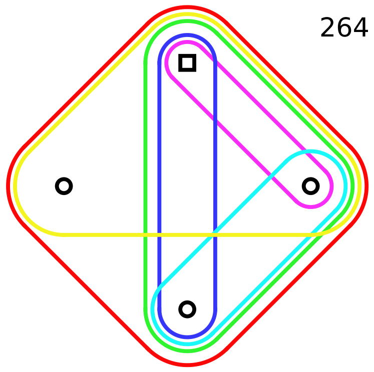
264

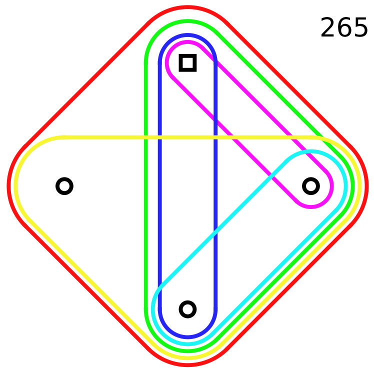
265

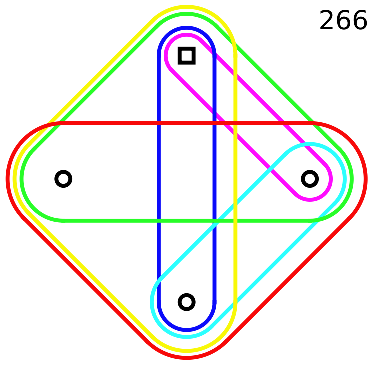
266

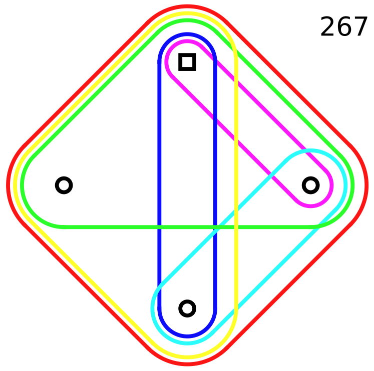
267

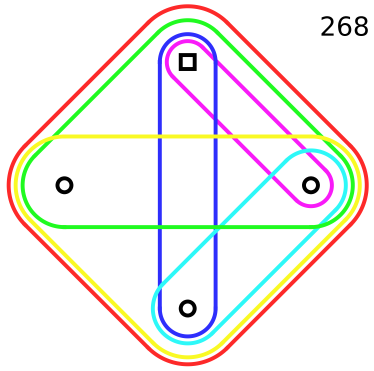
268

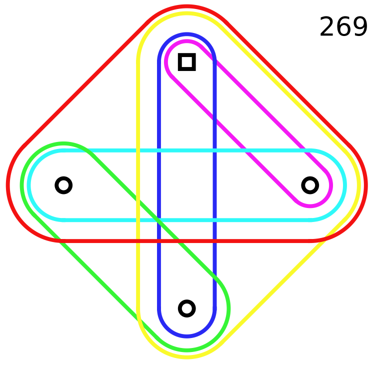
269

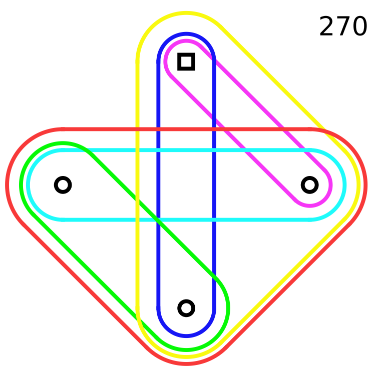
270

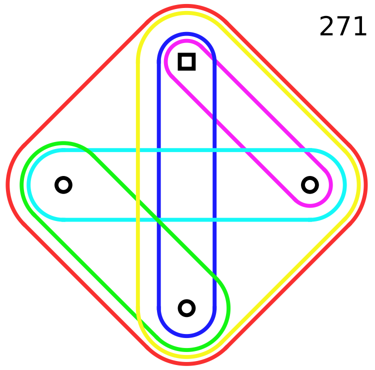
271

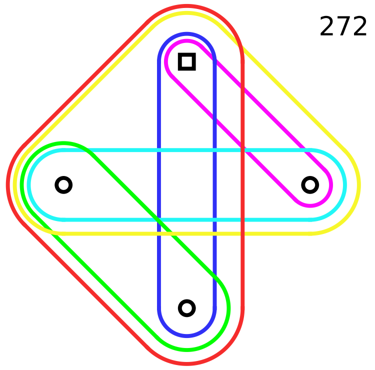
272

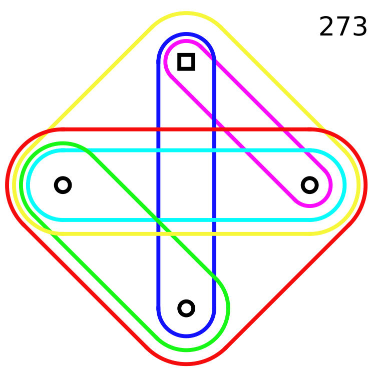
273

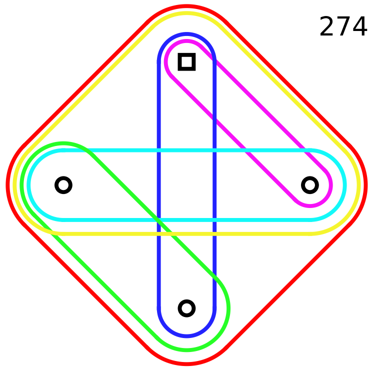
274

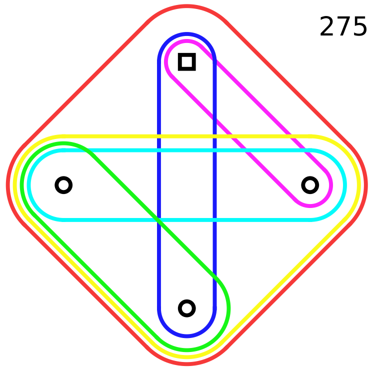
275

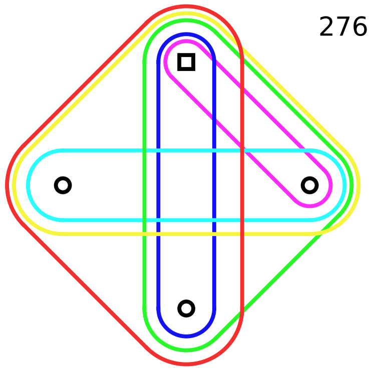
276

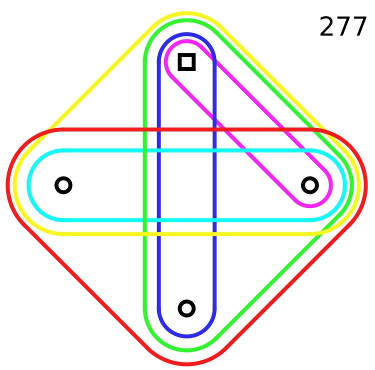
277

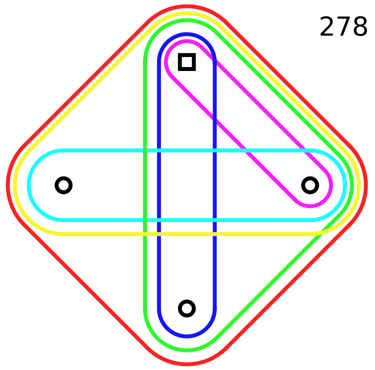
278

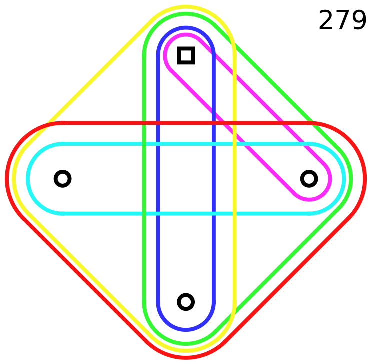
279

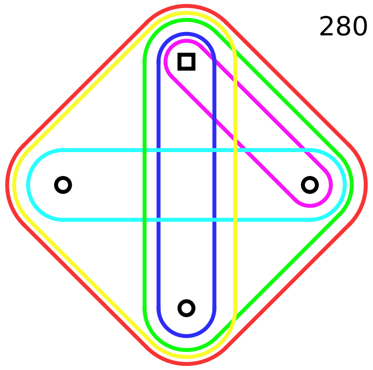
280

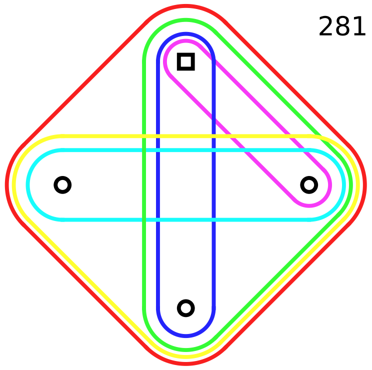
281

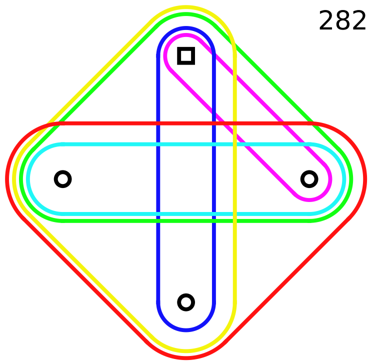
282

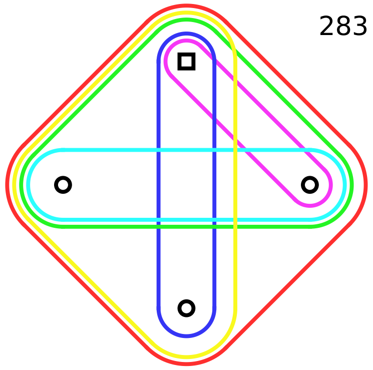
283

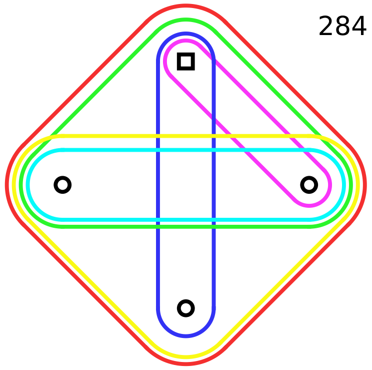
284

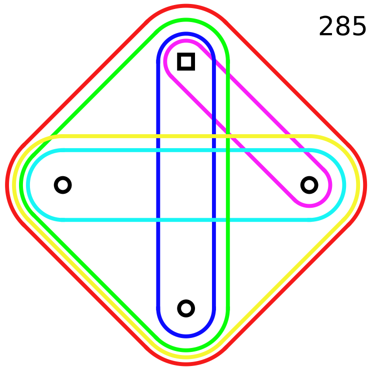
285

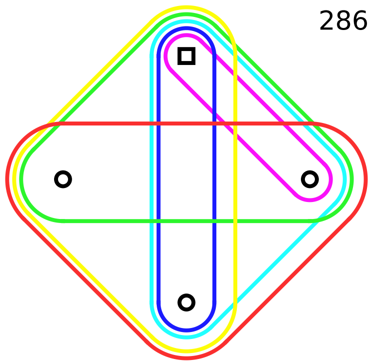
286

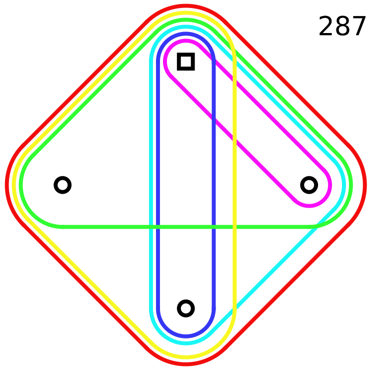
287

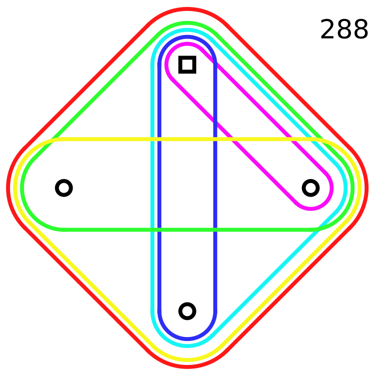
288

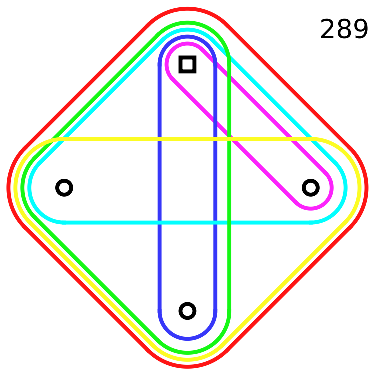
289

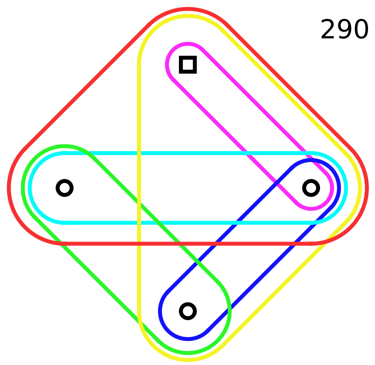
290

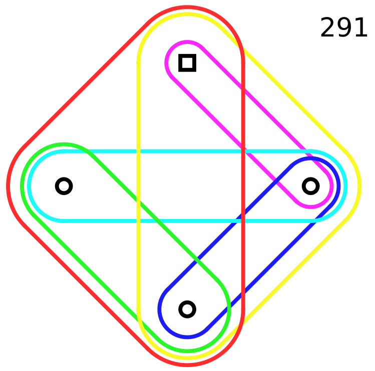
291

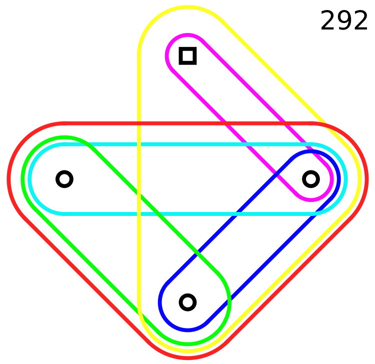
292

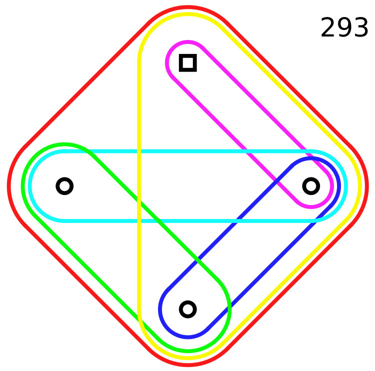
293

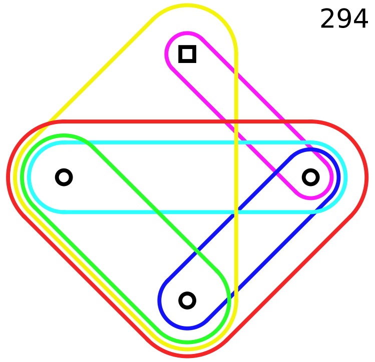
294

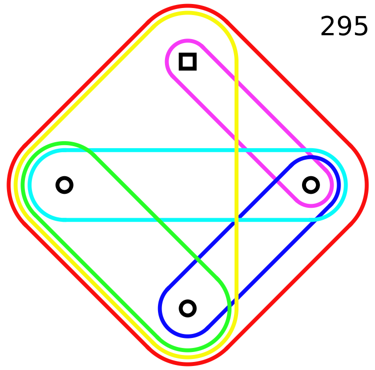
295

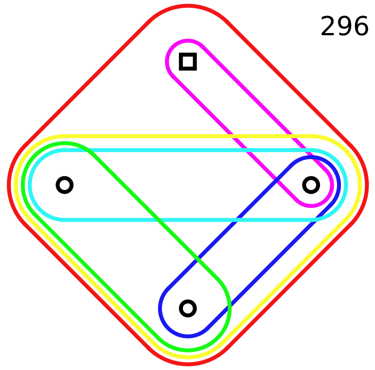
296

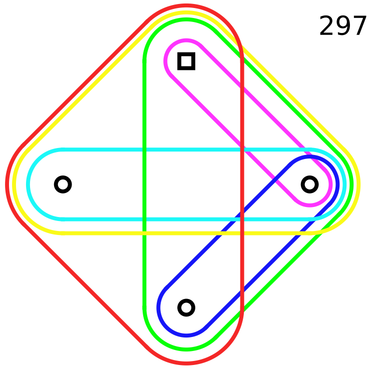
297

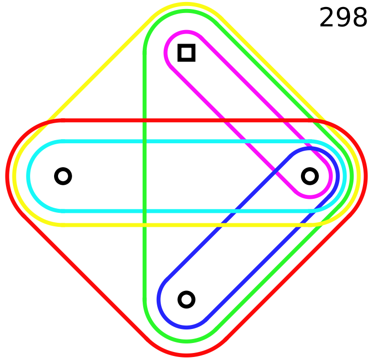
298

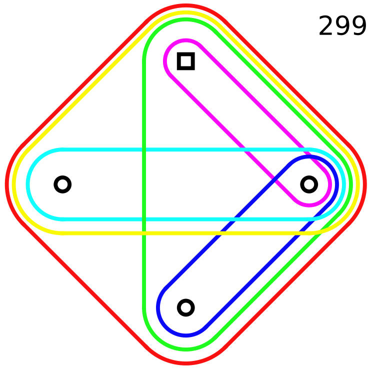
299

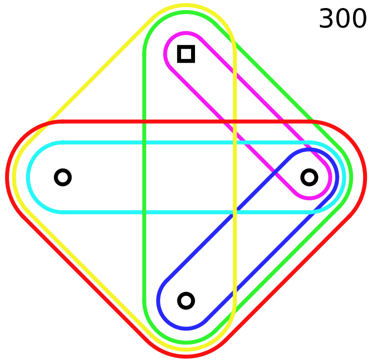
300

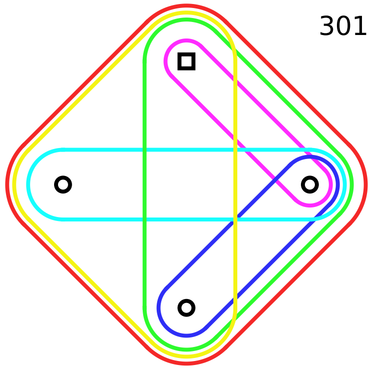
301

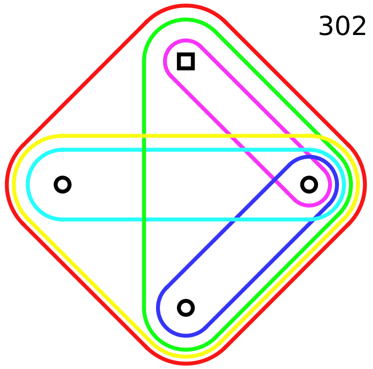
302

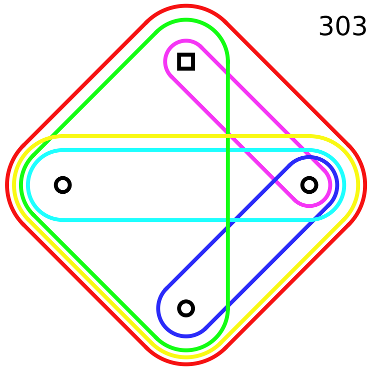
303

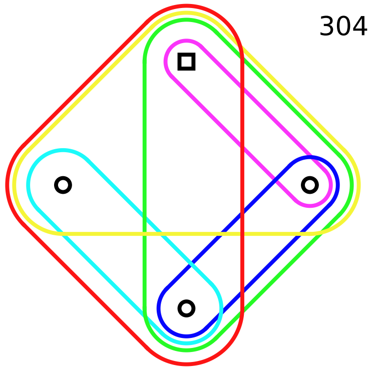
304

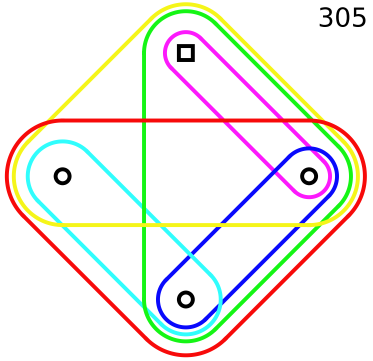
305

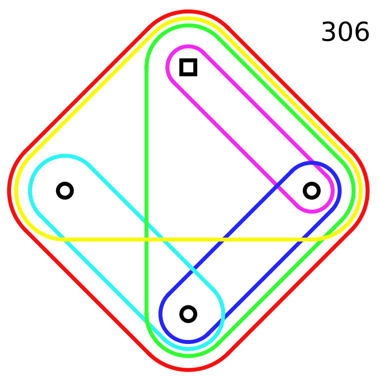
306

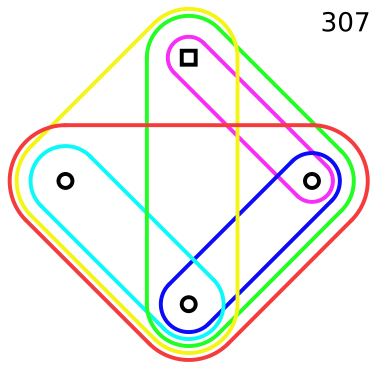
307

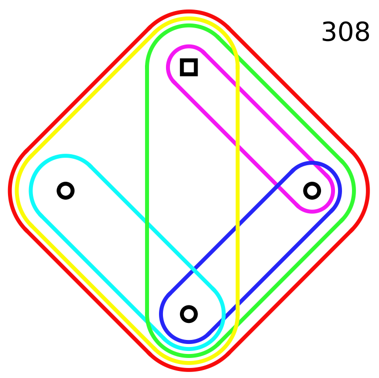
308

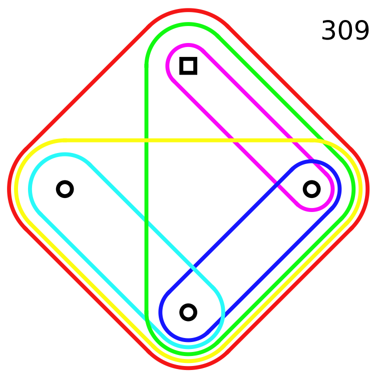
309

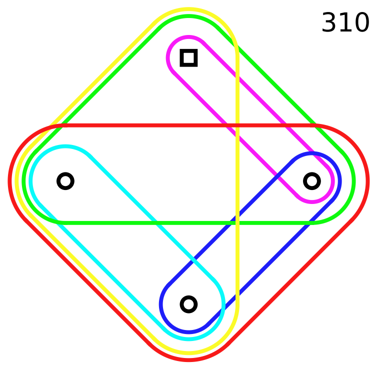
310

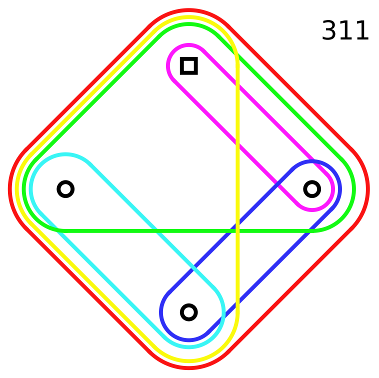
311

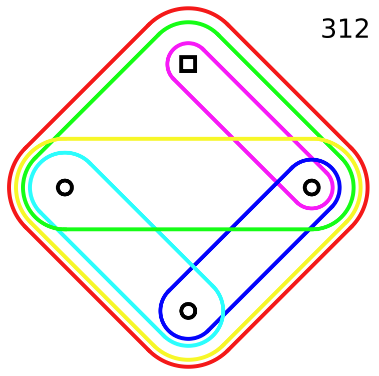
312

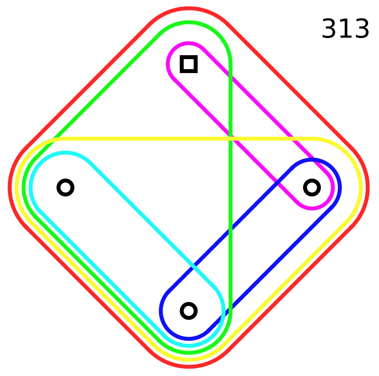
313

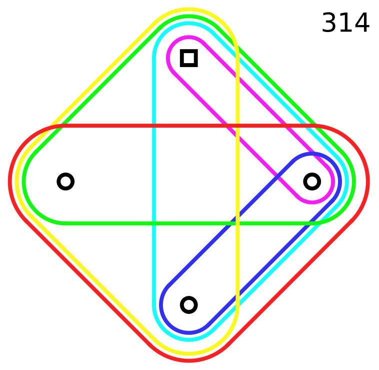
314

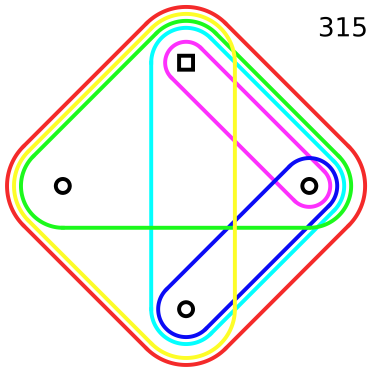
315

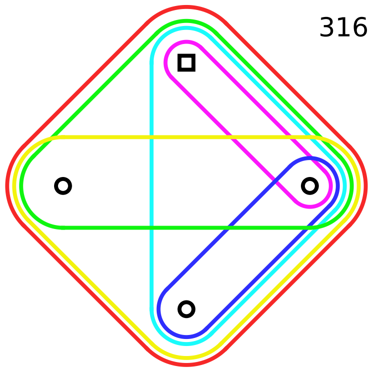
316

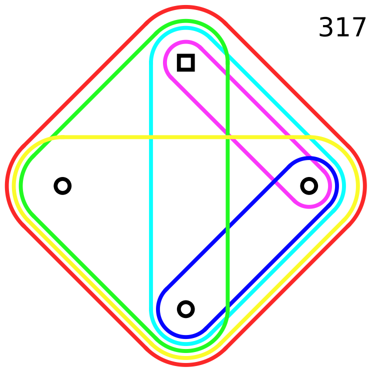
317

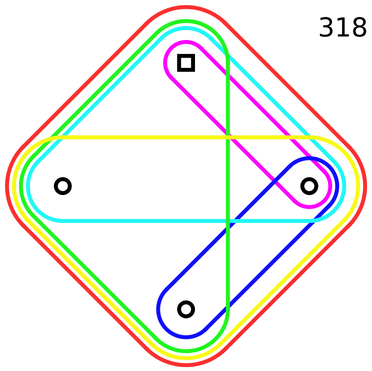
318

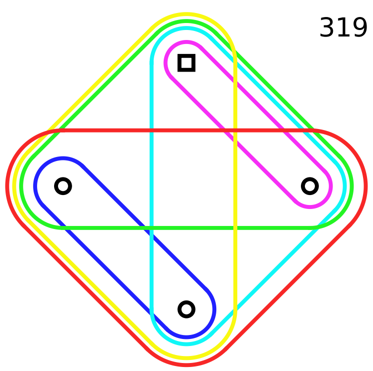
319

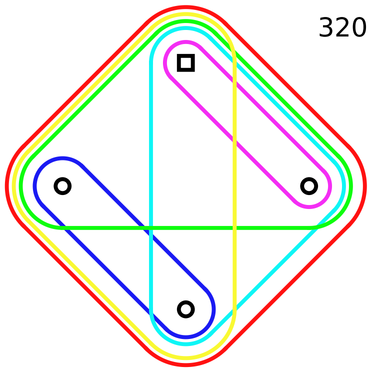
320

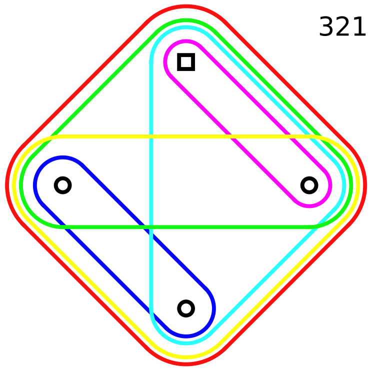
321

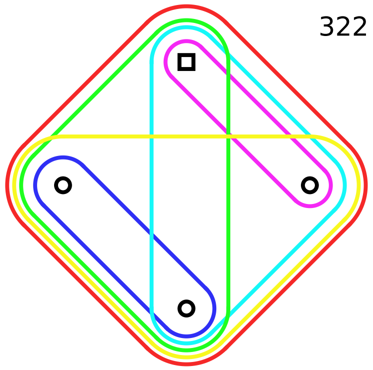
322

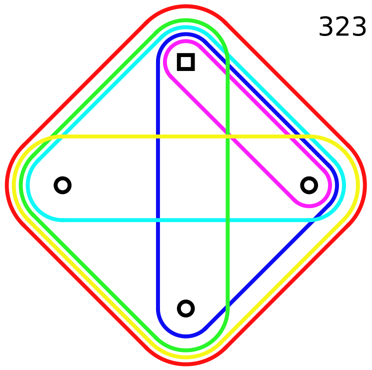
323

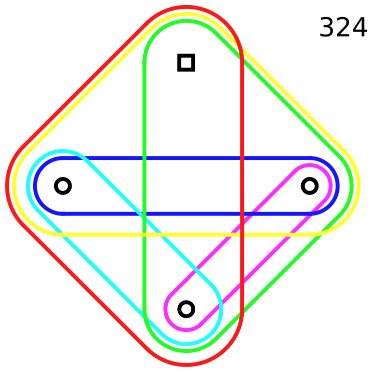
324

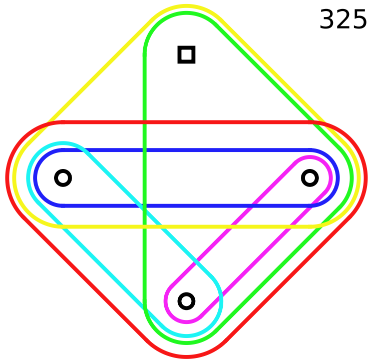
325

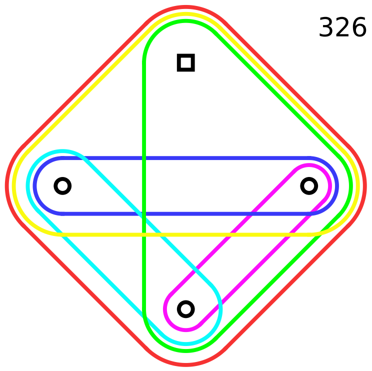
326

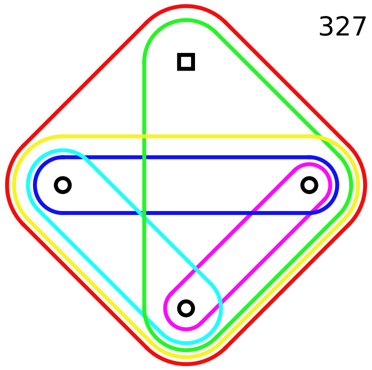
327

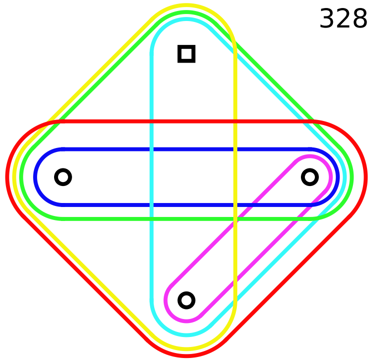
328

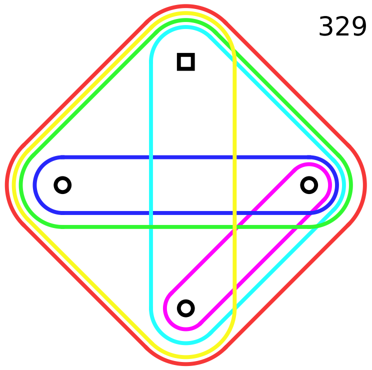
329

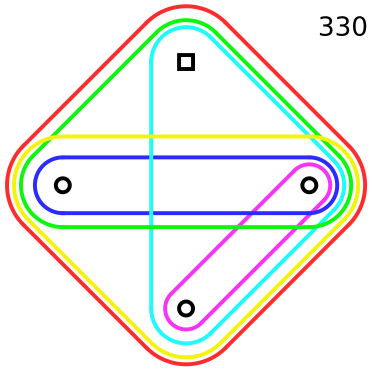
330

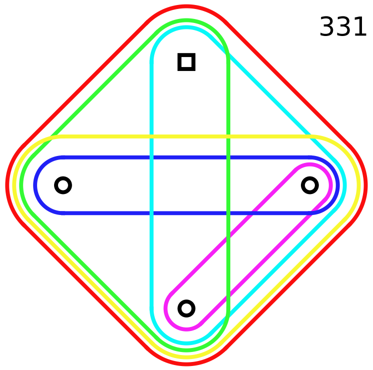
331

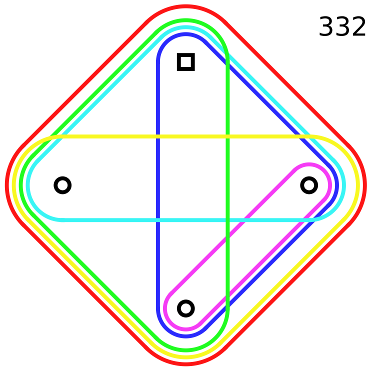
332

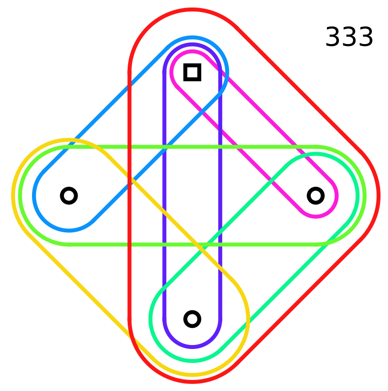
333

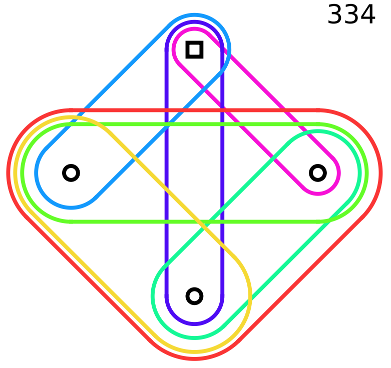
334

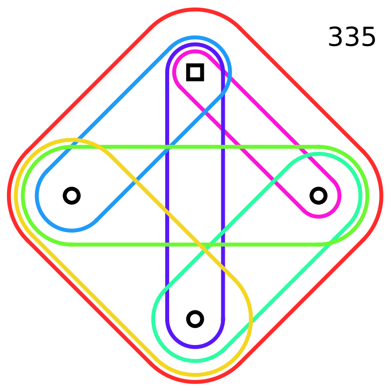
335

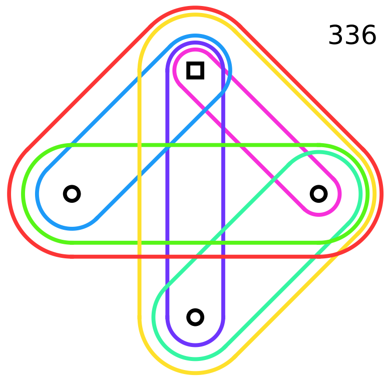
336

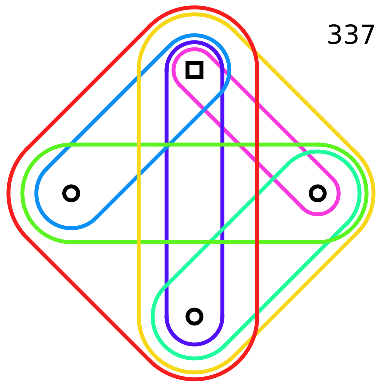
337

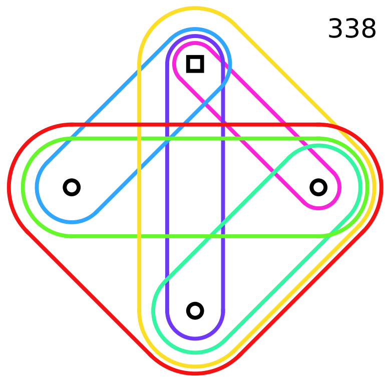
338

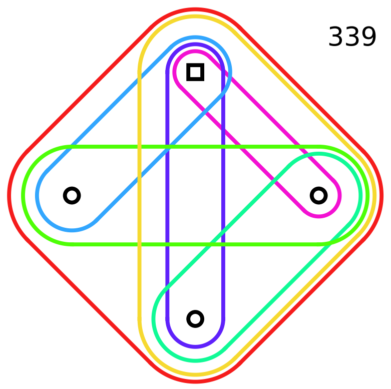
339

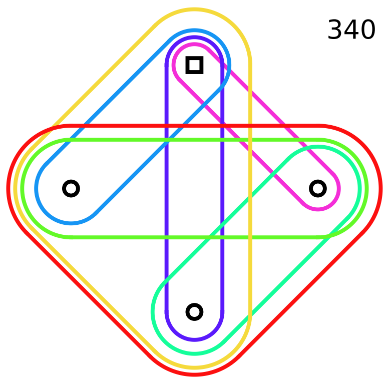
340

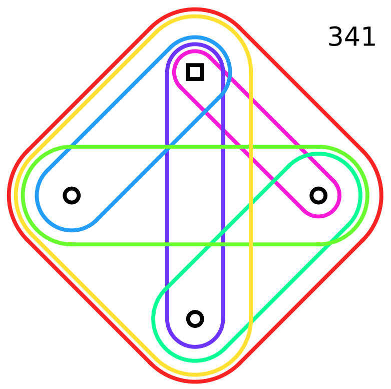
341

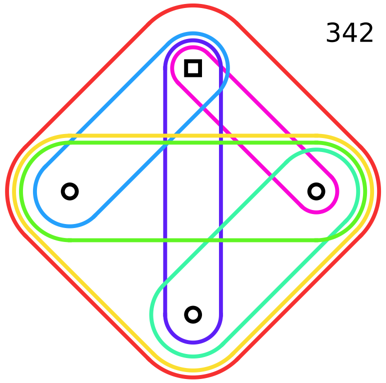
342

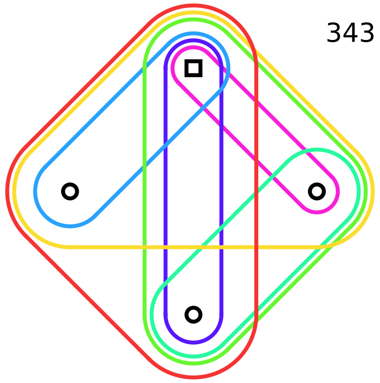
343

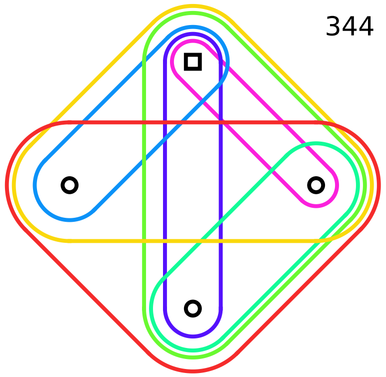
344

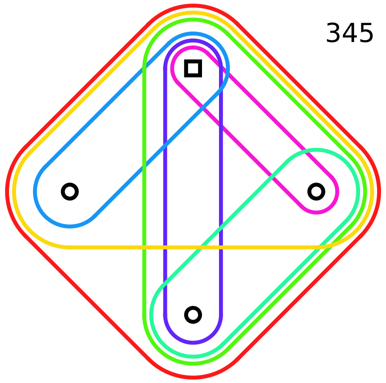
345

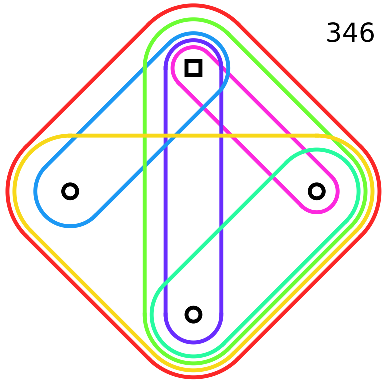
346

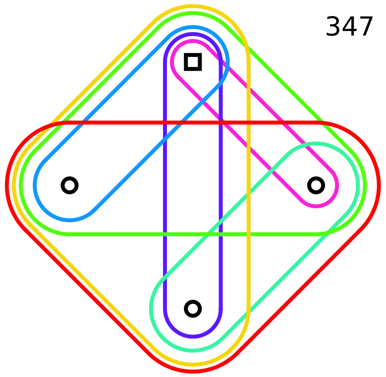
347

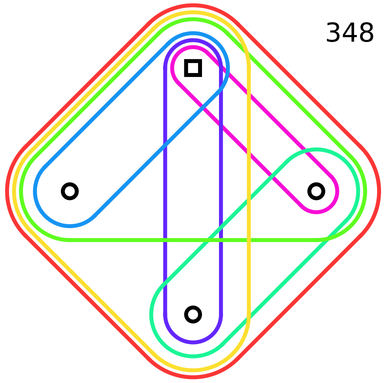
348

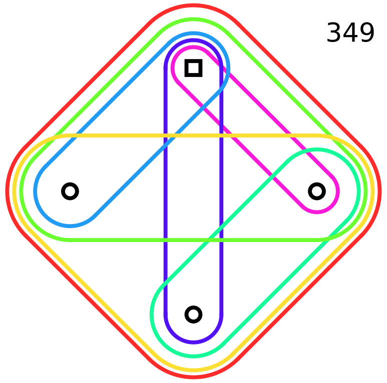
349

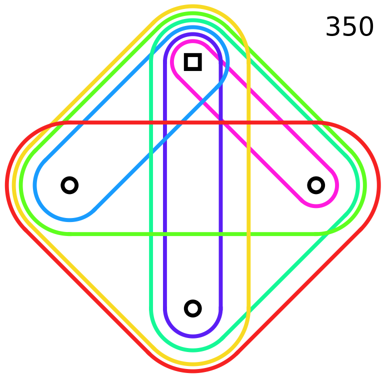
350

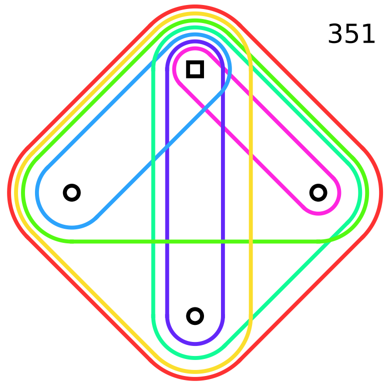
351

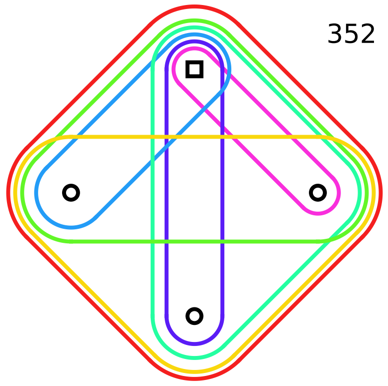
352

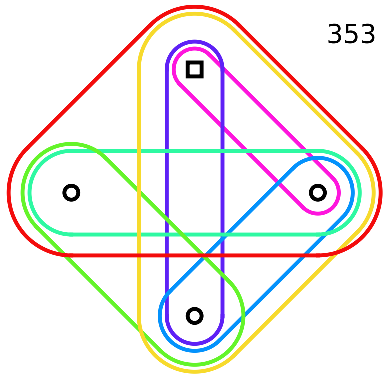
353

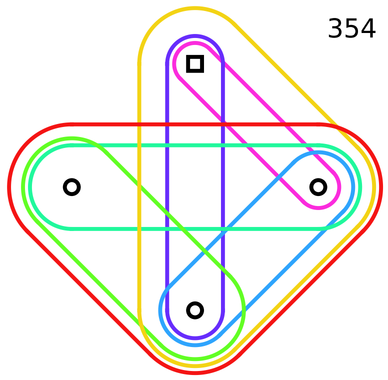
354

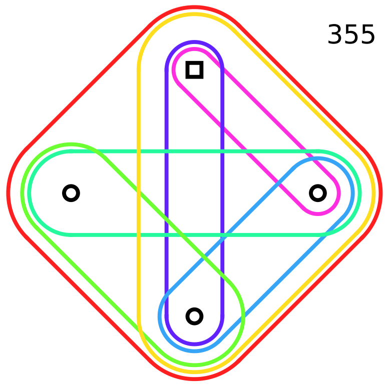
355

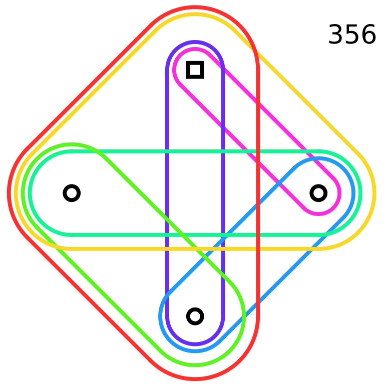
356

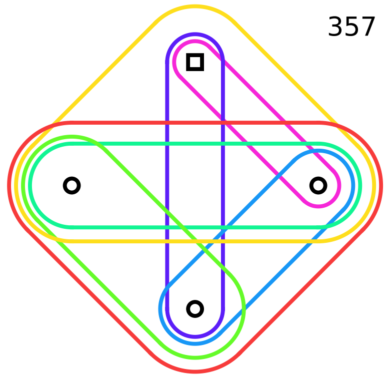
357

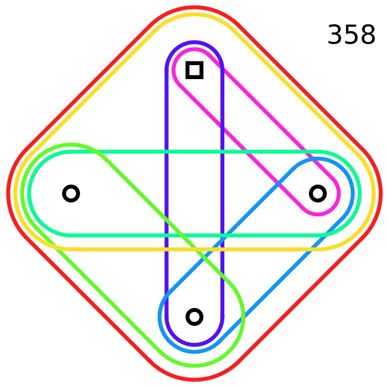
358

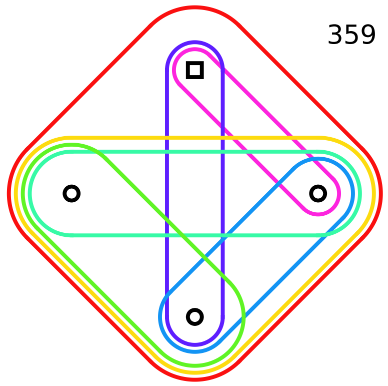
359

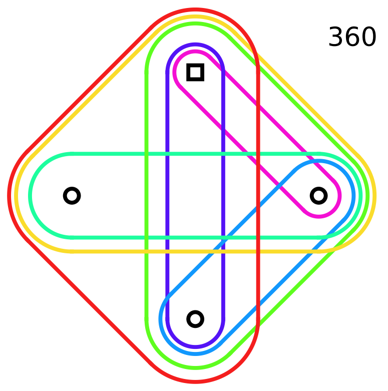
360

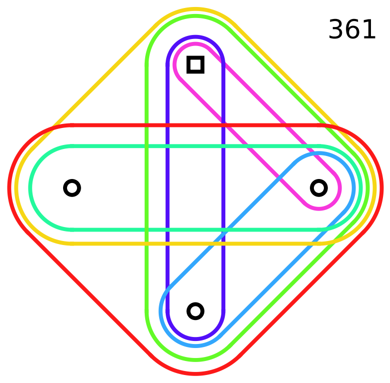
361

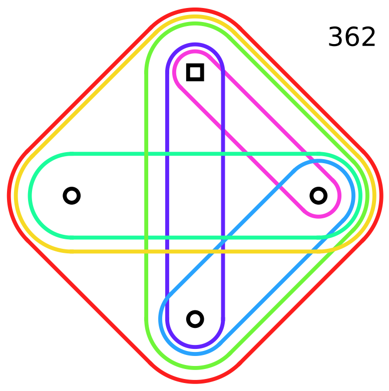
362

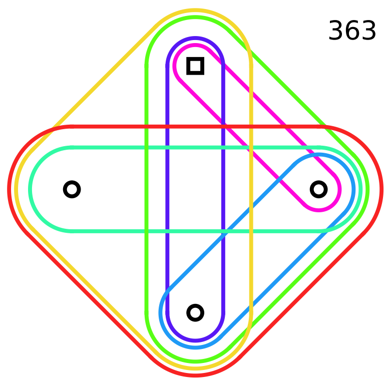
363

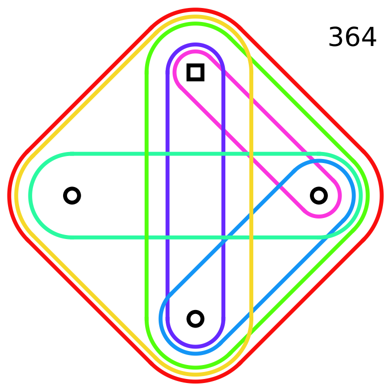
364

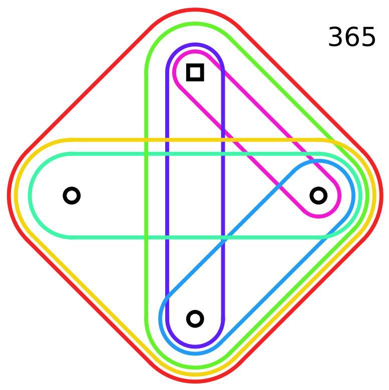
365

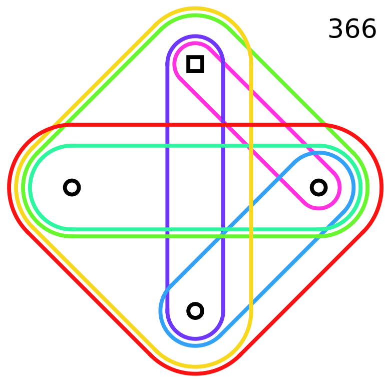
366

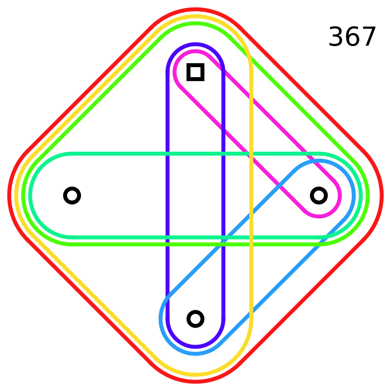
367

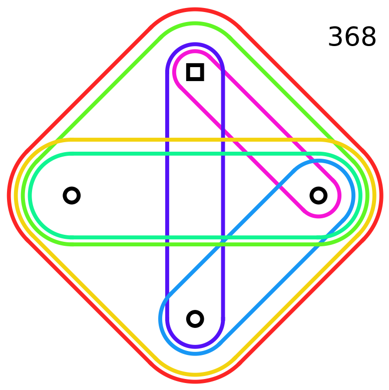
368

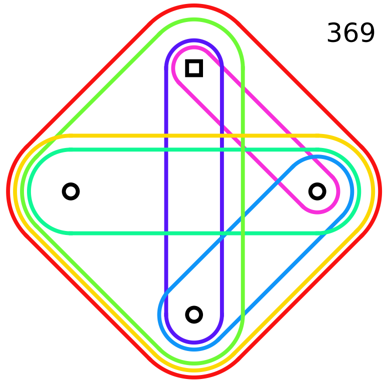
369

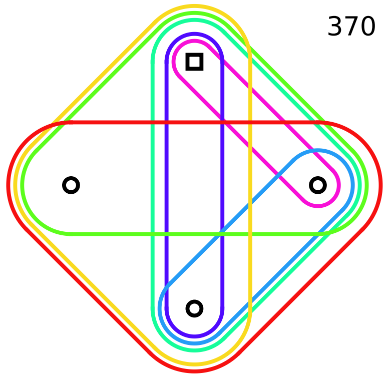
370

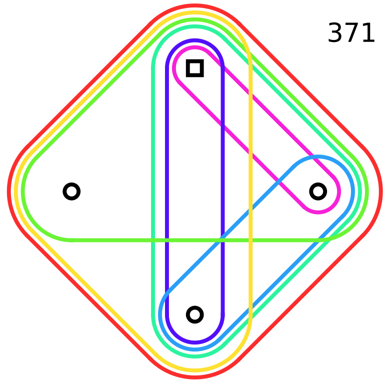
371

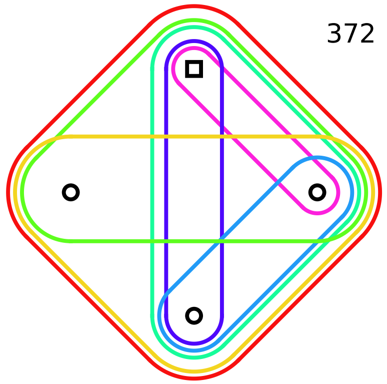
372

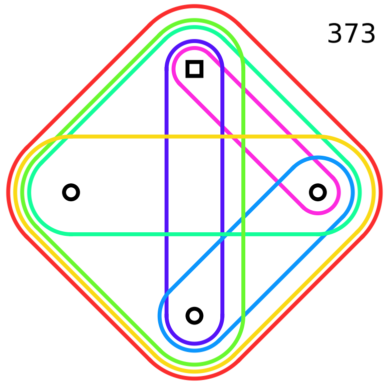
373

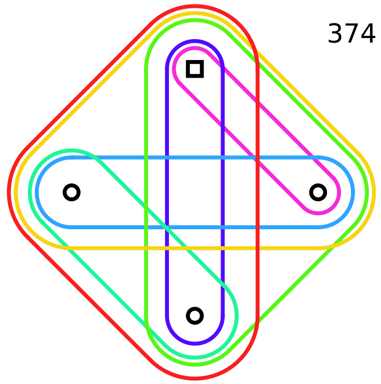
374

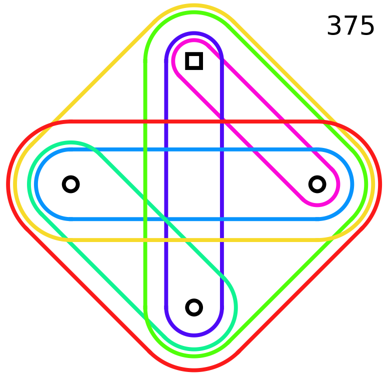
375

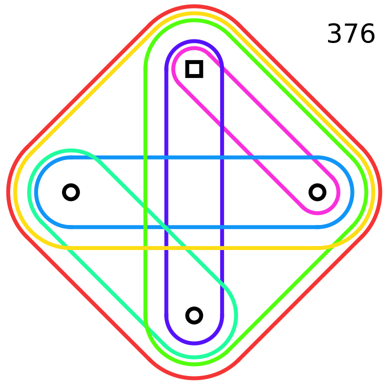
376

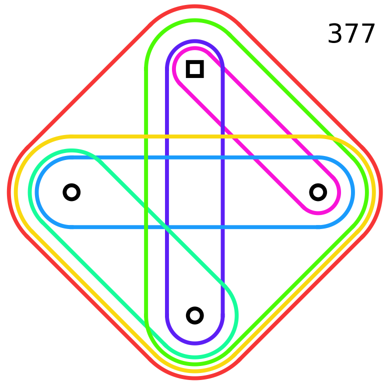
377

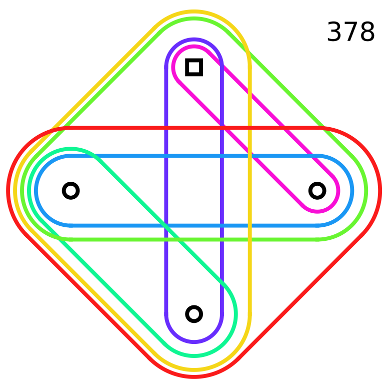
378

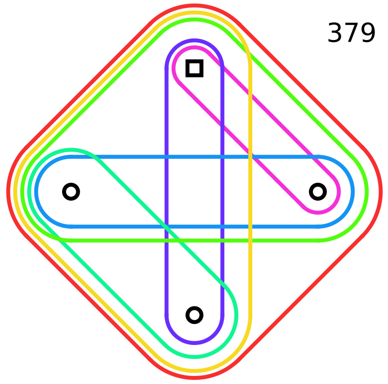
379

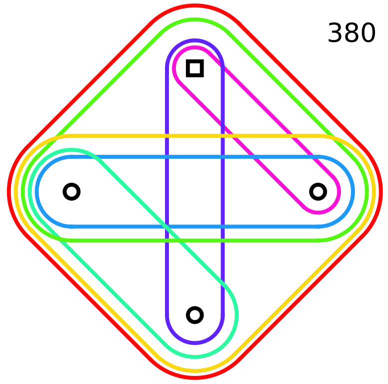
380

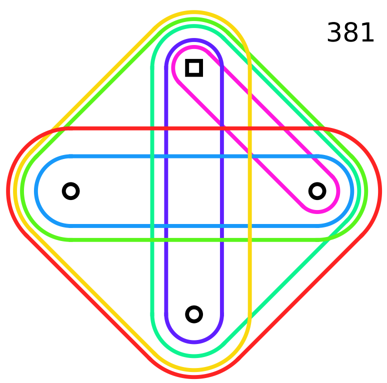
381

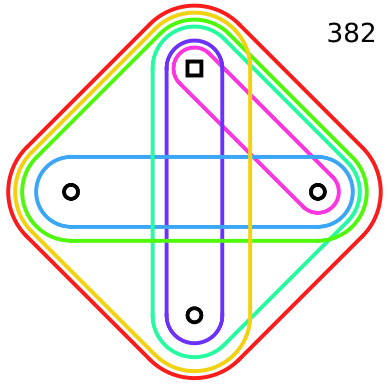
382

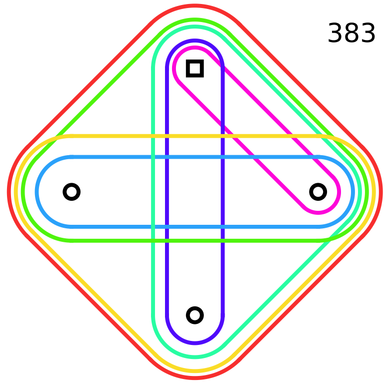
383

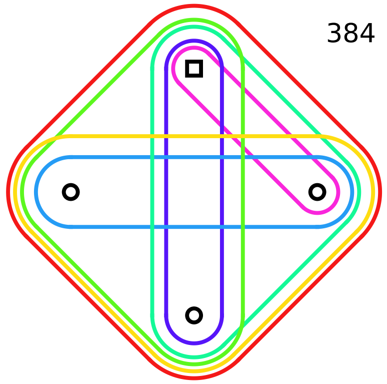
384

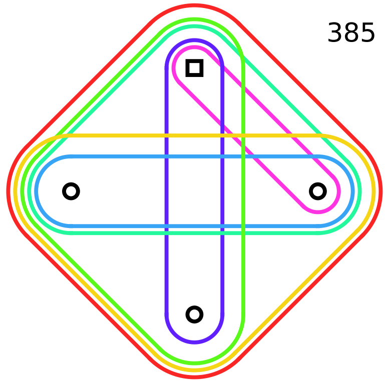
385

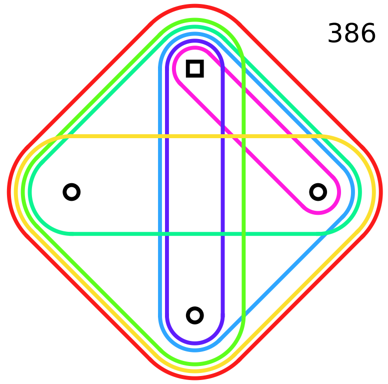
386

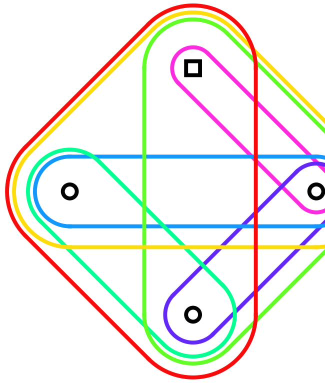
387

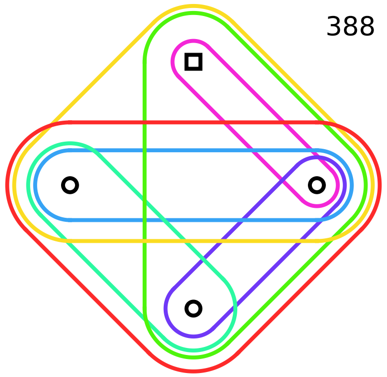
388

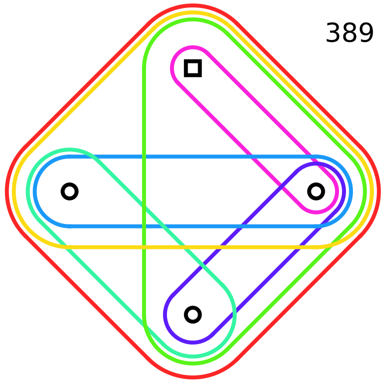
389

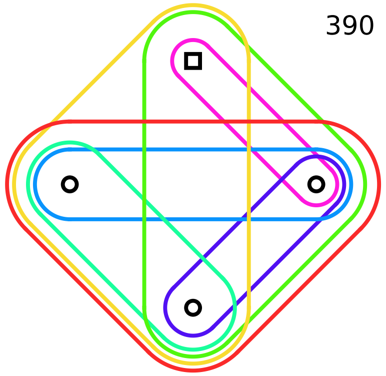
390

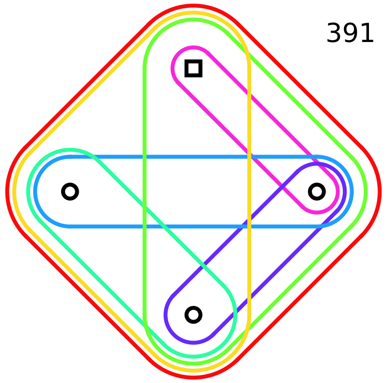
391

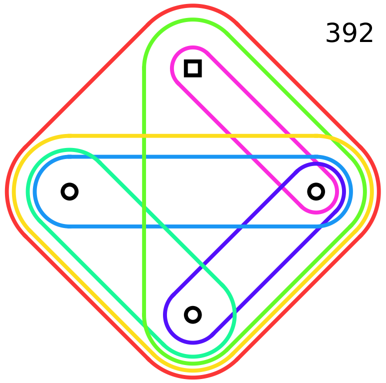
392

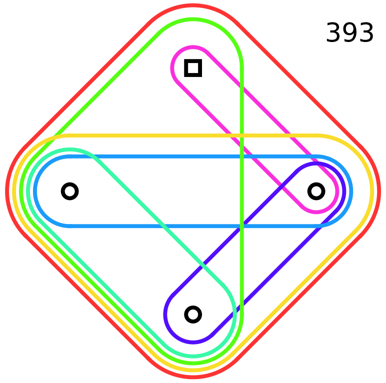
393

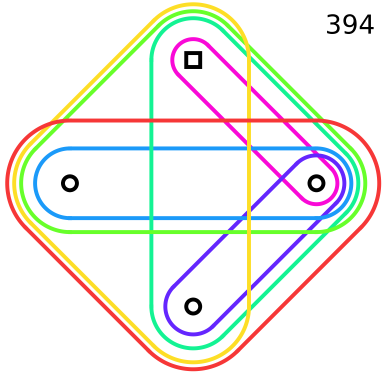
394

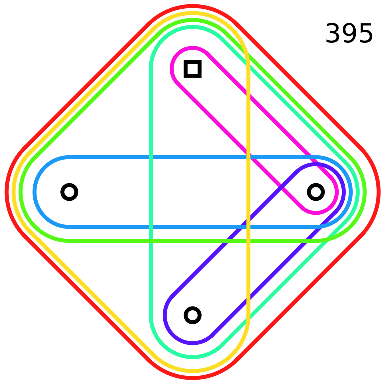
395

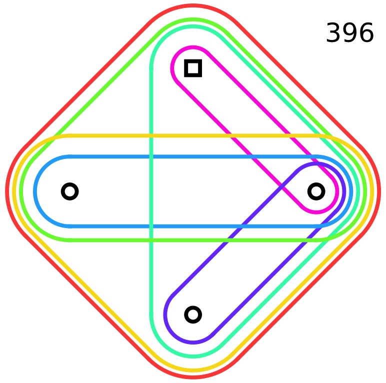
396

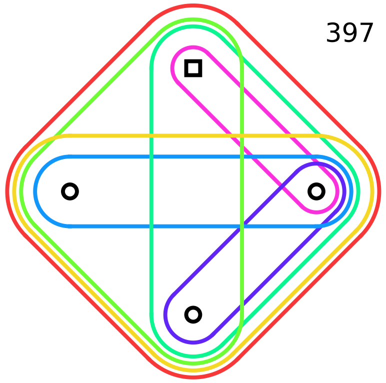
397

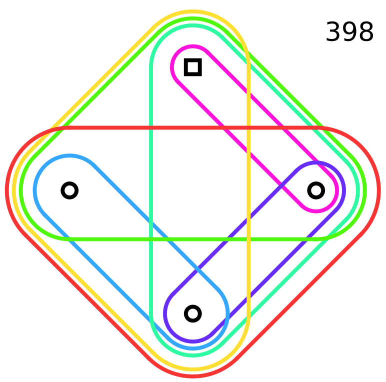
398

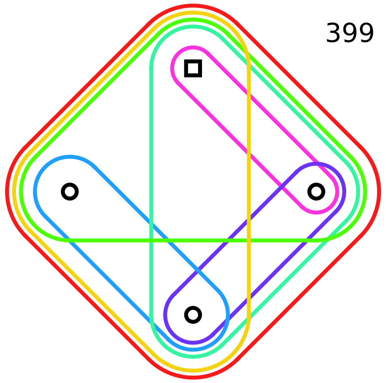
399

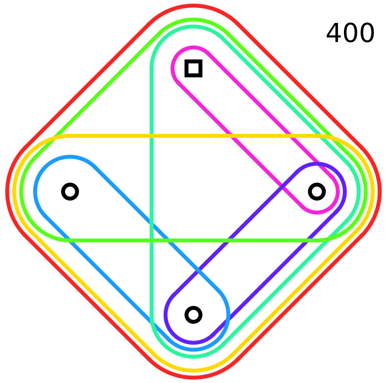
400

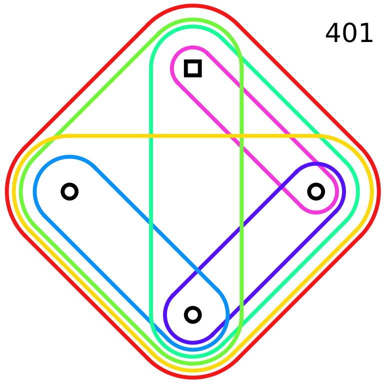
401

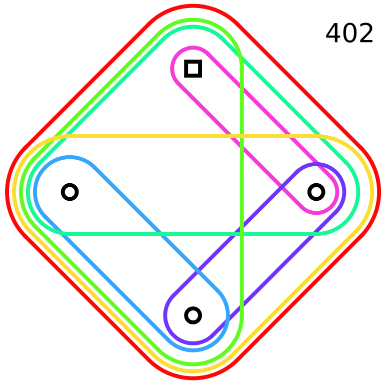
402

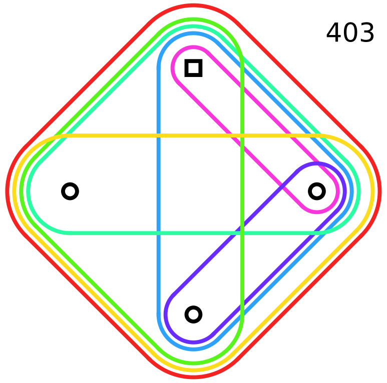
403

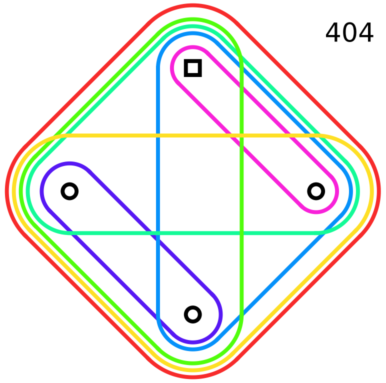
404

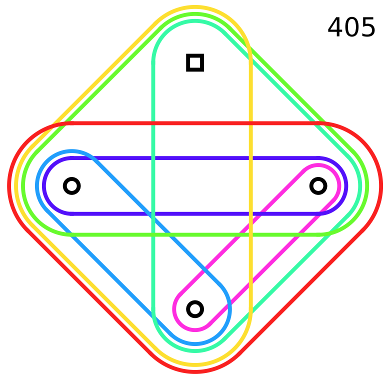
405

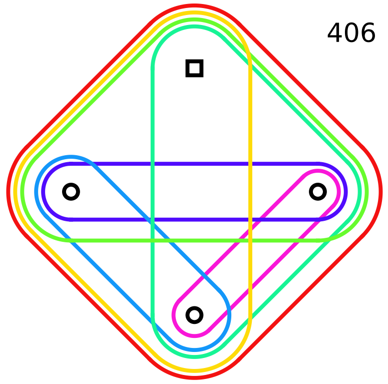
406

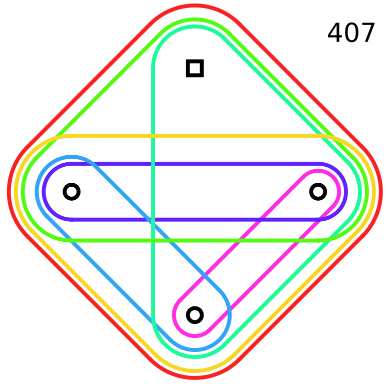
407

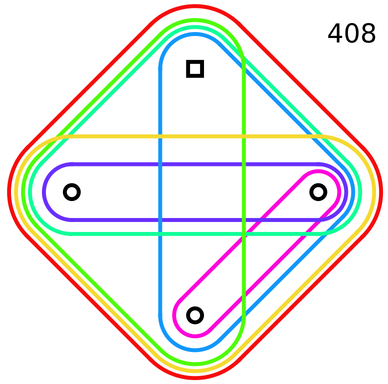
408

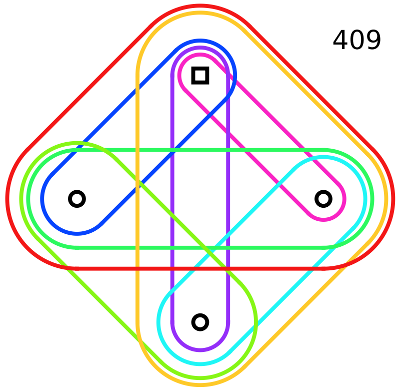
409

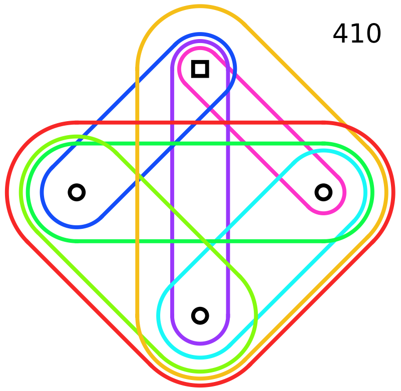
410

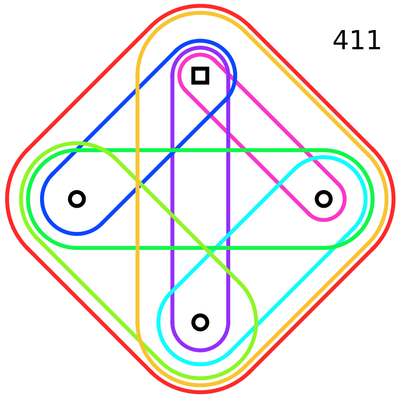
411

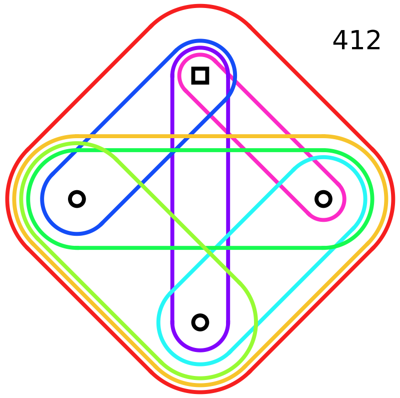
412

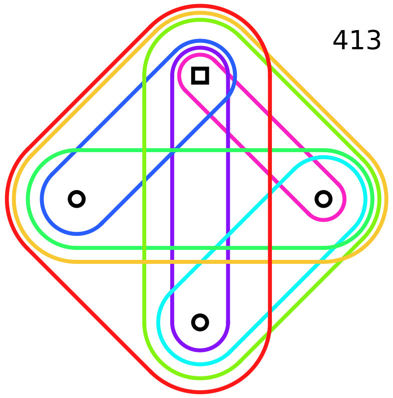
413

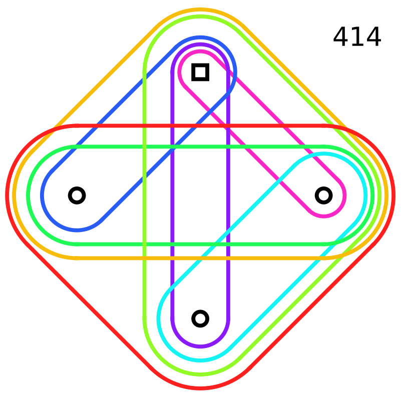
414

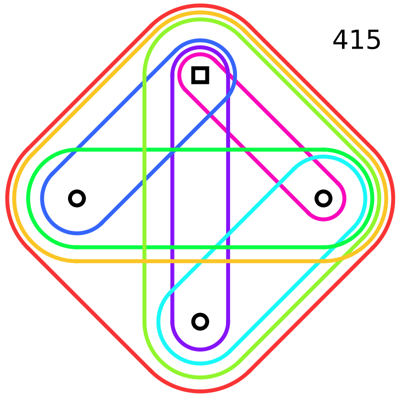
415

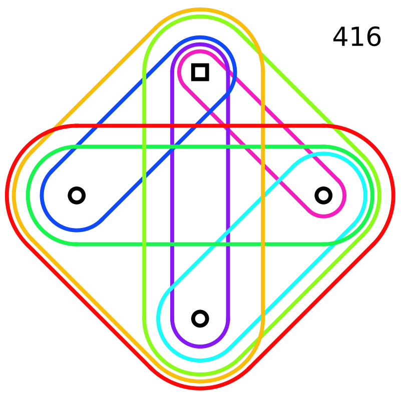
416

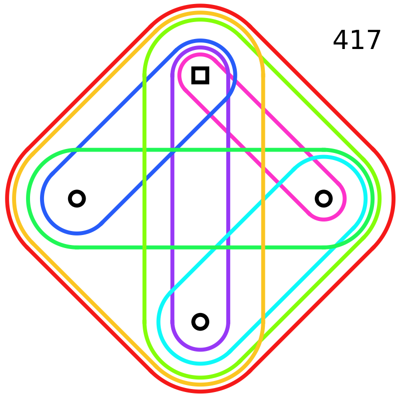
417

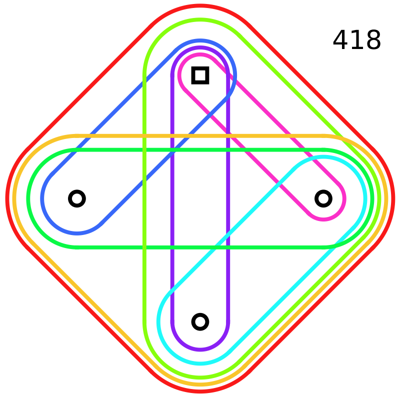
418

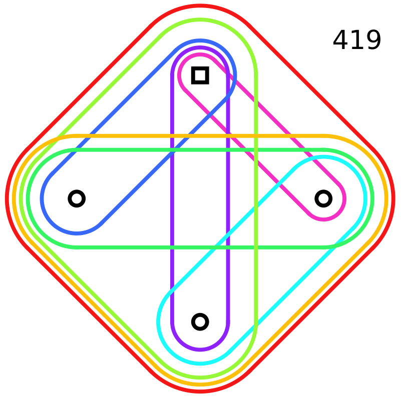
419

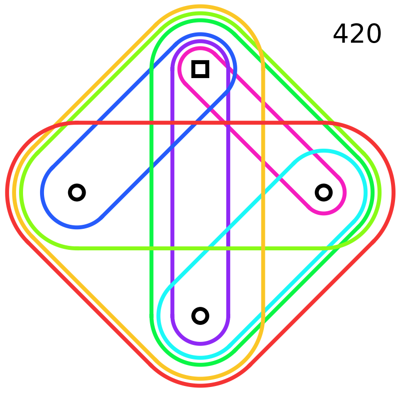
420

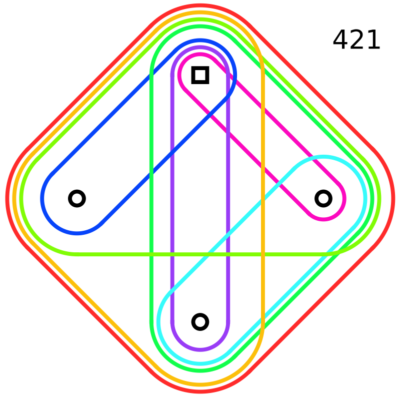
421

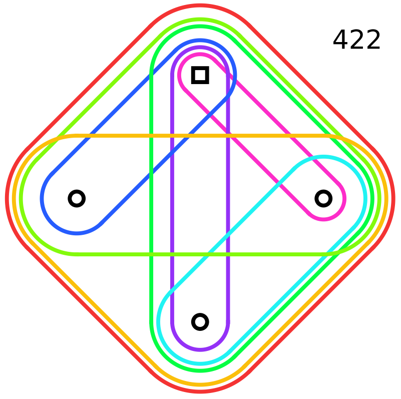
422

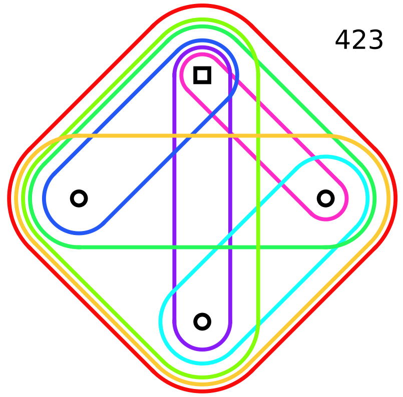
423

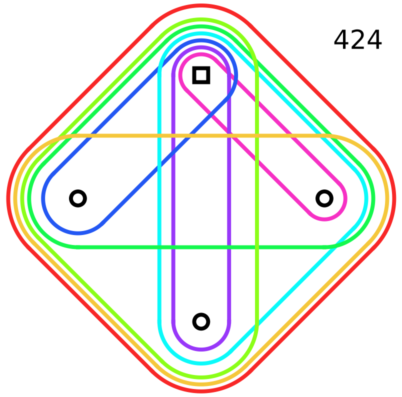
424

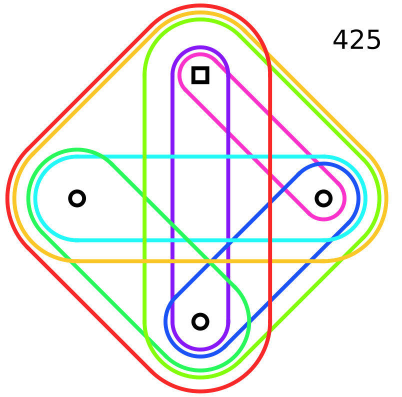
425

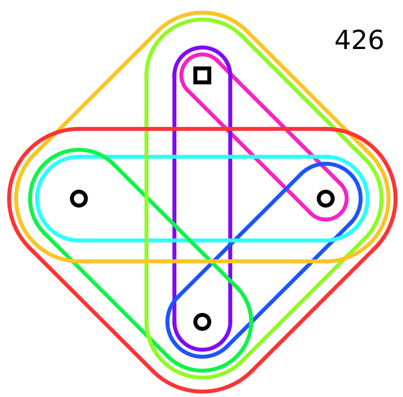
426

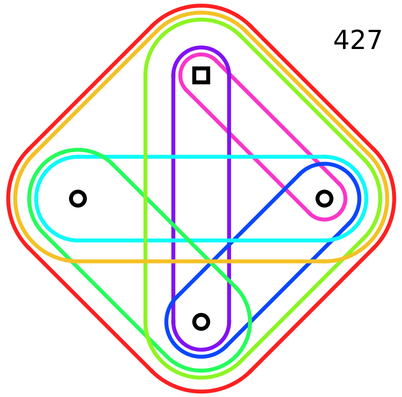
427

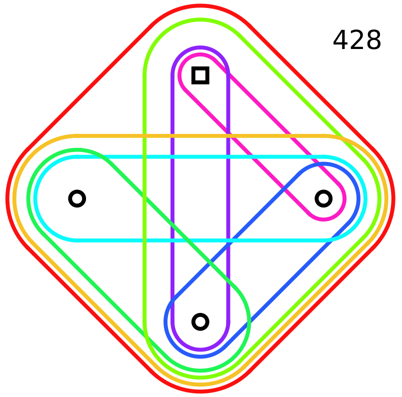
428

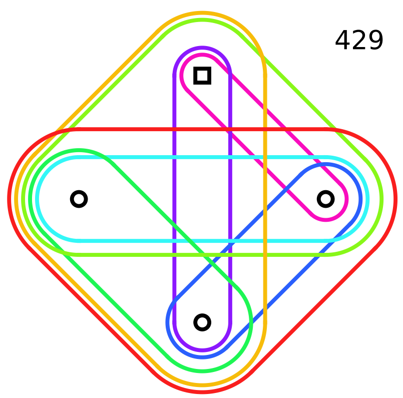
429

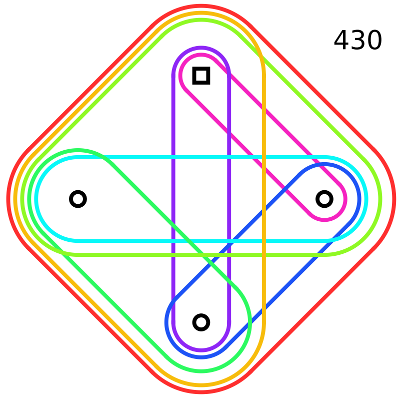
430

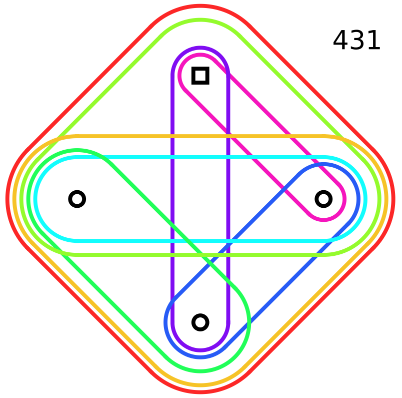
431

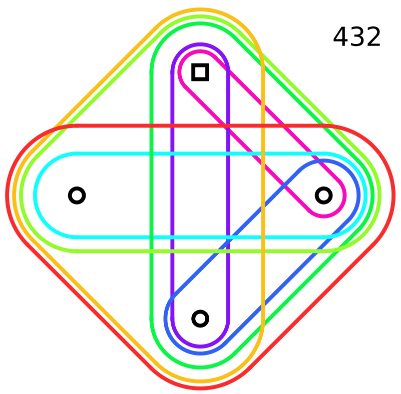
432

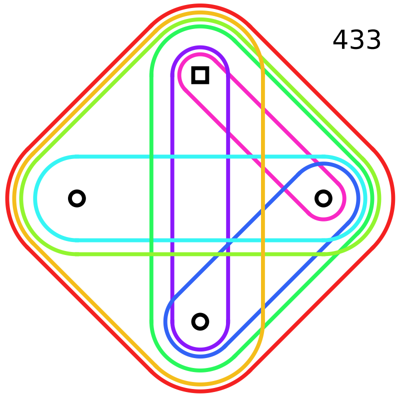
433

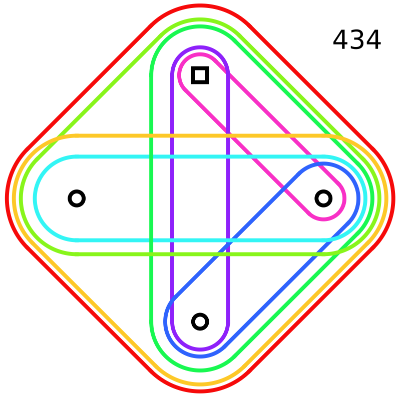
434

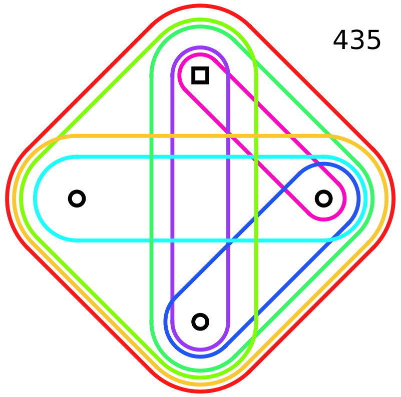
435

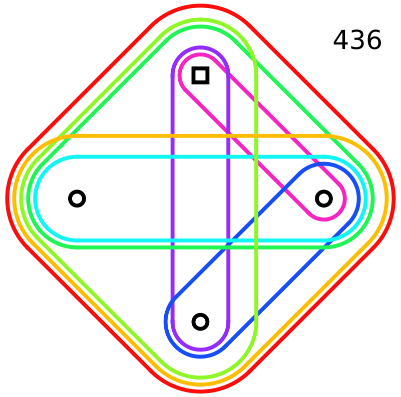
436

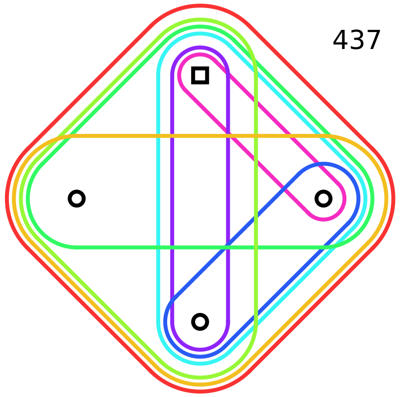
437

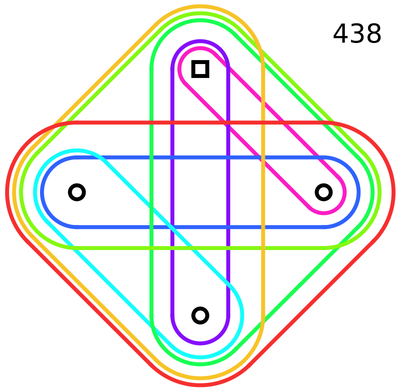
438

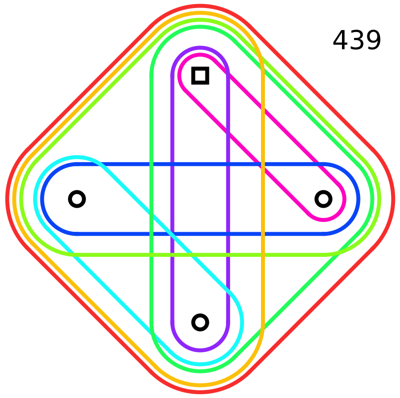
439

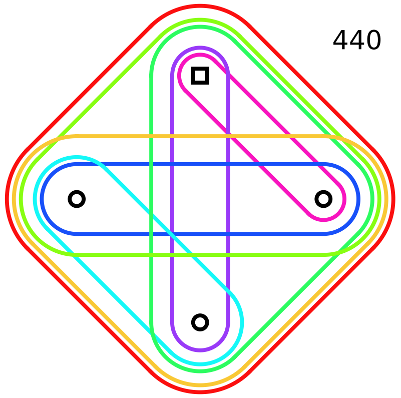
440

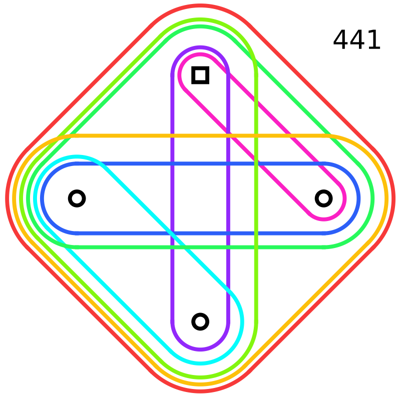
441

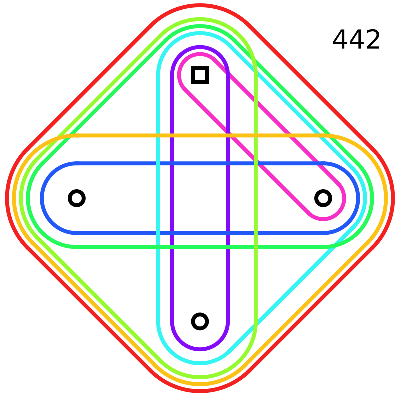
442

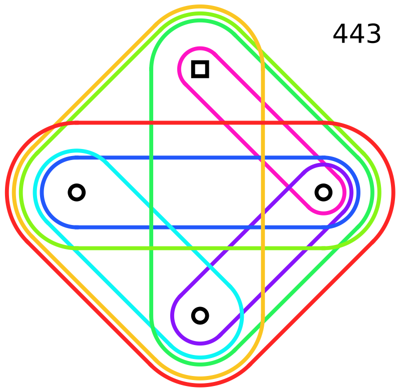
443

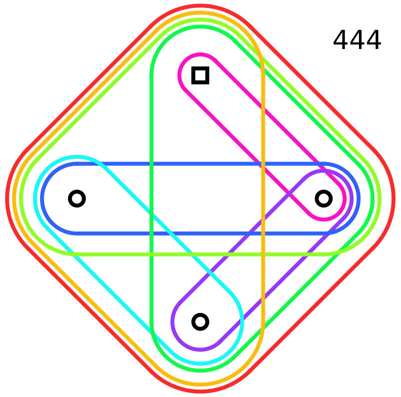
444

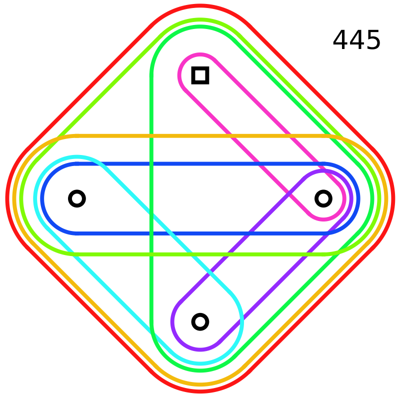
445

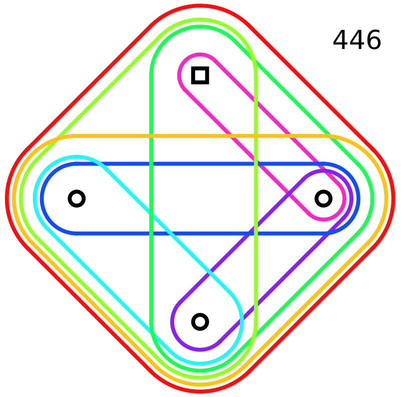
446

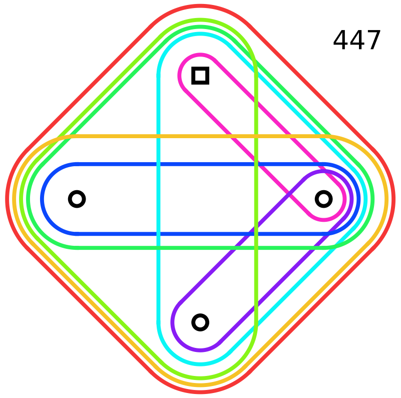
447

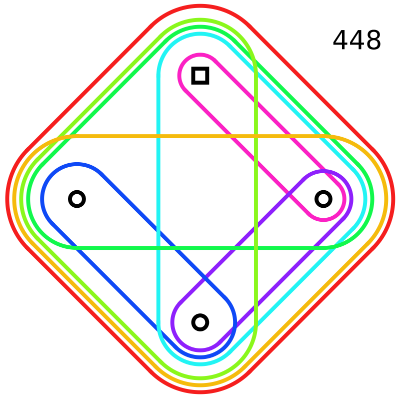
448

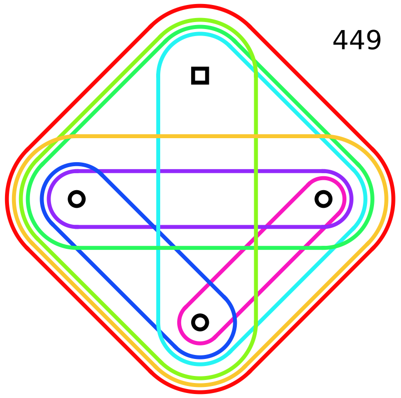
449

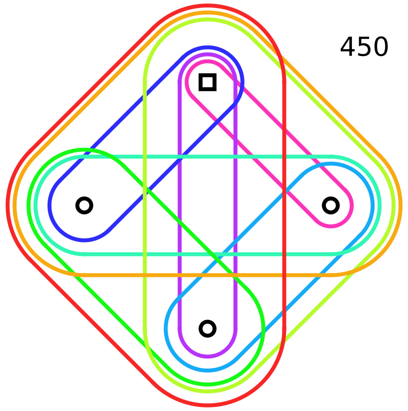
450

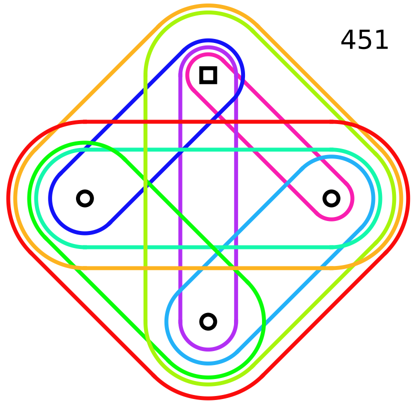
451

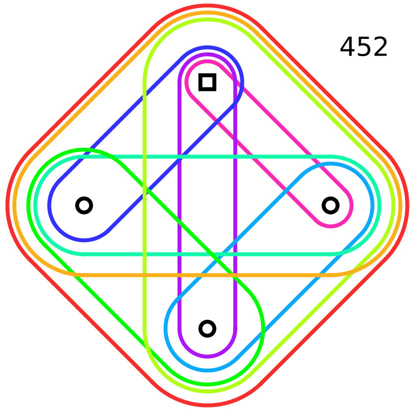
452

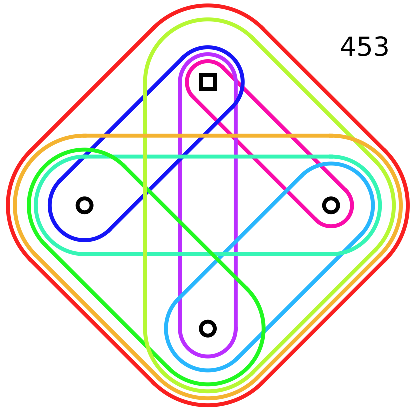
453

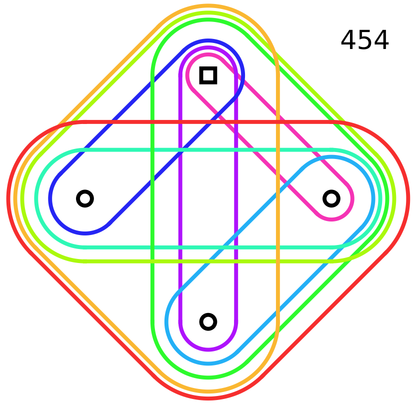
454

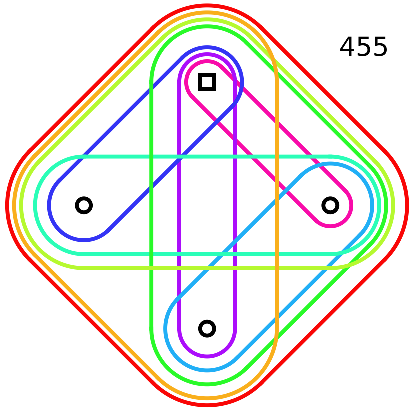
455

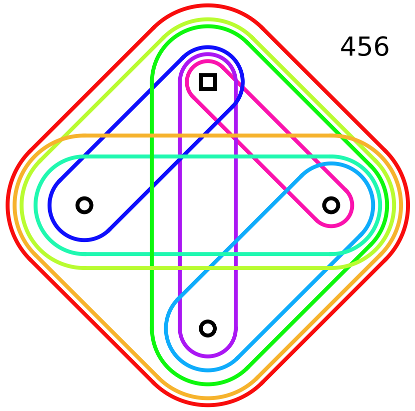
456

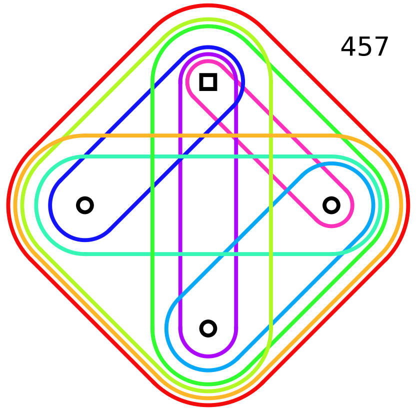
457

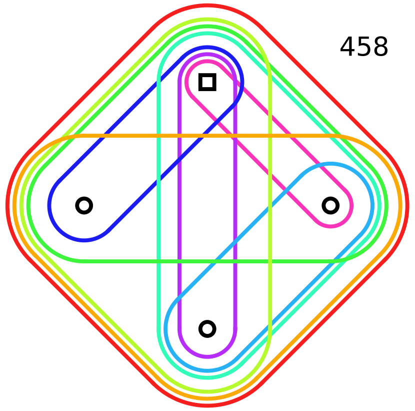
458

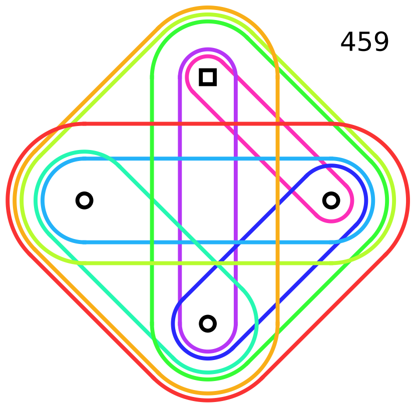
459

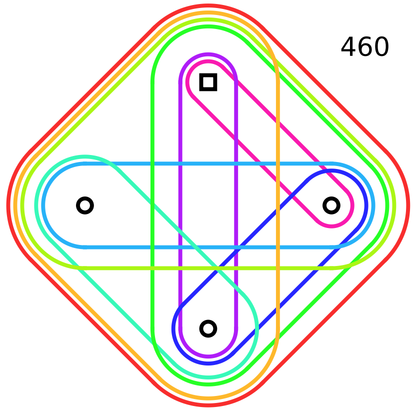
460

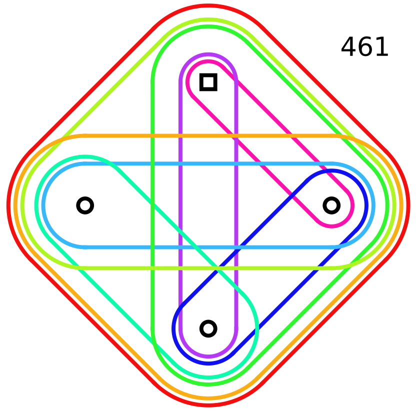
461

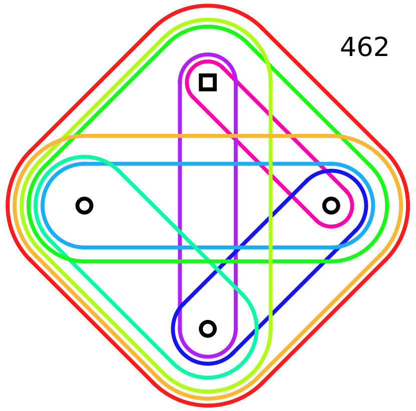
462

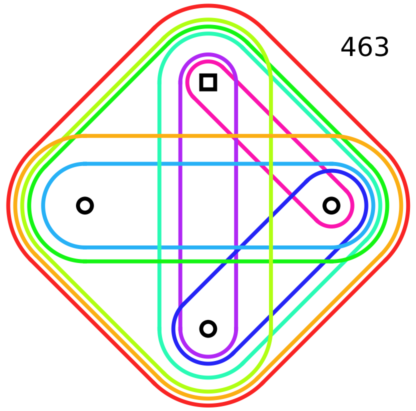
463

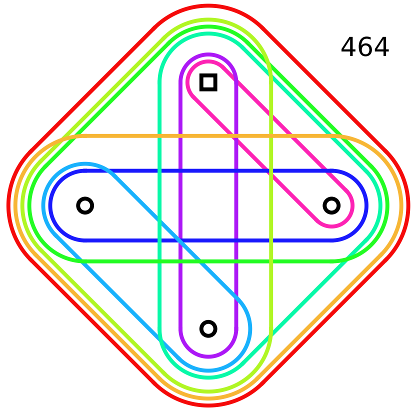
464

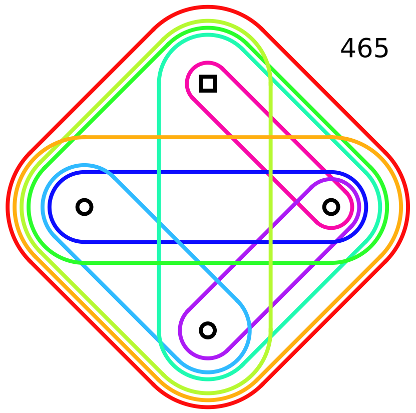
465

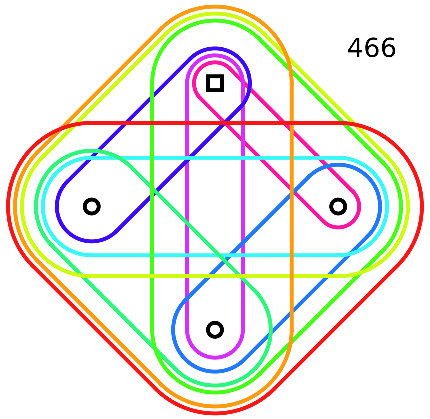
466

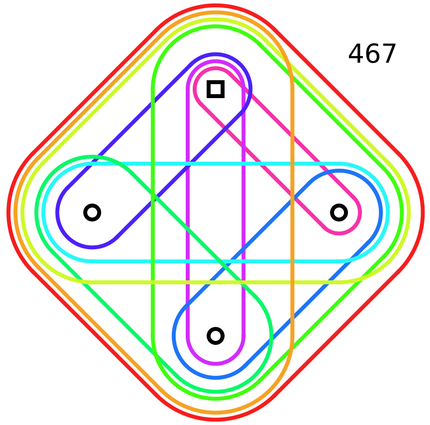
467

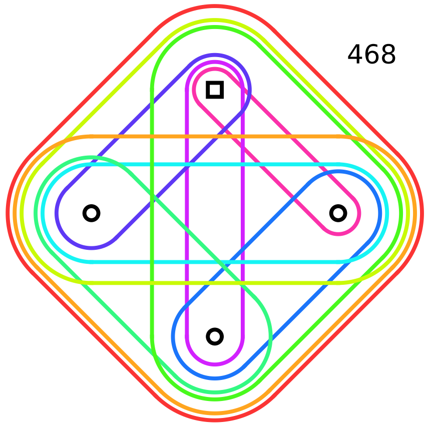
468

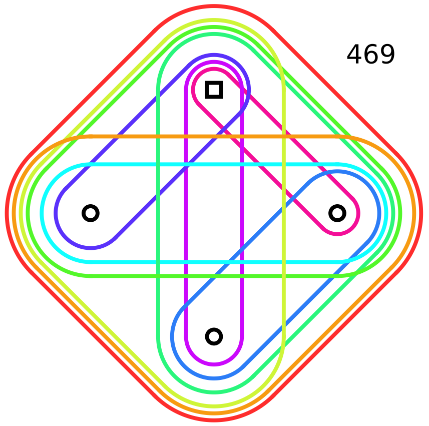
469

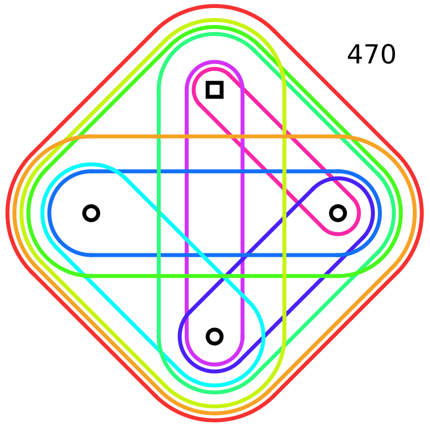
470

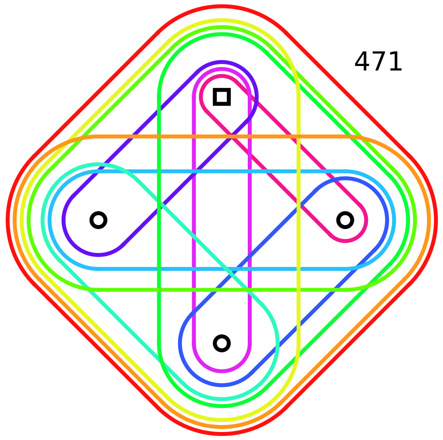
471